A. bisporus food web reconstruction and nematode analysis by stable isotope probing

by

Lucija Marjanović

A Graduation Research Submitted to

Faculty of Geosciences, Utrecht University

for the Degree of

MSc Earth Sciences (Earth, Life and Climate)

August 2022

Supervisors:

Madalina M. Vita, MSc

Prof. dr. Jack J. Middelburg

"All things are delicately interconnected."
Jenny Holzer. Truisms. 1978-1983

Abstract

The white button mushroom (*A. bisporus*) is one of the most important commercial mushroom cultivars worldwide, whose compost contains plentiful microbiota. However, little is known about the impact of nematodes on *A. bisporus'* growth and the carbon flow in the compost. To investigate this, a ^{13}C-glucose tracer study was performed, followed by counts of nematode densities which concluded with the build-up of a mathematical model of the carbon flow of this environment. First known application of LA-IRMS on nematodes for stable isotope analysis was performed, the results of which were coupled with results of PLFA biomarker studies, in order to build an interactive food web model for carbon flow tracing. Nematode population densities were shown to be too low to cause disease in *A. bisporus* primordia. Cultures without *A. bisporus* showed a lower overall number of nematodes than those with *A. bisporus*. Natural abundance $\delta^{13}C_{VPDB}$ measurements of nematodes agreed with literature values for soil nematodes and glucose tracer experiments suggested that nematodes uptake the tracer label indirectly through bacteria and fungi as second-level consumers. The model showed a drop in the bacterial and fungal biomass over the course of the experiment, with a simultaneous increase in *A. bisporus* biomass. Consistently with literature, simple sugars increased, and complex carbohydrates decreased over time, with increased emitted CO_2. These findings highlight that nematodes in commercial *A. bisporus* mushroom beds do not present danger to the mycelium, with *A. bisporus* acting as a direct competitor to nematode populations, which consume bacteria and fungi and in doing so, support carbon flow as top-level consumers.

Keywords: compost nematodes, casing nematodes, nematode stable isotope analysis, PLFA biomarker, compost food web modelling

Table of Contents

Introduction

Composting is a biochemical procedure whose final product is abundantly used in the commercial production of many cultivars, among them, edible mushrooms (Dunn-Coleman & Michaels, 1989). In Europe, this is particularly the case for the white button mushroom, *Agaricus bisporus*. Composting has a high economical value: the estimated worth of the edible mushrooms industry was $42 billion in 2018, out of which the genus *Agaricus* represents around 30% of all profits (Willis, 2018). Furthermore, the export market value of *A. bisporus* was €400 million in 2013, making the Netherlands the second largest producer of button mushrooms in Europe (Logatcheva et al., 2014). Additionally, natural forest beds include compost-based niches and are relevant in local and global nutrient cycles (Attiwill & Adams, 1993; Chang & Wasser, 2017). With its comparatively environmentally friendly production cycle, *A. bisporus* has found its purpose in agriculture as high-protein, high-vitamin food source, an alternative to non-biodegradable materials and as well as in medicine as a source of bioactive, anti-viral, anti-microbial and anti-cancer compounds (Atila et al., 2021; Bhushan & Kulshreshtha, 2018; Jagadish et al., 2009; Kozarski et al., 2011; Savoie & Mata, 2016).

The compost in which *A. bisporus* is grown undergoes two composting phases before the inoculation with the white button mushroom spawn (**Figure 1**). Starting with Phase I (PI), a basic mixture is formed from wheat straw, chicken or horse manure, gypsum and water, which will then be composted over the span of 3 to 7 days (Derikx et al., 1989; Straatsma et al., 1994). Compost-specific microbiota, composed largely of bacteria and fungi, establishes during this period (McGee, 2018). The activity of microbial organisms in compost raises the temperature in compost to about 80°C, and gradually, the mesophilic microbiota is replaced with thermophilic microbiota (Straatsma et al., 2000; Zhang et al., 2014). In phase II (PII), the residual phase I compost is pasteurised and conditioned at 45-50°C for 4 to 9 days, in order to selectively remove pests and prevent possible rotting and diseases (Mouthier et al., 2017). After phase II compost has conditioned and microbiota formed, *A. bisporus* is added to phase II-end compost as a spawn, on a rye grain inoculated with the fungal mycelium. The addition of the white button mushroom triggers phase III, during which the compost is kept at 25°C (Kabel et al., 2017). Over the course of 16 to 19 days, *A. bisporus* fully colonises the compost, removing in the process about 50% of monosaccharides (glucose) and polysaccharides (lignin, xylan) from the compost (Jurak et al., 2015). Phase IV (PIV) is triggered by addition of peat casing layer on top of the compost (Berendsen et al., 2010), which is further colonised by *A. bisporus*. Temperature and humidity are then lowered and ventilation is increased. Around 25 days after inoculation, pinning occurs and primordia form on the surface, which will grow into the sporocarp (fruitbody) of *A. bisporus*. The first flush occurs about 31 days after inoculation, with two to three series of harvest following afterward (Royse et al., 2008).

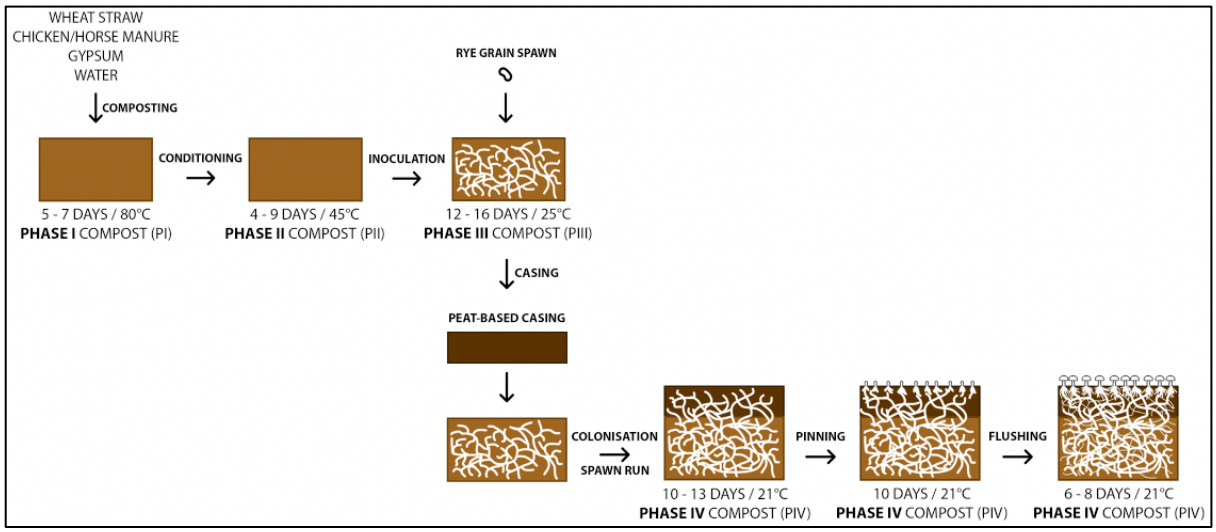

Figure 1: *Graphic representation of the cultivation process of A. bisporus.* Phase I commences with composting of a wet mixture of wheat straw, manure, gypsum and water over the course of 5 to 7 days at 80^0 C. Conditioning starts off phase II, during which compost is tempered at 45^0 C for 4 to 9 days. Phase III commences with the addition of rye grain inoculum to the compost, upon which the mushroom colonises the compost fully, over the course of 12 to 16 days. A layer of peat casing is added at 17 days post-inoculation, and at 25 days primordia start to form at the surface of the casing layer, commencing a fruiting phase of the cultivation. Around 31 days post-inoculation, primordia will develop into fruitbodies ready for harvest.

During edible mushroom production, used compost, commonly referred to as spent compost, remains rich in various nutrients (C, N and P) (Royse et al., 2008). Furthermore, a significant amount of carbohydrates is not taken up by any of the organisms active during the *A. bisporus* cultivation and is left behind in the post-cropping compost as waste, with each kg of produced mushrooms generating on average 5-6 kg spent compost (Rajavat et al., 2022). The amount of produced waste, which in the Netherlands alone is estimated to be around 800,000 tons, is problematic. While spent mushroom substrate is high in phosphate content and finds second life as fertiliser, circularity and reusability is limited, as residual waste can contaminate groundwater and natural resources without proper disposal solutions (Rajavat et al., 2022). The microorganisms in compost biologically cycle nutrients indispensable for life and alter their chemical structure, synthesising organic compounds which can be taken up by living organisms (Agnew & Leonard, 2003). The most commonly observed microorganism contributors in compost are bacteria, archaea and fungi (Kertesz & Thai, 2018; Steel et al., 2010). Aside from microbial life, many important participants from the kingdom Animalia have been observed in the compost, such as nematodes, centipedes, beetle, snails, mites and ants (Castilho et al., 2009; Muszynska et al., 2017; Reyes et al., 2004; Steel & Bert, 2012). Pests which inhibit growth of mushrooms or support diseases and rot are also naturally present, such as aphids and flies (Flint & Dreistadt, 1998; Gujarathi & Pejaver, 2011; Nardi, 2009).

Conversely to natural compost environments, *A. bisporus* is commercially raised in an artificial ecological niche. This niche is a cumulative effort of farmers across the world,

and a product of hundreds of years of agricultural effort, selective breeding and composting in a perfected environment to achieve conditions in which the sole goal is to harvest the white button mushroom to the best possible commercially viable extent. The artificial nature of this microenvironment led to a microbiota which is likewise truncated in comparison to any natural soil counterpart. The pre-extant microbiota (bacteria and fungi in the compost and casing) is altered through processes of casing, which supplies water, protects against desiccation and provides organic matter and structural support (Noble et al., 1999) and aeration, during which temperature, oxygen flow and humidity is controlled. These processes affect entire generations and types of microbial fauna present and lead to succession events. Notably, compost processed at lower temperatures (45-47°C) harbours a population of naturally-occurring bacteria and fungi, while compost processed at higher temperatures (65-68°C) lacks microbiota and is not selective for *A. bisporus* growth (Fermor & Grant, 1985; Fermor et al., 1985). Bacterial and fungal communities grow selectively depending on the environment they are suited to best. Mesophilic microbiota are the pioneer species proliferating during the creation of the compost mixture, while thermophilic microbiota overgrow them in a succession event with the increase of temperature and pH during Phase I (Kertesz & Thai, 2018; Mercer et al., 1996; Wood & Leatham, 1983). Finally, entire populations of large organisms (centipedes, mites, beetles and snails) and common pests (aphids, flies) are nearly non-existent in commercial *A. bisporus* production settings, in order to perpetuate a clean, viable and productive agricultural environment (Dias et al., 2013; Sharma et al., 2019). In this abbreviated biological environment, the carbon is exchanged among various compartment including bacterial biomass, fungal biomass, *A. bisporus* biomass, nematode biomass, recalcitrant sources of carbohydrates and lignin, readily available sources of broken-down sugars, and respired carbon dioxide.

Despite the overall removal of pests and large critters, nematodes have been consistently observed in *A. bisporus* casing and compost (Grewal, 1991; Grewal et al., 1992; Grewal, 1989). Studies done on similar substrates indicate possibilities of different nematode species co-existing in the compost, as well as successions occurring during composting (Steel et al., 2010). However, little is known about the role of nematode populations and their contribution to the carbon flow in commercial mushroom composts, and the literature body concerning their impacts on the biota present, as well as their interactions with *A. bisporus* itself, is scant. Nematode analysis is usually conducted through visual and morphological analysis. Post-extraction, visual analysis helps to establish population abundance and distinguish nematodes from nematode-looking debris (dark strands of plastic, particles of dust, or segments of straw or horsehair) (Wilschut et al., 2019). Morphological analysis aids in recognition of feeding habits of nematodes, and subsequently their classification, which bears importance in understanding their overall position in the food web (Bongers & Bongers, 1998; Bongers & Ferris, 1999). A nematode's head, and more precisely, its mouthpart, gives indication towards whether a nematode is preferentially herbivorous, bacterivorous, fungivorous, predatory or omnivorous

(Yeates et al., 1993). On living nematode samples, mouthpart organs, such as stylets or stomas, can be spotted under a large enough magnification under a dissecting microscope, compound microscope equipped with an imaging system, or a scanning electon microscope (SEM) (Hassan, 2013). For morphological analysis to be carried out correctly, it is important for the nematode samples to be fresh and still living, as sensitive mouthpart organs are most susceptible to decaying first, even when the structure of the nematode is well-preserved (Ingham, 1994). Several studies performed successful nematode rehydration on samples stored in preservatives for longer periods of time, to a degree of sufficient quality for morphological observations (Naem et al., 2010; Yoder et al., 2006). Moreover, some studies used microscope slide staining as a method of differentiation of nematodes in a sample from other living and dead material by distinguishing structural components depending on the stain used (Bybd Jr et al., 1983; Hallmann & Subbotin, 2018). Biological stains were used for this purpose, as they permeate the nematode cuticle and allow for rapid counting or taxonomy studies (Anderson et al., 1979).

Microbial contributors, together with large-scale contributors, combine nutrient cycles and intermingle through a natural interconnection of food chains in the compost ecological community. More specifically, this interconnection is called a food web, and graphically represents "what-eats-what" relationships of a certain ecological niche (Polis & Strong, 1996). Food webs explain the flow of nutrients (C, N, P) among different biological compartments and physical domains of a certain ecological niche, and they are represented as an intricate balance designed by even the most minute interactions between organisms present. The bacterial promotion of hyphal elongation (Kertesz & Thai, 2018), increase in efficiency of bacterial transport due to fungal hyphae (Kohlmeier et al., 2005; Simon et al., 2015; Warmink et al., 2011), bacteria and fungi serving as both collaborators that degrade polysaccharides which *A. bisporus* takes up, but also directly as its nutrient resource (Iiyama et al., 1994; Rashid et al., 2016; Sánchez, 2009) are just some of the observed interactions which shape the environment of the compost and its trophic interactions "behind the scenes". However, the full picture on the structure of *A. bisporus* food web remains elusive.

The natural abundance stable isotope ratios can indicate trophic transfers in food webs, and additions of label into the food web system can be traced, which allows precise elucidation of trophic pathways (Ruess & Chamberlain, 2010). Furthermore, isotopic signatures can be used to precisely identify groups of organisms, and even environmental conditions across different ecological niches (Chmura & Aharon, 1995). Stable isotope analysis is often performed using elemental analyser-coupled mass spectrometer (EA-IRMS), as a standard method allowing studies on isotopic values of the bulk materials and quantification of abundance (Grassineau, 2006). At Utrecht University, a laser ablation-coupled mass spectrometer is available (LA-IRMS), and this type of IRMS specifically and precisely targets individual specimens and their selected parts, ignoring possible debris (van Roij et al., 2017). The LA-IRMS setup is

commonly used for different types of pollens, dinoflagellates and other palynomorph forms (Moran et al., 2011).
In ecological studies, biomarker analysis is performed to aid with validation of the food web and in order to help reconstruct behavioural and trophic interactions between biological compartments (Boschker & Middelburg, 2002; Ruess et al., 2005). Phospholipid-derived fatty acids (PLFAs) can be extracted and analysed from samples containing bacterial or fungal biomass. PLFAs are present in the cell structures of both bacteria and fungi (including *A. bisporus*) (Ruess & Chamberlain, 2010), and some are taxonomically specific and can reliably be used as identifiers of organisms they are extracted from, as well as be used to calculate their total biomass (Frostegård et al., 2011; Treonis et al., 2004; Watzinger, 2015). Finally, PLFAs are often used in conjunction with stable isotope labelling procedures, as incorporation of label in the PLFAs allows for organism-specific uptake quantification (Dungait et al., 2011; Middelburg, 2014). The uptake signifies activity in the food web, essentially acting as a differentiator between active and deceased biomass. As PLFAs degrade rapidly after death of the originating organism, they are by natural indicators of living biomass. Tracers (such as ^{13}C-glucose) coupled with PLFAs demonstrate which group of organisms uptake the specific tracer in time, how rapidly and whether there is an uptake transfer from one biological group to the other (Boschker & Middelburg, 2002). Quantifications of living biomass are used as supplements to isotopic studies, which is a common biogeochemical approach often utilised in studies, though it has not been previously applied to *A. bisporus* compost food web.

Food web models are written in code and designed to output graphical representations (Soetaert & Herman, 2008). Graphicons serve as an easier and more intuitive way of observing carbon flow interactions between organisms, using differential equations which mathematically describe biological and behavioural interactions in a simplified manner over a pre-set time period (Richter et al., 2019). Depending on the parameters, state variables, behaviours and possible inhibitions, the code can be upgraded to output graphic interpretations of various scenarios, with the goal of elucidating trophic positions of living organisms involved in this ecological niche (de Vries & Caruso, 2016). Utilising different data sources and methods, such as biomarker studies coupled to stable isotope labelling techniques and morphological studies, in order to parametrise and reconstruct a food web is crucial for its accuracy. Food webs are considered to be limited representations of actual ecosystems, both due to constraints of dynamic differential equation modelling, and experimental and scientific understanding of processes which occur in real time. However, simplifications in terms of models are still an invaluable and irreplaceable resource in reaching a better understanding of ecosystems unseen to the naked eye (Pimm et al., 1991).

This study was incentivised by a need for better understanding of roles of biota in mushroom compost. Available literature focuses on trophic and behavioural interactions of the biological participants in soil networks, but detailed work on artificial decomposing environments is very scarce. Furthermore, unanswered questions

persist surrounding nutrients left unused in spent compost after mushrooms are harvested. Therefore, trophic interactions were evaluated through a modelling approach, where the goal was building a prototype food web model which would better explain trophic roles and forcing behaviours of participants involved. For this purpose, stable isotope analysis was performed on nematodes, mostly as an attempt to elucidate trophic positioning of nematodes in the compost food web, as well as to further understand preferential nutrition sources. PLFA biomarker studies were likewise performed and served as validation data for the built model, through an input of real-life, measured experimental values on fungi and bacteria present in the environment. The food web model was built for two scenarios to monitor carbon flow between bacteria, fungi, *A. bisporus*, sugars, compost and the atmosphere: the total carbon compost food web, intended as a general overview of carbon flow in normal compost settings between individual compartments, and the ^{13}C-glucose tracer supplemented compost food web, which dynamically traced the label uptake across compartments.

Methods

Experimental setup

All samples used in this work were collected from a previously set incubation experiment at Utrecht University. In short, 10 x 10 cm Petri dishes were prepared with 45 g of PII-end compost (CNC Grondstoffen©), inoculated with 10 grains of spawn (1.5% of the total wet weight) and duplicated for each sampling time point. ^{13}C-labeled glucose (Cambridge Isotope Laboratories, D-Glucose U-13C6, 99%) was added to the cultures at the start of the incubation. In addition, 20 grams of casing was added after the full colonization of the compost (**Figure 2**, day 14). The spawn run (day 0 to 21) was carried out at 22°C and 80% RH, while mushroom formation was induced by venting at 18°C and 80% RH (day 21 to 30). Destructive sampling was carried out at 0, 7, 14, 21 and 30 days of incubation, where 5 grams of compost and 5 grams of casing were collected for DNA extraction from the duplicates and stored at -20^{0}C, while the rest of the substrate was used for nematode extractions. Duplicates with ^{12}C-glucose were set in parallel as controls for each sampling point.

Nematode population study

Nematode extractions

Nematode extractions were performed on a total of 40 samples (**Figure 2**). Treatments on which extractions were performed were L- A+ (unlabelled environment containing casing and PIII-compost which had *A. bisporus* present), L+ A+ (environment with added ^{13}C-glucose containing casing and PIII-compost which had *A. bisporus* present) and L+ A- (environment with added ^{13}C-glucose containing casing and PII-compost which did not have *A. bisporus* present).

In total, duplicates were extracted from the casing and compost of the L- A+ treatment at each sampling time point (14, 21 and 30 days of the experiment), with additional two samples taken from compost at 30 days. Triplicates were extracted from the casing and compost of the L+ A+ treatment at each sampling time point. Duplicates were extracted from the casing and compost of the L+ A- treatment at each sampling time point, except at 30 days, as the lack of a presence of mushroom didn't yield mushroom formation.

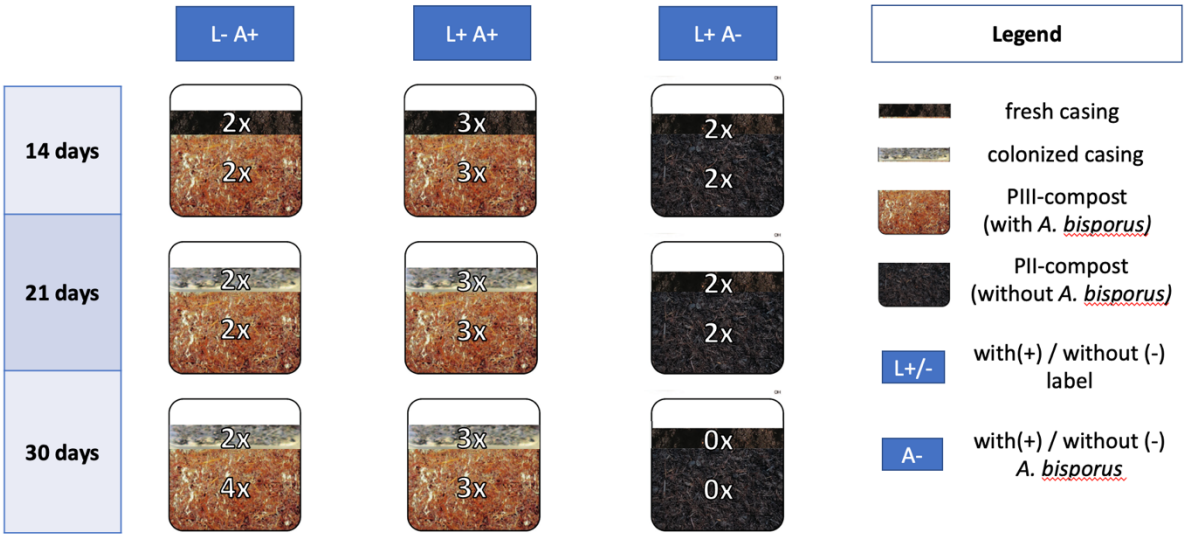

Figure 2: *Schematic representation of the experimental setup, outlining the nematode extraction procedure.*

Various tests were previously performed at NIOO-KNAW to evaluate which nematode extraction technique was more suitable for compost and casing. The substrates tested were PII compost, PIII compost, casing and PIII compost with added casing. The best results were obtained with misting over the course of 70 hours (Seinhorst, 1950), which was the method used on the samples in this work. In short, the compost was placed on mesh in a funnel in a closed chamber and sprayed at intermittent times with water mist. The nematodes were collected in a tube at the base of the funnel. The resulting solution was concentrated through centrifugation and finally suspended in 10mL of 75% molecular grade ethanol (Merck, Ethanol vr mol. biologisch suprapur 100%). The samples were preserved in glass vials at 4^{0}C.

Nematode counts

Nematode populations were counted for each sample as follows. Samples were transferred from their initial glass vial onto a sterile Petri dish, which was placed under a dissecting microscope (Nikon SMZ800, magnification 1.0 – 6.3x). Nematodes were counted and transferred to a clean 4 mL glass vial, using needles or Pasteur pipettes. During this process, nematodes were cleaned in fresh 75% ethanol in the attempt to remove as much debris as possible. All nematodes were transferred into the smaller vials, upon which the vial was labelled and used as a further working sample. For the purpose of calculations, counted nematodes were normalised per weight of the substrate, and per volume of the substrate. Visuals can be found in the Appendices (**Appendix A**).

Visual analysis and nematode morphology

Optical microscopy observations

Temporary samples were prepared on laboratory microscope slides. A drop of 75% ethanol was added onto a microscope slide, into which a single nematode would be placed using a needle. Each slide carried no less than 3 and no more than 5 nematodes, in order to prevent overlap. Positioning was checked under the microscope, after which a cover slide was carefully positioned on top. The cover slide was sealed with clear nail varnish, dried, and additionally sealed with Parafilm across the outermost edges. Long-term samples were prepared similarly, with the difference of using a fixative solution (4% formaldehyde and 0.5% glycerol) instead of 75% ethanol. 10 mL of the fixative solution were prepared, consisting of 9 mL 8% formaldehyde (Electron Microscopy Sciences, Paraformaldehyde 8% Aqueous Solution, EM Grade), 1 mL glycerol (VWR, Glycerol 99+%, Alfa Aesar) and 10 mL of MilliQ water.

Nematode rehydration

Nematode rehydration was performed utilising DESS solution and a rehydration protocol which previously saw success in rehydrating nematodes stored in up to 95% ethanol (Naem et al., 2010).

DESS is an abbreviation alluding to the components of the solution – dimethyl sulphoxide (Sigma-Aldrich, DMSO 99,9%, 20% v/v), disodium EDTA (Sigma-Aldrich, Ethylenediaminetetraacetic acid), and saturated NaCl (Merck, Sodium chloride). Final DESS solution (10 mL) was created using 2 mL DMSO, 3 mL water, 5 mL 0.25 M disodium EDTA and saturated with 3.5 g NaCl. Samples were transferred from 75% ethanol into DESS solution for 24, 48 and 72 hours. Immediately following immersion in DESS solution, nematodes were transferred into pure water for 5, 30 and 60 minutes, respectively, after which half of the samples were immediately observed under a dissecting microscope, and half of the samples were prepared into temporary and long-term microscope slides for observation under a compound microscope with an equipped imaging system (Leica DM2500 LED; Leica MC170 HD, magnification 10 – 100x).

Nematode staining

Staining was done as a wet mount preparation and involved taking up several drops of the original sample with a Pasteur pipette, in which besides nematodes, various straws and debris can be found. The drops were placed on a microscope slide and held over a Bunsen burner for 5-10 seconds to heat-fixate. Several drops of the dye of choice, iodine (Thermo Scientific™, Iodine, 99%+), fuchsin (Thermo Scientific™, Basic Fuchsin), or crystal violet (Thermo Scientific™, Crystal Violet) were placed on the entire surface of the dried sample for 5, 10 and 15 minutes, respectively. After dye

immersion, the sample was washed off with a decolorising agent and pure water before observation under an inverted microscope and a dissecting microscope.

Scanning electronic microscope (SEM) observations

Three batches of nematodes were prepared for the scanning electron microscope in order to better observe the details of nematode mouthparts. One to two nematodes were mounted on a nickel disk, to which they were attached to by their ends using very thin strips of copper tape. The nickel disk was further mounted on an SEM pin mount with double-sided carbon tape on top. The prepared sample was fully coated with a coat of mixed platinum and gold particles in order to make the biological sample electroconductive. The samples were imaged using a Benchtop SEM (JEOL JCM-6000) at high-vacuum, secondary electron images (SEI), 10 kV, 200x magnification settings.

Statistical analysis

Nematode counts, internematode variability of $\delta^{13}C$ values and nematode ^{13}C excess values were tested for significance ($p < 0.05$) among different sampling timepoints, soil types, and presence of ^{13}C label. Two-way analysis of variance (ANOVA), base 10 log-transformation, non-parametric Kruskal-Wallis one-way analysis of variance and Tukey's honest significant difference post-hoc test were used for data analysis. The data was tested for normal distribution before running statistical analyses, and non-parametric tests were applied to non-normal distributions. Analysis was run in R, using the **stats** package (Team, 2013). Due to the non-normality of the data, Kruskal-Wallis non-parametric statistical test was performed on all calculations concerning $\delta^{13}C_{VPDB}$ values.

Stable isotope analysis

Bulk analysis via elemental analyser coupled with an isotope ratio mass spectrometer (EA-IRMS)

Elemental analyser isotope ratio mass spectrometer (EA-IRMS, Thermo Delta V) was used to ascertain bulk $\delta^{13}C$ values of nematode samples. Sample trays for the EA-IRMS consisted of prepared standards, samples and blanks. Three samples were preselected and extracted from refrigerated storage vials onto a sterile Petri dish using Pasteur pipettes. Nematodes were individually collected from Petri dishes using needles under a dissecting microscope into clean, pre-weighed tin cups (4 x 6 mm, with tin cup size used generally depending on sample weight). About 50 nematodes, weighing in total from 26 to 31 micrograms, were collected into each of the three tin cups. Four tin cups were filled with the plant matter from the same three preselected samples. The tin cups were inserted into a multi-well tray, which was left for at least 48 hours to fully dry in the desiccator to eliminate traces of ethanol and water. After drying,

the filled tin cups were pinched closed at the opening and folded over several times inwardly until coiled into an approximately 1.5 mm diameter sphere. Three tin cups were filled with about 20 micrograms nicotinamide standard (containing 59.01% carbon (Foucreau et al., 2013)), four tin cups were filled with about 850 micrograms in-house sediment standard "GQ" (a graphite-quartzite from Naxos, Greece, containing 0.52% carbon (Broekmans et al., 1994)), three tin cups were filled with about 15 micrograms IAEA-CH-7 or polyethylene foil standard ($\delta^{13}C = -32.151 \pm 0.050‰$ relative to Vienna Pee Dee Belemnite (Coplen et al., 2006)) and folded over, in the same manner as the samples. Three tin cups were left unfilled and similarly folded over in order to serve as blank measurements. The folded spheres were placed into the wells of the well tray and a separate spreadsheet was filled out demarking the corresponding well tray position, content of the tin cups, and weight of the tin cups together with the sample.

Laser ablation coupled with an isotope ratio mass spectrometer (LA-IRMS)

Laser ablation coupled with continuous-flow mode isotope ratio mass spectrometer (LA-IRMS) is a Utrecht University in-house experimental setup combining laser ablation, nano combustion gas chromatography and isotope ratio mass spectrometry. The technique provides a viable alternative for $\delta^{13}C$ measurements of samples deemed too small for the EA-IRMS, or those where the amount of material is a limiting factor (Moran et al., 2011). The setup of the combustion device is based on a continuous gas flow system, where an ablation chamber is placed under a 193 nanometre, deep ultra-violet argon-fluoride exciplex laser beam (Basting & Marowsky, 2005) (COMPex 102; Lambda Physik, Göttingen, Germany), with a direct online link to the isotope ratio mass spectrometer (Delta V Advantage; ThermoFinnigan, Bremen, Germany) via a GCIII combustion interface (ThermoFinnigan, Bremen, Germany) (van Roij et al., 2017). The ablation chamber is custom-made for the experimental setup, consisting of a metal cylinder which is hollow in the centre for the placement of samples (van Roij et al., 2017). A nickel disk which carries the specimen is positioned on a screw-top pedestal and locked against the ablation chamber by inserting the pedestal carrying the sample from below. Nickel disks are used as a background surface area for sample ablation due to the resistance of nickel to being ablated with various frequencies of laser pulsation (Semerok et al., 1999), which prevents a skew of measured values.

Nematodes were acquired from pre-cleaned working samples derived from original nematode extraction samples for the LA-IRMS analysis. 1 to 7 nematodes were measured per pre-selected sample as follows. From L+ A+ treatment, 6 casing samples and 6 compost samples (sampled at day 14, day 21 and day 30) were selected for measurements, with casing and compost samples being sourced from the same replicate. Likewise, from L- A+ treatment, 6 casing samples and 6 compost samples (sampled at day 14, day 21 and day 30) were selected for measurements. Preselected samples were extracted from refrigerated storage vials onto a Petri dish using Pasteur pipettes, and nematodes were individually collected under a dissecting microscope onto clean nickel disks (6 mm diameter), concave side up. Depending on the size of

nematodes, a minimum of one nematode and a maximum of five were placed on one nickel disk. Nematodes were positioned to be centred on the disk as much as possible to avoid sample loss due to field of vision differences. During the collection of nematodes, they were cleaned of plant material and debris, either in a wash of clean 75% ethanol, or by mechanically removing debris using needles. The samples were placed in a desiccator for a minimum of 48 hours to fully dry out the ethanol and water lingering on the nematode specimens. After drying, the stacked nickel disks containing the sample were carefully taken out, inspected under a dissecting microscope for any changes in the positioning of nematodes and pressed with a hydraulic press at the pressure of 1 tonne. Higher pressure is not recommended, as it flattens out the disk, rendering it incapable of fitting into the ablation chamber. After pressing, the disks were separated and the one containing the nematodes was supplemented with a small amount (2 mm x 2 mm) of the IAEA-CH-7 polyethylene foil standard ($\delta^{13}C = -32.151 \pm 0.050‰$) and loaded into the ablation chamber from below, while the empty one was discarded for cleaning. The ablation chamber was closed and positioned under a connected optical microscope and the ArF laser beam for ablation procedure. Nitrogen was set at 1.5 bars. After pre-heating, the laser tube would be closed off and ran for 5 minutes at 10 Hz. The energy level was tested after the warm-up procedure was completed, by running the laser at 2 Hz, allowing the adjustment of voltage based on the energy needed to properly ablate the sample. For the standard, the energy was calculated to be 100 mJ, with the sample generally needing 20 mJ energy beam for proper ablation. The laser would shoot the standard one to four times for several seconds, after which material was shot, likewise each time for several seconds, over the course of the 70 minutes of the run. Between measurements, various waiting times were employed, with a goal to reduce $\delta^{13}C$ to background levels. Peaks which shared elevated baselines were discarded, as they would present wrong values. Post-measurement, peaks were integrated with Isodat 3.0 Thermo Fischer software, where values were checked for elevated baselines and twinned peaks, after which the data was extracted to Excel for further processing.

Isotope analysis

Isotope analysis was performed on nematodes using the LA-IRMS technique, which gives measured output in the form of $\delta^{13}C_{VPDB}$ for each laser hit. The formula for this delta notation is (Urey, 1948):

$$\delta^{13}C_{VPDB} = \frac{R_{sample}}{R_{VPDB}} - 1 \qquad (2.1)$$

where δ expresses the abundance of ^{13}C over ^{12}C (R_{sample}) in a sample, relative to the abundance of ^{13}C over ^{12}C (R_{VPDB}) in the Vienna Pee Dee Belemnite isotopic standard. R_{VPDB} is the international standard for carbon, with an isotope ratio of $^{13}C/^{12}C = 0.0112373$.

Using these measured values, ratios were calculated for each laser hit in both labelled and unlabelled nematodes, using the formula (Hayes, 2004):

$$R = \left(\frac{\delta^{13}C}{1000} + 1\right) * R_{VPDB} \quad (2.2)$$

Fractions were calculated in both labelled and unlabelled nematodes, using the formula (Hayes, 2004):

$$F = \frac{R}{(R+1)} \quad (2.3)$$

where R is the previously calculated ratio.

Unlabelled nematodes were used to derive the background ^{13}C fraction. Fractions were averaged in order to get an average background fraction. These average fractions were subtracted from the fractions of the corresponding labelled samples. The resulting value represent the excess of ^{13}C over the background. Negative excess values were considered to be 0:

$$Excess = F_{L+sample} - \overline{F_{L-sample}} \quad (2.4)$$

Excess was also calculated from pre-existing PLFA biomarker datasets for the purposes of validating the food web model. Data points for excess were averaged to get average excess ^{13}C per compartment in mmol/gram compost.

Phospholipid-derived fatty acid (PLFA) biomarker studies

Extraction

The samples were immediately freeze-dried and sealed after sampling. A small quantity of each freeze-dried sample (1-2 grams) was homogenized using a bead beater (Retsch MM200) and stored at -20^{0}C. The original purpose of this batch was to preserve the compost that was used for DNA extractions. The larger batch of samples had been kept sealed at room temperature. In order to extract PLFAs, solid samples of casing and compost were milled to a fine, powdery, homogenous consistency. Larger quantities of freeze-dried compost (3-4 grams) samples were homogenised using a laboratory pulverizing mill (Herzog HP-MA/HP-PA) and casing samples were milled by hand, using a mortar and pestle.

The extractions were completed according to a modified Bligh and Dyer method (Bligh & Dyer, 1959) which includes three distinctive steps (De Kluijver et al., 2021). In the first step (**Appendix B, Figure 30**), milled casing or compost samples were submerged in a solution of MeOH:CH_2Cl_2:P-buffer with a 10:5:4 mixing ratio, sonicated for 10 minutes and centrifuged for 3 minutes, after which the resulting supernatant was

collected. The procedure was repeated three times in total, after which equal parts of P-buffer and dichloromethane (DCM) were added to collected supernatants in order to induce phase separation. The resulting DCM phase was collected into pre-weighed vials, the procedure repeated four times in total, and the vials dried under nitrogen flow.

The second step involved silica column chromatography (**Appendix B, Figure 31**), where the total lipid fraction sample was passed through a column of activated silica in order to separate apolar, neutral and polar lipids via elution in DCM, acetone, and methanol respectively. The methanol-eluted fraction was collected and dried to obtain the polar lipids.

The third and final step (**Appendix B, Figure 32**) involved adding toluene:methanol (1:1, v:v), methanolic NaOH and C19:0 fatty acid methyl ester (FAME) standard to the vials containing dried methanol-eluted polar lipid fraction. Methylation reaction occurred for 30 minutes at 37°C and was stopped with the addition of acetic acid and Milli-Q water. Hexane was subsequently added to the sample with the resulting separated layer being collected and dried under nitrogen flow for a total of three repetitions. In order to ensure removal of any leftover impurities, the dried sample was eluted with DCM through a centimetre thick AlOx and Na_2SO_4 column and fully dried. In order to be injected into the GC and GC-IRMS, the polar lipid fractions in the samples need to be suspended in hexane along with C12:0 internal standard.

Analysis

PLFA samples were analysed using gas chromatography (GC, Hewlett-Packard HP 6890 Series GC System with an Agilent Chrompack CP-Sil 5 CB capillary non-polar column) and gas chromatography isotope ratio mass spectrometry (GC-IRMS, Agilent 8890 GC System combined with Elementar GC5 interface and Elementar isoprime visION IRMS).

GC was used for calculation of PLFA concentrations, and chiefly served to validate extraction procedures as correct. GC-IRMS was used to obtain isotopic values of the samples through quantification of ^{13}C enrichment present in the PLFAs and to calculate the absolute ^{13}C uptake in each PLFA. The total uptake was calculated from PLFA concentrations and served for comparison against active biomass. Therefore, the output results of the GC-IRMS allowed for the calculation of bacterial and fungal biomass, as well as excess by using averaged ratios from unlabelled samples as sources of background values for labelled samples according to sampling time.

PLFAs were identified based on retention times from raw output files by comparing them to those of the fatty acid methyl ester (FAME) standards (Supelco 37 Component FAME Mix) and equivalent chain lengths (ECL) based of the retention times of C12:0, C16:0 and C19:0. The list of PLFAs utilised in the calculations for particular biota can

be found in **Table 1**. PLFA concentration analysis and isotope ratio results were analysed in R, using the **Rlims** package, which processes GC-IRMS lab analysis results (Soetaert et al., 2015).

Table 1: PLFA biomarkers corresponding to particular food web model compartments.

Compartment	PLFA biomarker	Reference
BACTERIA	i-C14:0, i-C15:0, i-C17:0, ai-C15:0, ai-C17:0, C16:1w7, C18:1w7c, cy-C17:0, cy-C19:0	(Ahlgren et al., 1992); (Bååth et al., 1992); (Bowman et al., 1993); (Dijkman et al., 2010); (Francisco et al., 2016); (Frostegård et al., 1993); (Gillan et al., 1988); (Kroppenstedt, 1985); (Nichols et al., 1985); (O'Leary et al., 1988); (Vestal & White, 1989); (Willers et al., 2015); (Zelles, 1997); (Zelles, 1999)
FUNGI	C18:2w6c	(Federle et al., 1986); (Stahl & Klug, 1996); (Vestal & White, 1989)
A.BISPORUS	C18:2w6c	(Frostegård & Bååth, 1996); (Zelles, 1999)

Compost food web model design

The model used for the reconstruction of the compost food web has been adapted from the nutrient-phytoplankton-zooplankton-detritus (NPZD) marine biogeochemical model (Meire et al., 2013), which was used to track carbon flow through the food web compartments.

The compost food web model makes use of the **deSolve** package (Soetaert et al., 2010) in order to solve differential equations, **shiny** package (Chang et al., 2015) to build an interactive user interface which allows real-time reactive change in graphical outputs and **shinyWidgets** (Perrier et al., 2019) for creating user-friendly custom input controls to manipulate applications built with the shiny package.

The biogeochemical theoretical basis of the model is described in the following sections, complete with the corresponding data, both sourced and calibrated. Full code is available in the Appendices (**Appendix C**).

Total carbon food-web model

In this model, naturally abundant, ^{12}C isotope of carbon was the main nutrient and model currency. The state variables are BACTERIA, FUNGI, A. BISPORUS, SUGARS, COMPOST AND CO_2. The total amount of carbon distributed in the food web came from compost (45 grams, 30% carbon) and readily available sugars.

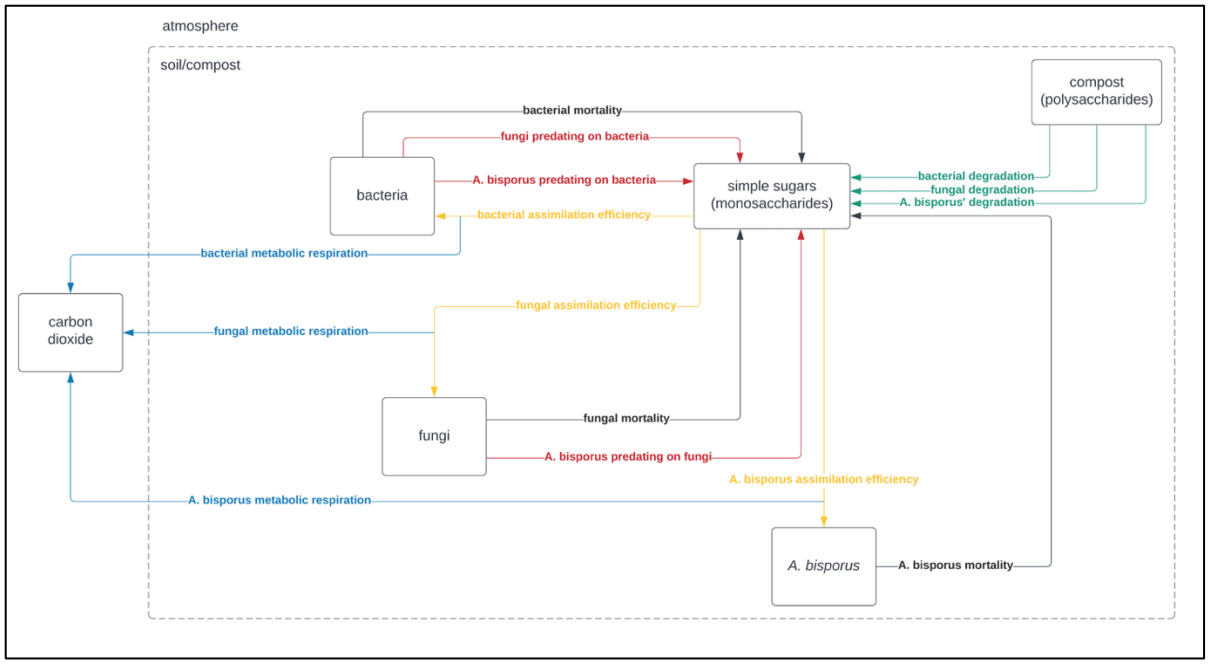

Figure 3: Conceptual model diagram for the total carbon food-web model.

Bacteria, fungi and *A. bisporus* release monosaccharides by degrading recalcitrant polysaccharides from compost, adding into the total sugars pool. From the pool of sugars, bacteria, fungi and *A. bisporus* uptake carbon to serve as food, a certain percentage of which is integrated into the overall biomass and used for growth and metabolism, while the rest is respired from the compost domain (where all important processes take place) into the atmosphere domain in the form of CO_2 (Vos et al., 2017).

Together with direct uptake of simple carbohydrates, the organisms display predation and inhibition behaviours towards one another. Bacteria are indirectly and directly predated on by fungi and *A. bisporus*, inhibiting their biomass growth, while *A. bisporus*, likewise indirectly and likely enzymatically, predates upon fungi. Predation and inhibition behaviours, together with susceptibility to natural organism mortality, are modelled to cyclically add to the total sugar pool. Mortality is modelled as a linear function of biomass, in comparison to commonly used quadratic function of biomass, because mortality is lower in controlled environments (**Figure 3**). The full list of mass balance equations governing these behaviours can be found in **Table 2.**

Table 2: Mass balance equations for the total carbon scenario.

$$\frac{dBACTERIA}{dt} = Ef.bac * BacUptake - FunPredationBac - BispPredationBac - MortalityBac$$

$$\frac{dFUNGI}{dt} = Ef.fun * FunUptake - BispPredationFun - MortalityFun$$

$$\frac{dA.BISPORUS}{dt} = Ef.bisp * BispUptake - MortalityBisp$$

$$\frac{dSUGARS}{dt} = BacDegradation + FunDegradation + BispDegradation - BacUptake - FunUptake - BispUptake + FunPredationBac + BispPredationBac + BispPredationFun + MortalityBac + MortalityFun + MortalityBisp$$

$$\frac{dCOMPOST}{dt} = -BacDegradation - FunDegradation - BispDegradation$$

$$\frac{dCO2}{dt} = (1 - Ef.bac) * BacUptake + (1 - Ef.fun) * FunUptake + (1 - Ef.bisp) * BispUptake$$

Data used for the parametrisation of the model has partially been sourced from pre-existing literature which concerns similar ecological niches and similar organisms and partially from existing experimental data done beforehand in the same project. Parameters which were impossible to source have been calibrated using the model itself and fitted to empirical projections and pre-existing outcomes. The full list of rate expressions can be found in **Table 3**. The full list of parameters, as well as their values and sources, can be found in the Appendices (**Appendix D**).

Table 3: Rate expressions for processes between carbon compartments.

$$BacDegradation = k.deg.bac * BACTERIA$$
$$FunDegradation = k.deg.fun * FUNGI$$
$$BispDegradation = k.deg.bisp * A.BISPORUS$$
$$BacUptake = k.bac.uptake * \frac{SUGARS}{(SUGARS + kSUGARS.bac)} * \frac{kBISPORUS}{(A.BISPORUS + kBISPORUS)} * BACTERIA$$
$$FunUptake = k.fun.uptake * \frac{SUGARS}{(SUGARS + kSUGARS.fun)} * \frac{kBISPORUS}{(A.BISPORUS + kBISPORUS)} * FUNGI$$
$$BispUptake = k.bisp.uptake * \frac{SUGARS}{(SUGARS + kSUGARS.bisp)} * \left(\frac{1 - A.BISPORUS}{MAX.A.BISPORUS}\right) * A.BISPORUS$$
$$FunPredationBac = k.fun.pred.bac * BACTERIA * FUNGI$$
$$BispPredationBac = k.bisp.pred.bac * BACTERIA * A.BISPORUS$$
$$BispPredationFun = k.bisp.pred.fun * FUNGI * A.BISPORUS$$
$$MortalityBac = k.bac.mort * BACTERIA$$
$$MortalityFun = k.fun.mort * FUNGI$$
$$MortalityBisp = k.bisp.mort * A.BISPORUS$$

^{13}C carbon flow food web model addition

In these experiments, ^{13}C-enriched glucose was added to the compost as a one-off injection to the pool of otherwise predominantly naturally abundant ^{12}C monosaccharide carbon (**Figure 4**). After the addition of glucose, the compost was incubated in conditions which mimic the cropping process. Over the course of a month and a half, the surplus ^{13}C slowly begun to be taken up by the living biomass in the compost. It was assumed that as the time of the experiment progresses, surplus ^{13}C would accumulate in the biomass of the living organisms that uptake it. The second trophic step organisms, which do not consume labelled or unlabelled simple sugars but feed on organisms that do, consumed the label through incorporation of biomass labelling of smaller organisms.

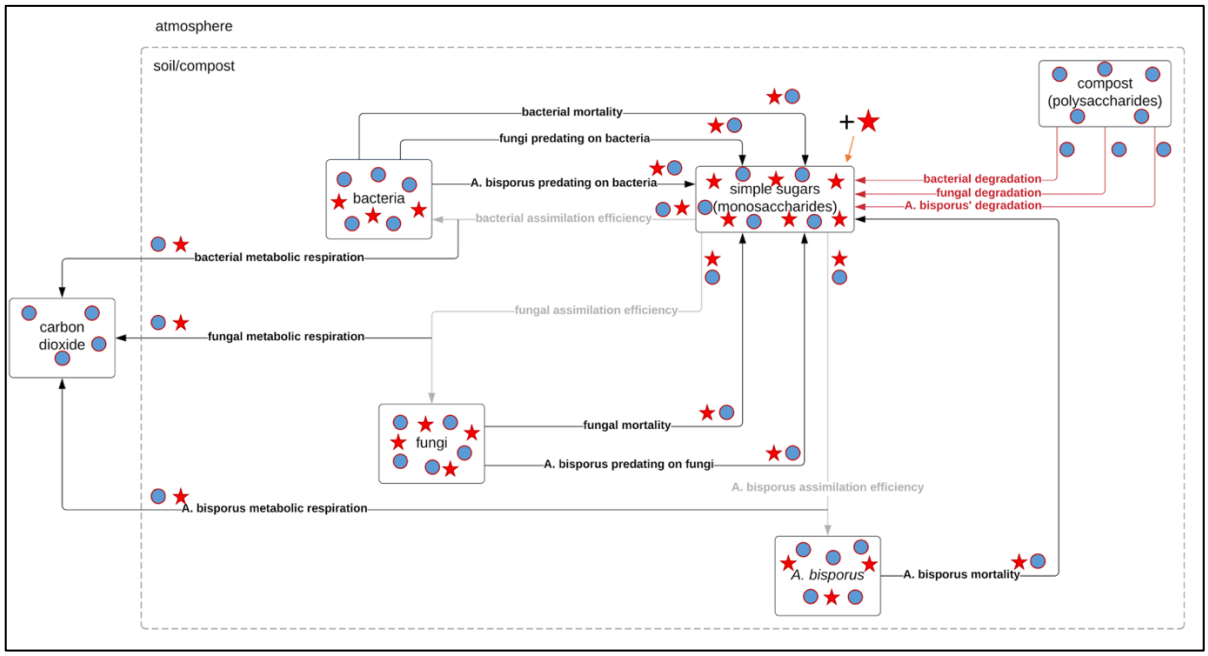

Figure 4: Conceptual model diagram of the ^{13}C-tracer tracking addition. The tracer isotope is added into the pool of simple sugars (denoted with a star). Bacteria, fungi and *A. bisporus* uptake the tracer isotope through assimilation of sugars, and incorporate it into their biomass, along with developing unlabelled biomass (denoted with a circle). Upon dying, respiration and predation, the label gets propagated through the entire system.

The ^{13}C carbon flow in the food web was tracked using the calculation of excess ^{13}C, which was sourced from PLFA extractions. Excesses are calculated from ratios and fractions, which were calculated from biomarkers corresponding to particular organisms, after which they were summed up to get the total excess value for a particular compartment.

State variables for the ^{13}C model addition are BACTERIA.13C, FUNGI.13C, A.BISPORUS.13C, SUGARS.13C and CO2.13C. The variables serve to aid tracking of the incorporation of ^{13}C label by a particular organism. Additional mass balance equations used for the ^{13}C model addition can be found in **Table 4**, as they are amended

with amount-of-substance fraction rate expressions of the source, which can be found in **Table 5**. The full list of parameters can be found in the Appendices (**Appendix E**). Other mass balance equations and rate expressions remain valid and unchanged, unless stated otherwise.

Table 4: Mass balance equations, updated for tracer uptake tracking through the compost network.

$\frac{dBACTERIA.13C}{dt} = Ef.bac * BacUptake * x13C.sugars - FunPredationBac * x13C.bac - BispPredationBac * x13C.bac - MortalityBac * x13C.bac$
$\frac{dFUNGI}{dt} = Ef.fun * FunUptake * x13C.sugars - BispPredationFun * x13C.fun - MortalityFun * x13C.fun$
$\frac{dA.BISPORUS}{dt} = Ef.bisp * BispUptake * x13C.sugars - MortalityBisp * x13C.bisp$
$\frac{dSUGARS}{dt} = BacDegradation + FunDegradation + BispDegradation - BacUptake * x13C.sugars - FunUptake * x13C.sugars - BispUptake * x13C.sugars + FunPredationBac * x13C.bac + BispPredationBac * x13C.bac + BispPredationFun * x13C.fun + MortalityBac * x13C.bac + MortalityFun * x13C.fun + MortalityBisp * x13C.bisp$
$\frac{dCO2}{dt} = (1 - Ef.bac) * BacUptake * x13C.sugars + (1 - Ef.fun) * FunUptake * x13C.sugars + (1 - Ef.bisp) * BispUptake * x13C.sugars$

Table 5: Rate expressions for tracer uptake.

$x13C.bac = \frac{BACTERIA.13C}{BACTERIA}$
$x13C.fun = \frac{FUNGI.13C}{FUNGI}$
$x13C.bisp = \frac{A.BISPORUS.13C}{A.BISPORUS}$
$x13C.sugars = \frac{SUGARS.13C}{SUGARS}$
$x13C.co2 = \frac{CO2.13C}{CO2}$

Results

Results of method comparisons for nematode extraction

In both phase II-end and phase III-end compost, no nematodes were extracted after 14 or 40 days of incubation with any of the methods used (**Table 6**). Conversely, nematodes were extracted from casing samples at both sampling times, with all methods, and displayed a 50% decrease in numbers over time. A similar trend was noticed in PIII compost with added casing, where nematodes were likewise extracted using all available methods at both sampling times, however, with a nearly 900% increase in nematode numbers.

Table 6: Results of nematode extraction method testing performed on various substrate types.

	Nematode count (number per gram substrate)			
Incubation time	PII compost	PIII compost	Casing	PIII compost + casing
14 days	none	none	6	1.5
40 days	none	none	3	14.5

Effect of incubation treatments on nematode counts

Nematode populations were fully counted for all extracted samples from all treatments: non-labelled cultures containing *A. bisporus* (L- A+), labelled cultures with *A. bisporus* (L+ A+) and labelled cultures without *A. bisporus* (L+ A-). Counts were then compared to ascertain the effect of different substrates (casing versus compost), the effect of different sampling times (14, 21 and 30 days), and the effect of label addition.

Nematodes were counted in compost and casing samples which had been sampled at day 14, day 21 and day 30 of the experiment, belonging to labelled (L+) and unlabelled (L-) treatments, containing (A+) or not containing (A-) *A. bisporus* (**Appendix F**, **Table 12**). The absolute counts yielded from the direct counting of specimens from extracted samples were divided by the weight of every corresponding sample (**Appendix F**, **Table 13**). Likewise, nematode counts were divided by volume, yielding normalised nematode counts per volume of substrate. Nematode counts normalised per weight were used for further statistical testing.

Substrate type effect on counts

In the L+ A- treatment, lower nematode counts were present in casing than in compost at day 14 (**Figure 5**, light green with red outline). In the same treatment, higher nematode counts were present in casing than in compost at day 21 (**Figure 5**, light orange with red outline).

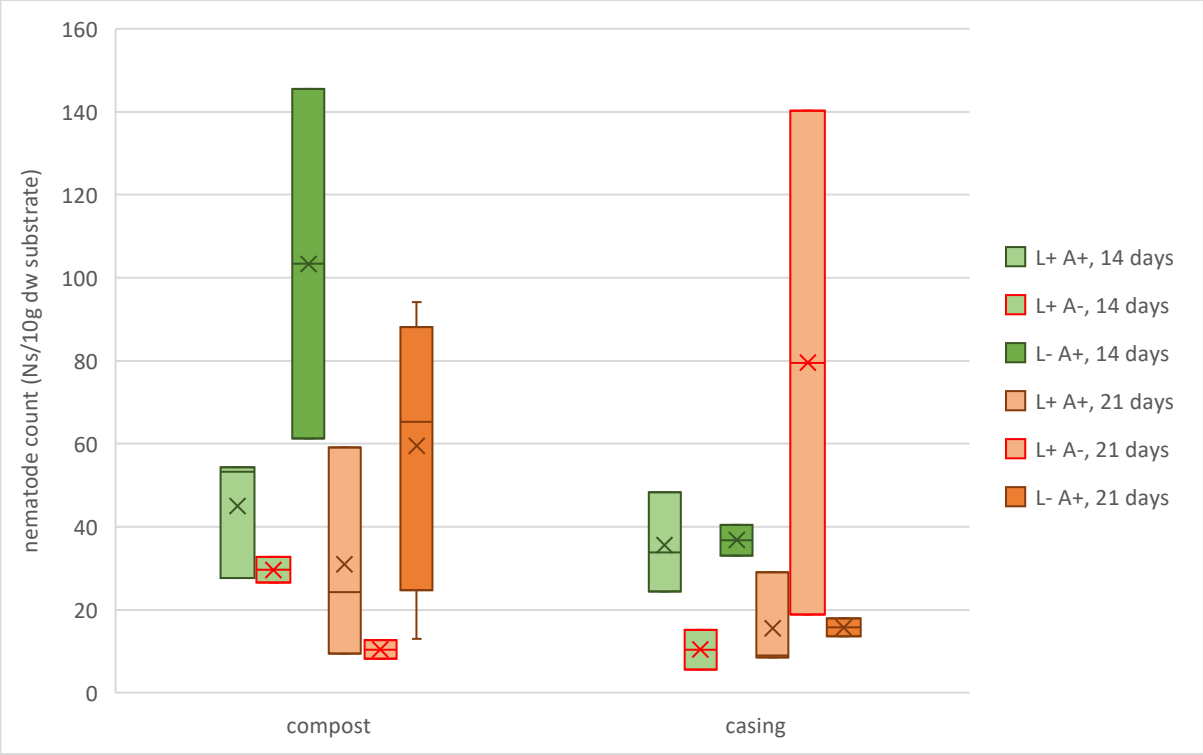

Figure 5: *Comparison of nematode numbers between L- A+, L+ A+ and L+ A- treatments during the first 21 days of the experiment, normalised per substrate weight.* Nematode counts in L- A+ treatment samples (denoted in dark green and dark orange), L+ A+ treatment samples (denoted in light green and light orange), and L+ A- treatment samples (denoted in light green and light orange with a red outline) normalised per 10 grams of compost or casing, respectively.

In the L- A+ treatment (**Figure 6**, dark green, dark orange and dark yellow), nematode counts in casing were, on average, lower at all sampling timepoints than nematode counts in compost, but the difference between the two substrate type treatments was not significant [$F(1, 9) = 1.11409$, $p = 0.318705$]. A similar observation was made for the L+ A+ treatment (**Figure 6**, light green, light orange and light yellow), but the difference between soil type treatments was also not significant [$F(1, 16) = 0.44456$, $p = 0.514429$].

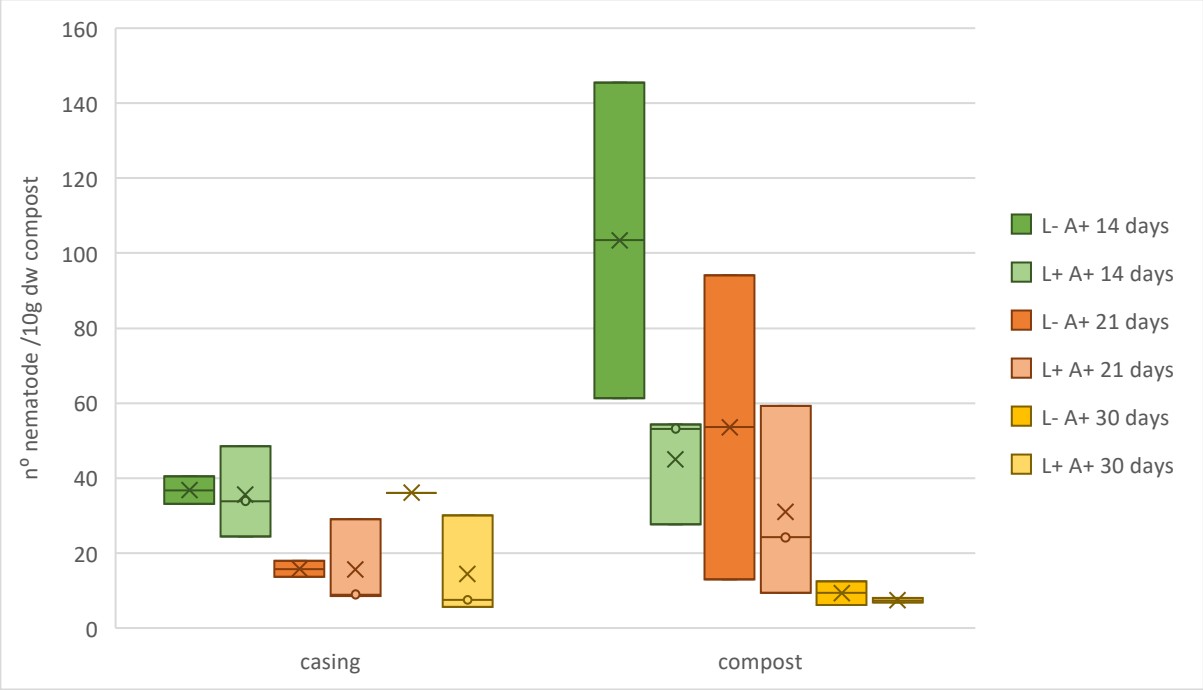

Figure 6: *Number of nematodes in L- A+ and L+ A+ treatments, normalised per substrate weight.* Nematode counts in L- A+ treatment samples (denoted in dark green, dark orange and dark yellow) and L+ A+ treatment samples (denoted in light green, light orange and light yellow), normalised per 10 grams of compost or casing, respectively.

In L- A+ and L+ A+ samples which were normalised per substrate volume (**Figure 7**), similar observations were made, with the only difference being that the number of nematodes in casing and compost were found to be on a similar scale, with nematodes sourced after 14 and after 30 days being more abundant in casing of both labelled and unlabelled treatments than compost counterparts.

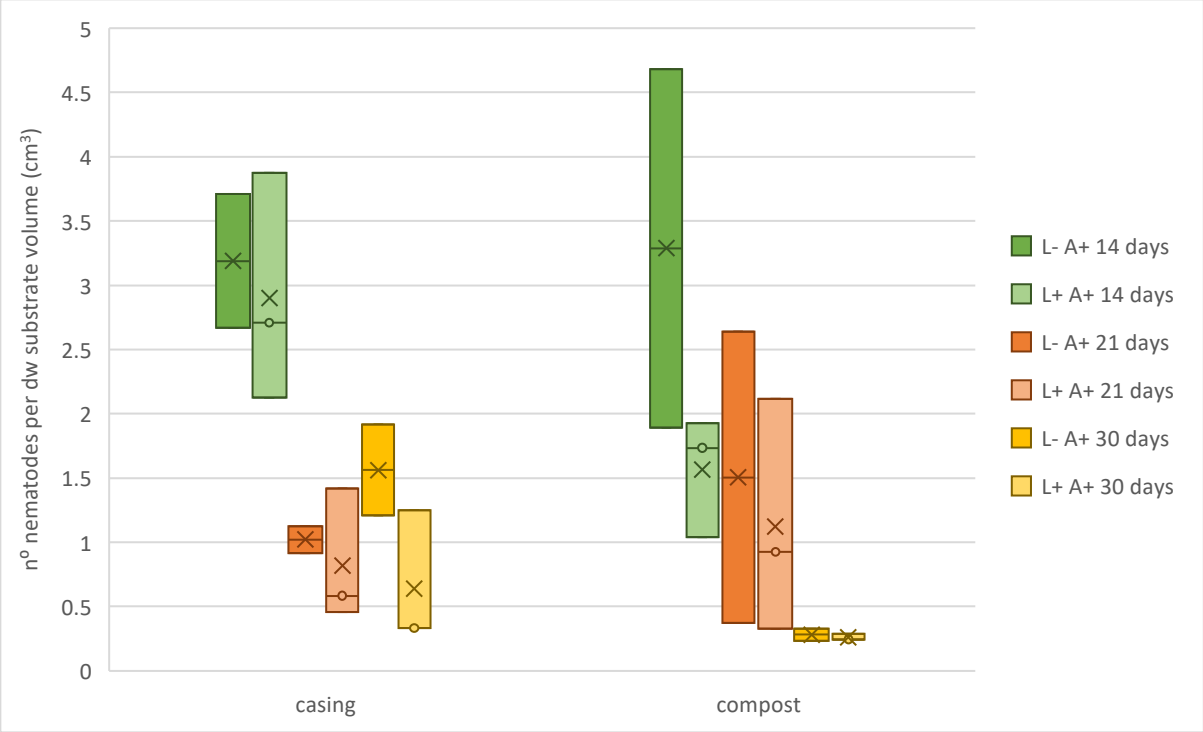

Figure 7: *Number of nematodes in L- A+ and L+ A+ samples normalised per substrate volume.* Nematode counts in L- A+ treatment samples (denoted in dark green, dark orange and dark yellow) and L+ A+ treatment samples (denoted in light green, light orange and light yellow), normalised per volume of sampled compost or casing, respectively.

Sampling time and label addition effect on counts

Comparing the L+ A- treatment with the other two treatments showed that treatments which had *A. bisporus* present had higher and more variable counts of nematodes during the first 14 days than treatments which contained *A. bisporus*, regardless of whether the environment was labelled or unlabelled (**Figure 5**). This trend was similar after 21 days in compost. However, after 21 days in casing, the treatment without *A. bisporus* exhibited very variable and higher counts of nematodes than both labelled and unlabelled counterparts which contained *A. bisporus*.

Nematode counts were observed to decrease in both casing and compost samples, as the time of the experiment progressed. Among compost samples, nematode counts were observed to be generally lower in labelled than unlabelled samples (**Figure 7**). Nematode counts in L- A+ and L+ A+ treatments were found to be significantly different between both sampling timepoints [$F(1, 2) = 5.112$, $p < 0.01$] and labelling treatments [$F(1, 2) = 3.318$, $p < 0.05$]. Tukey's post-hoc Honest Significant Difference test was conducted and showed that the sampling timepoint at day 14 and sampling timepoint at day 30 differed significantly ($p = 0.011$). Other sampling timepoints did not differ significantly. Unlabelled and labelled groups did not differ significantly but showed elements of a trend ($p = 0.07$).

Compost-casing ratio of nematode counts

The values of normalised numbers of nematodes in compost were divided by values of normalised numbers of nematodes in casing for each replicate, respectively. The ratios were averaged and plotted per phase and sampling timepoint. The ratio represented a numeric expression of the number of nematodes in compost samples, compared to the casing samples from the same replicate, at the same sampling time point (e.g. a ratio of 2 would indicate twice as many nematodes in compost than in casing of the same replicate, **Figure** 8).

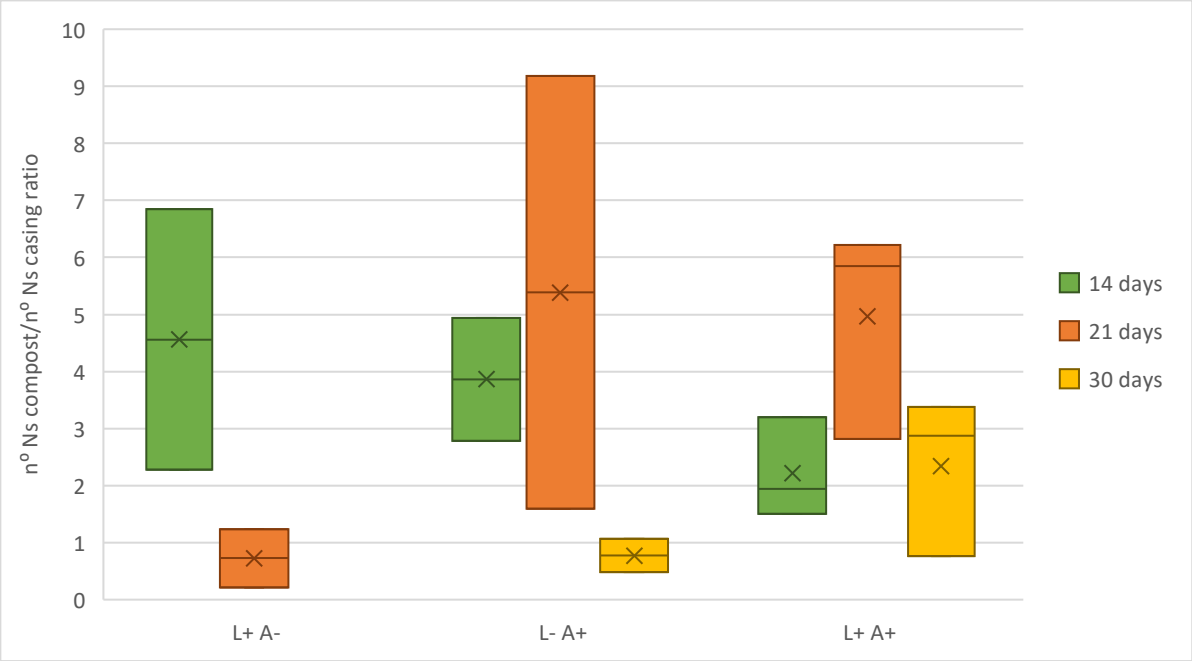

Figure 8: *Compost:Casing ratios for L+ A-, L- A+ and L+ A+ treatments.* Higher compost to casing ratio indicated a higher count of nematodes in the compost sample, rather than in the casing sample, in the same replicate, at the same sampling timepoint. A ratio of 1 indicated an equal number of nematodes, while ratios below 1 indicated a higher count of nematodes in casing sample, than in the respective compost sample counterpart.

The ratio showed that in L+ A- treatment, higher counts of nematodes were found in compost at day 14, than at day 21. In L- A+ treatment, lower counts were found in compost at day 14, peaking at day 21, and lowering considerably after day 30. In the L+ A+ treatment, the trend was similar, with even lower nematode counts found in compost after day 14, peaking similarly high at day 21 as in L- A+ treatment, and lowering again after day 30, though to higher respective counts than in L- A+ treatment. In all cases had with a considerably higher number of nematodes than respective casing sample counterparts.

Visual observations of nematode mouthparts, nematode rehydration and staining

Observations conducted on nematodes and their mouthparts did not yield results which could be utilised for either confirmation of the species, or of their possible feeding habits (**Figure 9**). The observations did not yield results of quality sufficient for certain determination on both dissecting and compound optical microscopes, as well as on the SEM, on all utilised magnifications and settings.

The conducted process of rehydration yielded results on the bodies of the nematodes, mostly on the cuticle, but not on the mouthparts, which were not of sufficient quality for either species or feeding preference determination by the end of the rehydration process. The rehydration process was equally unsuccessful at all conducted lengths of the experiment (**Figure 10**).

The process of biological staining was likewise unsuccessful and did not allow for unequivocal determination of feeding habits or taxa. When the experiment was conducted for 5 minutes, fuchsin had fully stained the detritus, but no nematodes, while the iodine had fully stained thicker plant stems, but no other detritus. Upon conducting the experiment for 10 minutes, both iodine and fuchsin had fully stained all the detritus present. When the experiment was ran for 15 minutes, both iodine and fuchsin had fully stained all the nematodes and all the detritus present. In the case of crystal violet, the dye had stained all nematodes and all detritus, regardless of the duration of the experiment (**Figure 11**).

Photographs of nematodes and nematode mouthparts before and after rehydration (at various durations of the rehydration process) were created on the imaging system equipped to the compound microscope, and can be found in the Appendices (**Appendix G**).

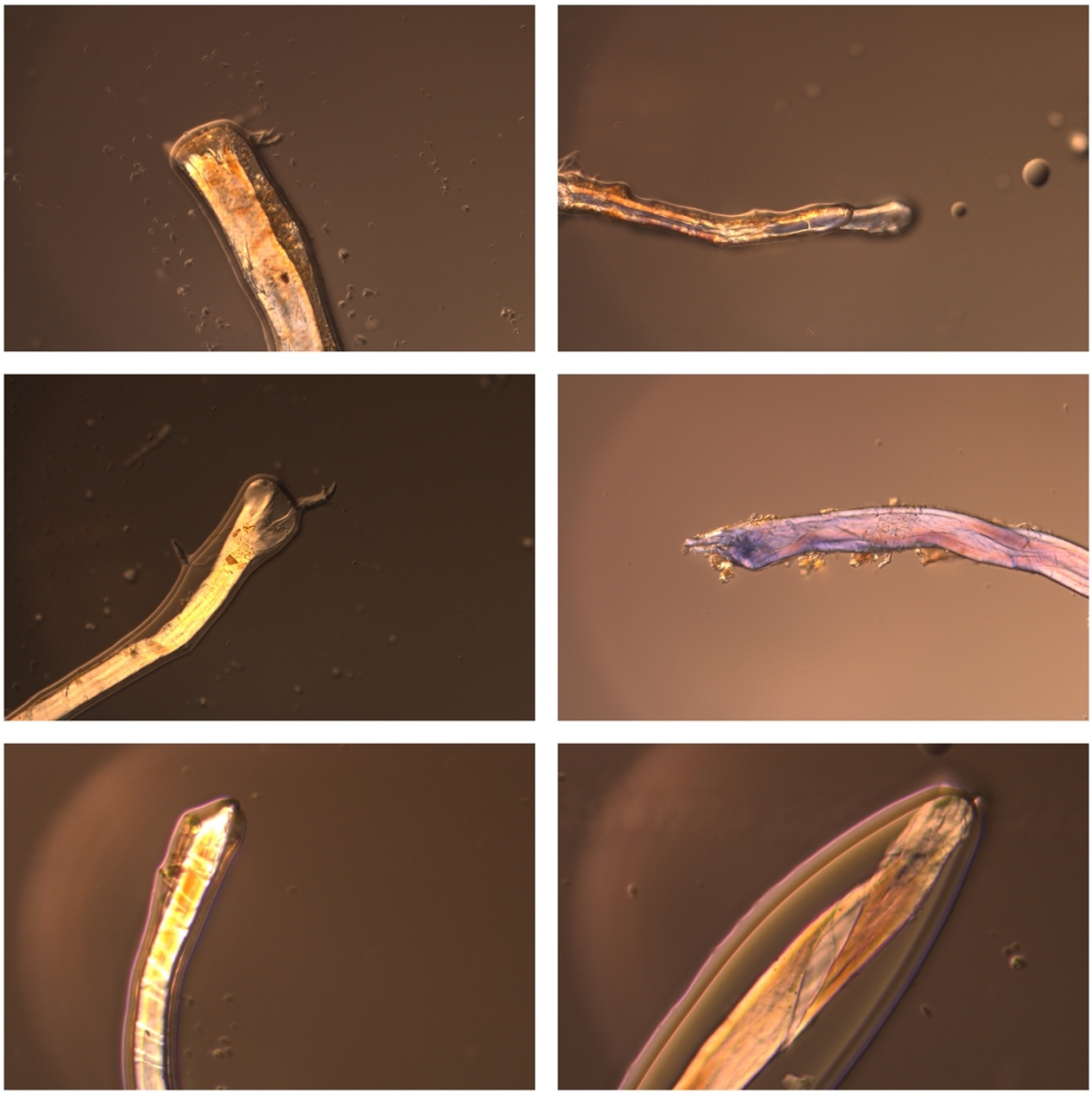

Figure 9: Images of nematode mouthparts before rehydration process. Top row are nematodes sourced from casing after 14 days, middle row are nematodes sourced from compost after 14 days replicate A and bottom row are nematodes sourced from compost after 14 days replicate B.

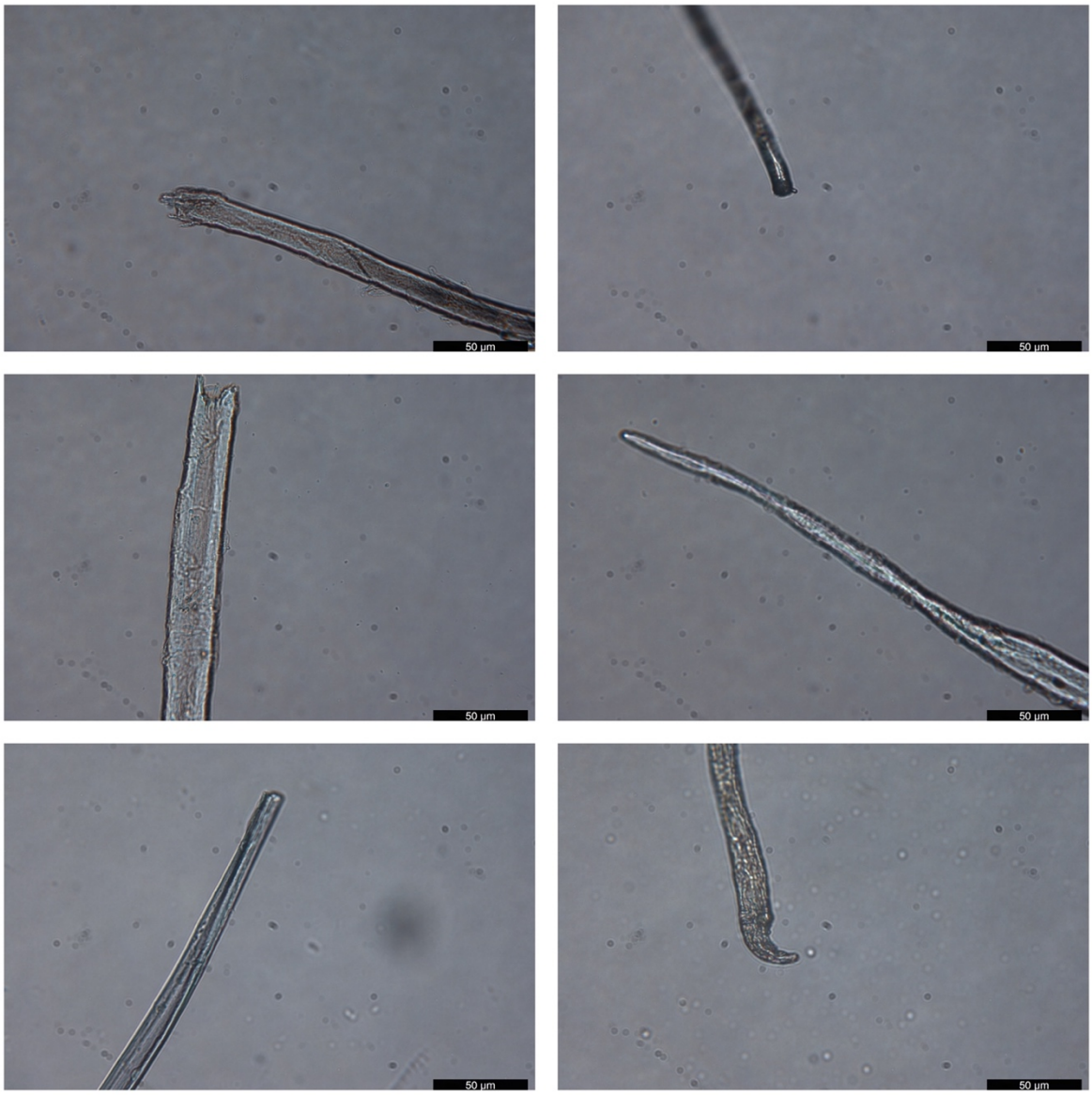

Figure 10: Nematodes after 65 hours rehydration, the longest possible rehydration period. Top row are nematodes sourced from casing after 14 days, middle row are nematodes sourced from compost after 14 days replicate A and bottom row are nematodes sourced from compost after 14 days replicate B.

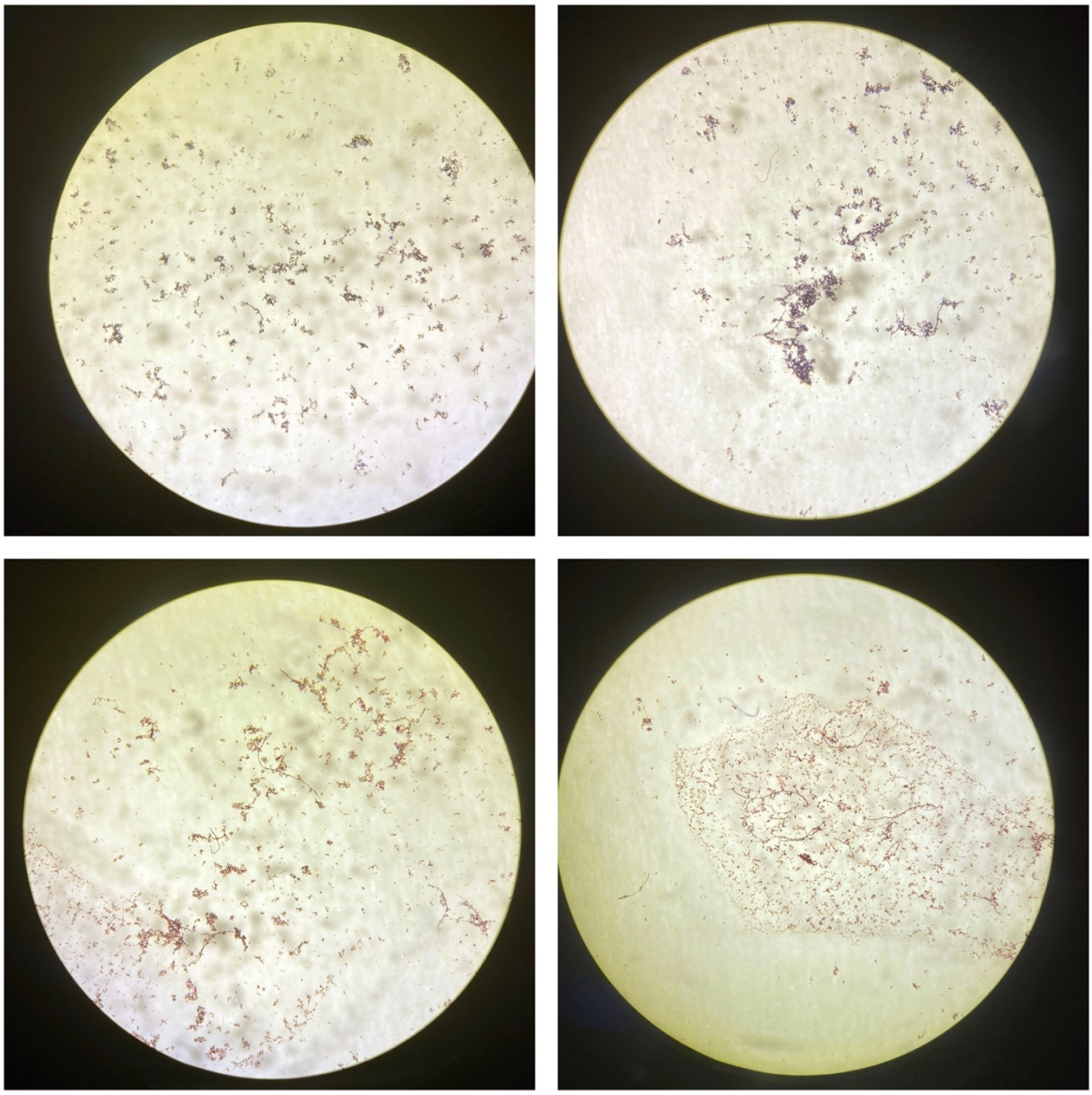

Figure 11: Nematodes after dye immersion for 15 minutes. Nematodes in the top row were immersed in crystal violet, showing a blue tint evident in detritus and nematodes. Nematodes in the bottom row were stained with fuchsin, showing a pink tint evident in detritus and nematodes. The presence of both dyes in the entire sample disabled biological staining from being used as an identification method for nematodes.

Isotopic values of bulk nematodes

Bulk nematodes were analysed for total amounts of carbon (%C, **Figure 12**) and natural abundance $\delta^{13}C_{VPDB}$ isotopic values (**Figure 13**). L- A+ treatment compost sample, which was sampled at day 21, contained 31 micrograms of nematodes, consisted of 35.85% carbon, and had a $\delta^{13}C_{VPDB}$ value of -26.75‰. L- A+ treatment compost sample, which was sampled at day 14, contained 30 micrograms of nematodes, consisted of 33.31% carbon, and had a $\delta^{13}C_{VPDB}$ value of -25.84‰. L- A+ treatment casing sample, which was likewise sampled at day 14, contained 26 micrograms of

nematodes, consisted of 35.46% carbon, and had a $\delta^{13}C_{VPDB}$ value of -26.05‰. On average, the carbon content was 34.87% and the average $\delta^{13}C_{VPDB}$ isotopic values were -26.21‰, displaying consistent values among the samples.

Isotopic values of all samples measured were between $\delta^{13}C_{VPDB}$ = -25.85‰ and -26.80‰, accounting for 1‰ difference in isotopic values between samples. Carbon percentages of all samples measured were between 33.3% and 35.9%, accounting for 2.6% difference in carbon content between samples. No labelled samples were measured on the EA-IRMS due to low counts in these types of samples.

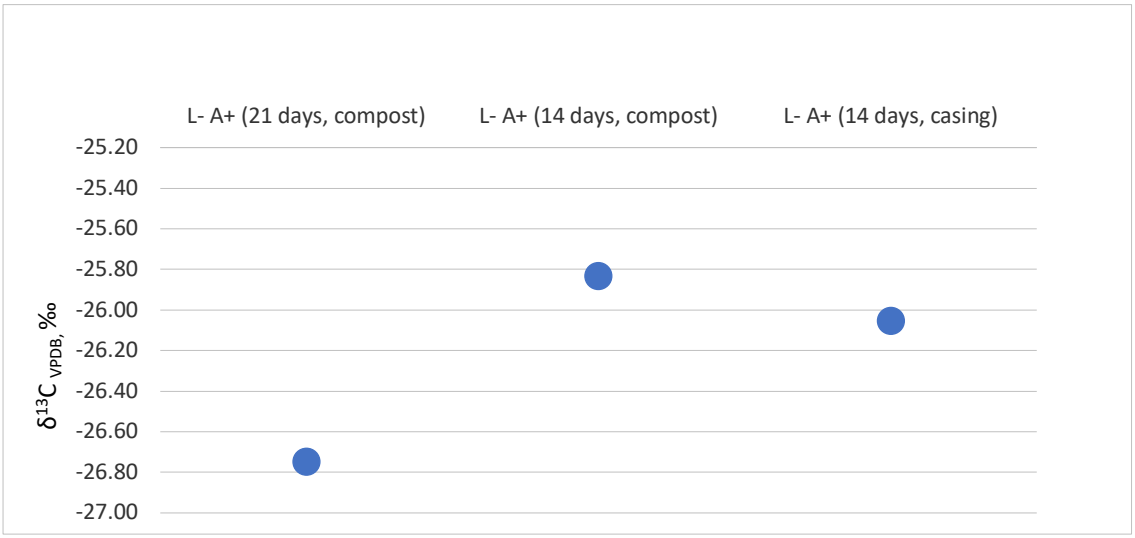

Figure 12: *EA-IRMS $\delta^{13}C$ measurement results.* Natural abundance $\delta^{13}C_{VPDB}$ isotopic values of three analysed bulk nematode samples (n ≈ 50 individuals).

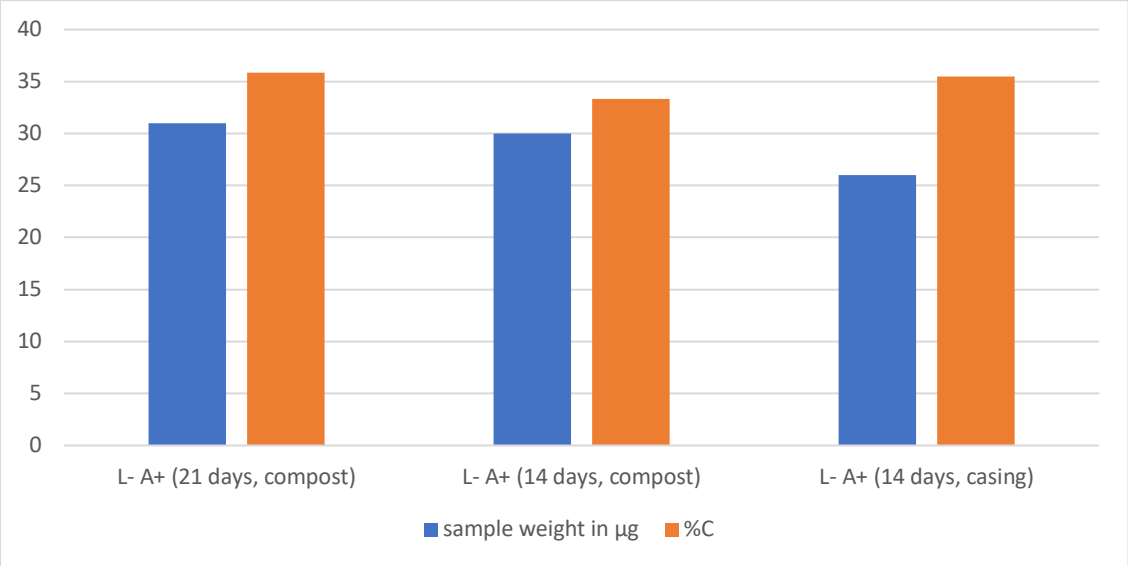

Figure 13: *Percentage of carbon contained in bulk samples of nematodes vs the weight of the nematodes in sample.* Percentage of carbon was expressed in %C, total weight of the nematodes was expressed in micrograms, with each bulk nematode sample totalling 50 individuals.

Isotopic values of individual nematodes

A hit completed on the LA-IRMS represents a single point of measurement, usually taken within a 5 second duration, and distinguished by the ablation laser hitting the surface of the nematode, and slowly burning away the sample.

Isotopic values of nematodes from unlabelled samples

Distribution of averages of measured natural abundance $\delta^{13}C_{VPDB}$ hits per corresponding unlabelled sample, including all replicates for the sample, can be seen on **Figure 14**. A full overview of descriptive statistics per substrate and sampling time for unlabelled nematodes can be found in **Table 7**.
Between casing and compost samples sampled at day 14, Kruskal-Wallis non-parametric test did not show significant differences [H(1) = 0.2228, p = 0.63695]. However, between casing and compost samples sampled at day 21, Kruskal-Wallis non-parametric test showed significant difference [H(1) = 17.2927, p = 0.00003]. Similarly to day 14, comparison between casing and compost samples sampled at day 30 using Kruskal-Wallis non-parametric test did not show significant difference [H(1) = 0.0408, p = 0.83986]. A prominent trend for unlabelled nematodes was the uniformity of median and mean values, with no evidently enriched values with later time points. The trend persists equally for both casing and compost-sourced nematodes, with a markedly smaller value spread evident in minimum and maximum natural abundance $\delta^{13}C_{VPDB}$ values, especially compared to labelled nematodes.

Table 7: Overview of natural abundance $\delta^{13}C_{VPDB}$ values in unlabelled nematode samples, with calculated minimums, maximums, medians and means for two types of substrate (casing and compost), divided by sampling times.

	Day 14		Day 21		Day 30	
Substrate	Casing	Compost	Casing	Compost	Casing	Compost
Min. $\delta^{13}C$	-35.95‰	-40.63‰	-33.43‰	-32.29‰	-32.38‰	-35.33‰
Max. $\delta^{13}C$	-21.69‰	-8.4‰	-24.29‰	-22.3‰	-23.46‰	-22‰
Median $\delta^{13}C$	-27.56‰	-27.71‰	-27.15‰	-28.34‰	-27.24‰	-27.58‰
Mean $\delta^{13}C$	-27.92‰	-27.77‰	-27.27‰	-28.36‰	-27.25‰	-27.4‰

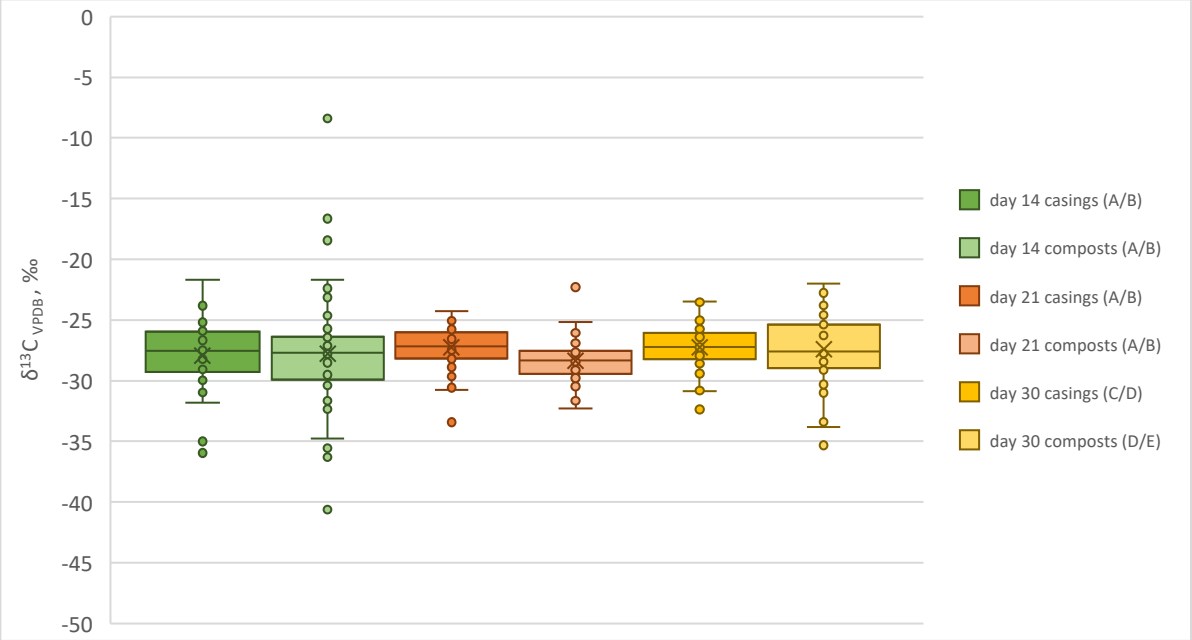

Figure 14: *Average natural abundance $\delta^{13}C_{VPDB}$ value distribution per substrate and per sampling time in L- samples.* Distribution of averages of measured $\delta^{13}C_{VPDB}$ hits per corresponding L- sample, including all replicates (A, B, C...) of the sample within a certain substrate. Darker colours correspond to casing substrate samples, and lighter colours correspond to compost substrate samples (green indicating day 14 samples, orange indicating day 21 samples and yellow indicating day 30 samples).

Isotopic values of nematodes from labelled samples

Distribution of averages of measured tracer $\delta^{13}C_{VPDB}$ hits per corresponding labelled sample, including all replicates for the sample, can be seen on **Figure 15**. A full overview of descriptive statistics per substrate and sampling time for labelled nematodes can be found in **Table 8**.

Between casing and compost samples sampled on day 14, Kruskal-Wallis non-parametric test showed significant difference [$H(1) = 6.2382$, $p = 0.0125$].This was also the case for casing and compost samples sampled at day 21, where Kruskal-Wallis non-parametric test likewise showed significant difference [$H(1) = 16.3692$, $p = 0.00005$]. Conversely, between casing and compost samples sampled at day 30, Kruskal-Wallis non-parametric test did not show significant difference [$H(1) = 3.1392$, $p = 0.07643$]. Labelled nematodes presented with an overall trend of progressively higher tracer $\delta^{13}C_{VPDB}$ values with further sampling time points, visible in both progressively higher mean values and in the number spread between minimum and maximum recorded tracer $\delta^{13}C_{VPDB}$ values. While this trend is present in casing substrates (1.35‰ higher value at day 30 compared to day 14), it has been shown to be much more evident in compost substrates (3.85‰ higher value at day 30 compared to day 14).

Table 8: Overview of tracer $\delta^{13}C_{VPDB}$ values measured in labelled nematode samples, with calculated minimums, maximums, medians and means for two types of substrate (casing and compost), divided by sampling times.

	Day 14		Day 21		Day 30	
Substrate	Casing	Compost	Casing	Compost	Casing	Compost
Min. $\delta^{13}C$	-30.76‰	-35.29‰	-34.205‰	-31.48‰	-52.22‰	-35.52‰
Max. $\delta^{13}C$	-20.5‰	-21.799‰	-12.965‰	+4.74‰	-0.17‰	+4.47‰
Median $\delta^{13}C$	-26.17‰	-24.5‰	-26.63‰	-24.15‰	-25.16‰	-23.11‰
Mean $\delta^{13}C$	-25.98‰	-23.29‰	-26.24‰	-22.64‰	-24.63‰	-19.44‰

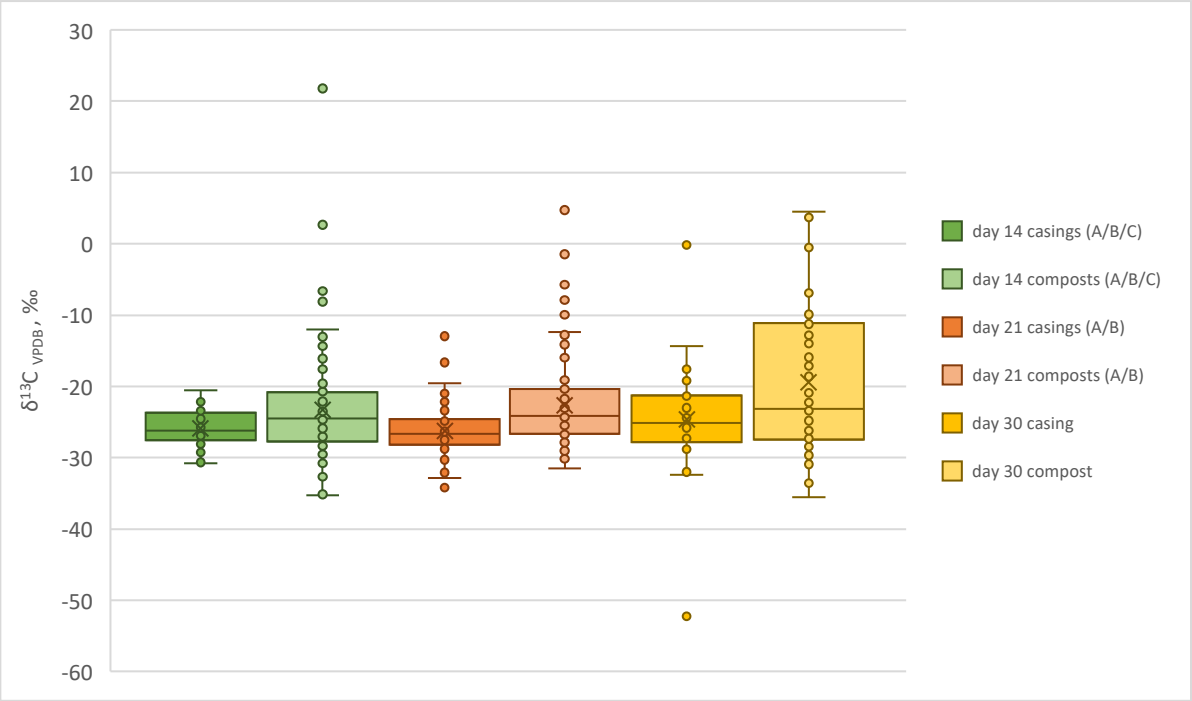

Figure 15: *Average tracer $\delta^{13}C_{VPDB}$ value distribution per substrate and per sampling time in L+ samples.* Distribution of averages of measured $\delta^{13}C_{VPDB}$ hits per corresponding L+ sample, including all replicates (A, B, C...) of the sample within a certain substrate. Darker colours correspond to casing substrate samples, and lighter colours correspond to compost substrate samples (green indicating day 14 samples, orange indicating day 21 samples and yellow indicating day 30 samples).

Comparing $\delta^{13}C_{VPDB}$ values of nematodes from L+ treatments with nematodes from L- treatments

Direct comparisons of $\delta^{13}C_{VPDB}$ values were performed between labelled (L+, tracer carbon) nematodes from casing samples, and unlabelled (L-, natural abundance carbon) nematodes from casing samples. Likewise, comparisons were performed between L+ nematodes from compost samples, and L- nematodes from compost samples. An overview of outcomes for both comparisons can be seen in **Table 9**.

$\delta^{13}C_{VPDB}$ values of nematodes from both casing and compost samples sampled at day 14 were found to be statistically different between L+ and L- experiments. $\delta^{13}C_{VPDB}$

values of L+ nematodes from casing samples were compared to those of L- nematodes from casing samples, and found to be significantly different, which was also the case for $\delta^{13}C_{VPDB}$ values of L+ nematodes from compost samples were compared to those of L- nematodes from compost samples. $\delta^{13}C_{VPDB}$ values of nematodes from casing samples sampled at day 21 were not found to be statistically different between L+ and L- experiments. However, $\delta^{13}C_{VPDB}$ values of nematodes from compost samples were found to be statistically different between L+ and L- experiments. $\delta^{13}C_{VPDB}$ values of nematodes from both casing and compost samples sampled at day 30 were found to be statistically different between L+ and L- experiments. In the case of casing samples, $\delta^{13}C_{VPDB}$ values between nematodes of the two treatments were significantly different, and similarly, $\delta^{13}C_{VPDB}$ values between nematodes of L+ and L- treatments were also significantly different.

In general, nematodes from L+ experiments showed a larger spread and variability of tracer $\delta^{13}C_{VPDB}$ values in every sample than the nematodes from corresponding L- experiments. The results and statistical analysis showed significant differences in natural abundance and tracer $\delta^{13}C_{VPDB}$ values between L+ and L- nematodes in all but one instance.

Table 9: Overview of calculated significant differences between labelled and unlabelled nematodes at various sampling time points between various substrates.

	Day 14		Day 21		Day 30	
Substrate	L-	L+	L-	L+	L-	L+
Casing	Yes. $H(1) = 13.2153$, $p = 0.00028$		No. $H(1) = 2.5407$, $p = 0.11095$		Yes. $H(1) = 9.3337$, $p = 0.00225$	
Compost	Yes. $H(1) = 25.1003$, $p < 0.00001$		Yes. $H(1) = 69.3221$, $p < 0.00001$		Yes. $H(1) = 13.4377$, $p = 0.00025$	

Variability of $\delta^{13}C_{VPDB}$ values between and within nematodes of the same sample

Inter-nematode variability of $\delta^{13}C_{VPDB}$ values considered the distribution of values within the nematodes of the same sample, and the extent of the range over which these values varied. In both L+ and L- samples, instances were found where $\delta^{13}C_{VPDB}$ values varied widely depending on the nematode analysed, as well as instances where $\delta^{13}C_{VPDB}$ values were nearly identical between the nematodes of the same sample. Generally, L+ samples seemed to display a wider scope of nematodes whose isotopic values varied extensively from one another in a single sample, while L- samples tended to have less variability between natural abundance $\delta^{13}C_{VPDB}$ values in nematodes of the same sample.

In L+ experiments, several samples stood out as highly intervariable, most notably the compost sample sampled at day 30 (**Figure 16**). This sample featured high intra-nematode variability (e.g. Nematode 2, with a span of 18.2‰ between the highest (-

10.2‰) and lowest (-28.3‰) $\delta^{13}C_{VPDB}$ tracer value in the nematode), as well as high inter-nematode variability (span of 31‰ between the highest (+4.5‰) and lowest (-35.5‰) tracer $\delta^{13}C_{VPDB}$ value in the sample). Conversely, the casing sample sampled at day 21 (**Figure 17**), was a notable example of a sample featuring low intra-nematode variability and inter-nematode variability in tracer $\delta^{13}C_{VPDB}$ values. Inter-nematode variability spanned 9‰ between the highest (-20.9‰) and lowest (-29.9‰) tracer $\delta^{13}C_{VPDB}$ value in the sample, while average intra-nematode variability spanned 2.92‰.

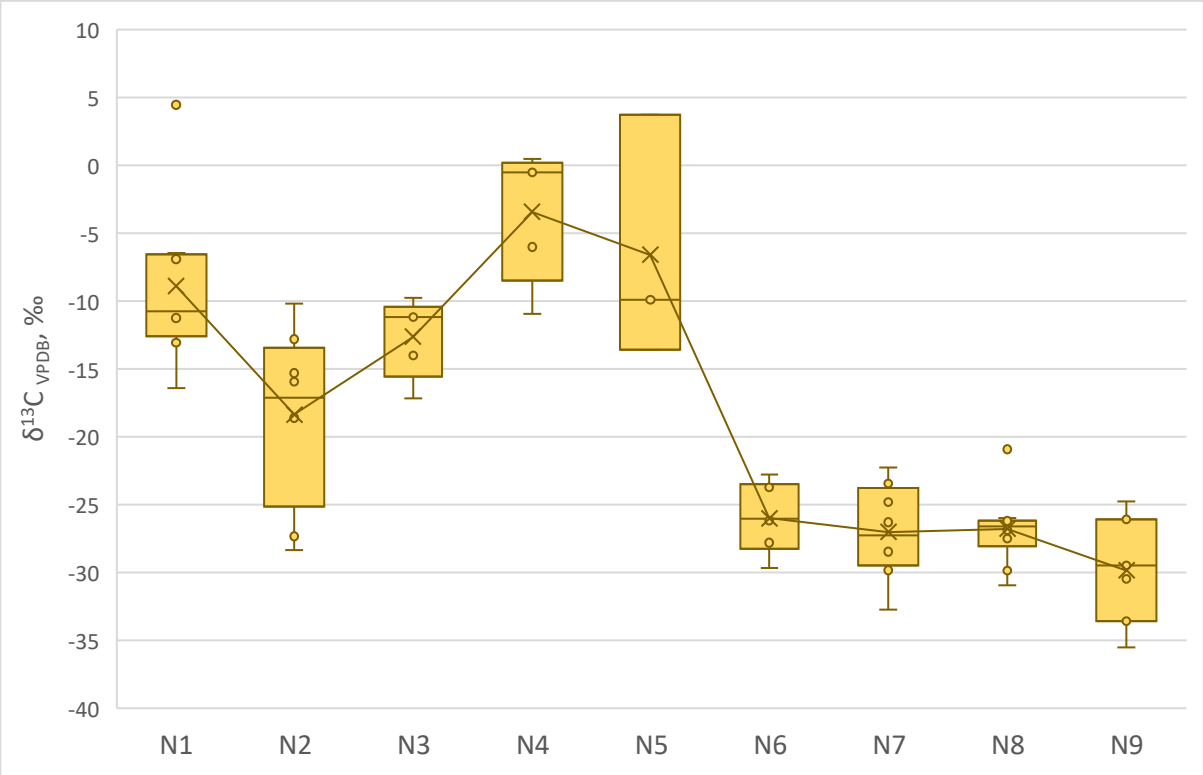

Figure 16: *Example of high tracer $\delta^{13}C_{VPDB}$ inter-nematode variability in a labelled compost sample.* The nematodes for the sample were extracted at day 30. N stands for nematode, demarking the numerical order of the nematode with all its belonging measurements.

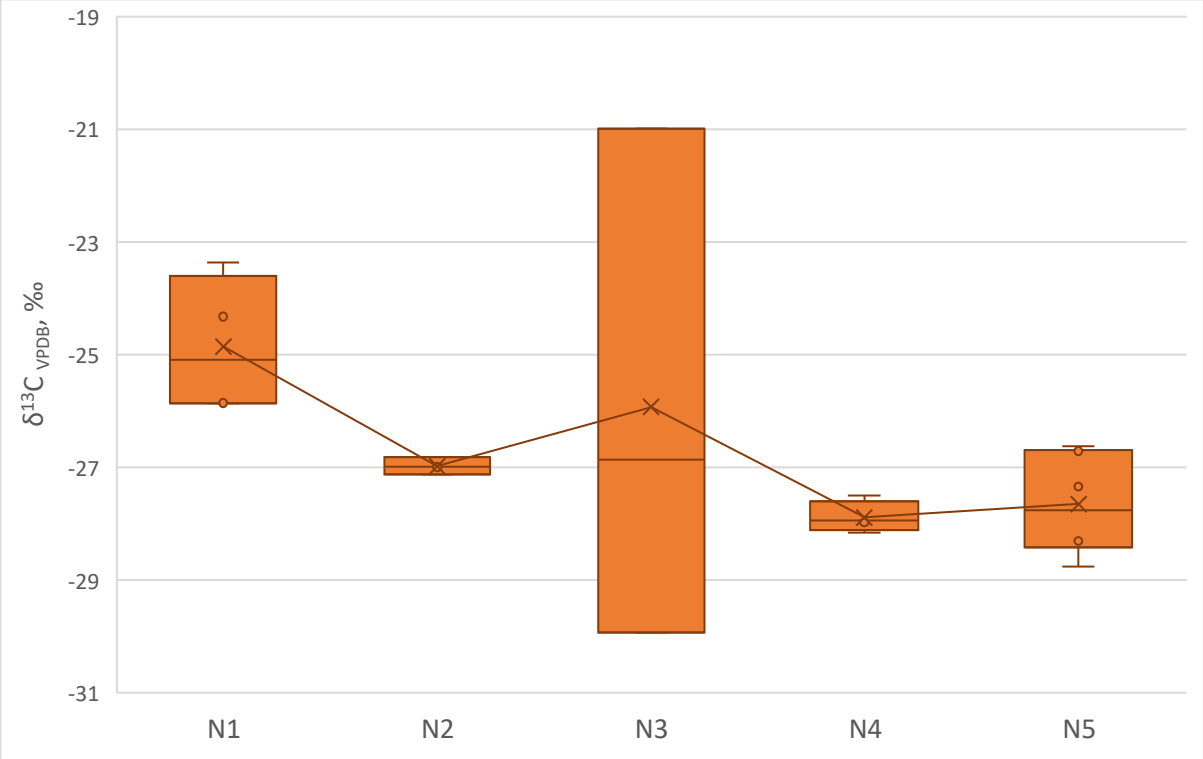

Figure 17: *Example of low tracer $\delta^{13}C_{VPDB}$ inter-nematode variability in a labelled casing sample.* The nematodes for the sample were extracted at day 21. N stands for nematode, demarking the numerical order of the nematode with all its belonging measurements.

L- experiments were marked by lower inter-nematode variability. The most notable example of high inter-nematode variability was in a casing sample collected at day 21 (**Figure 18**). Highest intra-nematode variability was observed in Nematode 6, with a span of 8‰ between the highest (-25.4‰) and lowest (-33.4‰) natural abundance $\delta^{13}C_{VPDB}$ value. Inter-nematode variability in the sample spanned 9.1‰ between the highest (-24.2‰) and lowest (-33.4‰) natural abundance $\delta^{13}C_{VPDB}$ value. The sample with the lowest inter-nematode variability was in a casing sample sampled at day 14 (**Figure 19**), with a span of 5.6‰ between the highest (-25.1‰) and lowest (-30.7‰) natural abundance $\delta^{13}C_{VPDB}$ value.

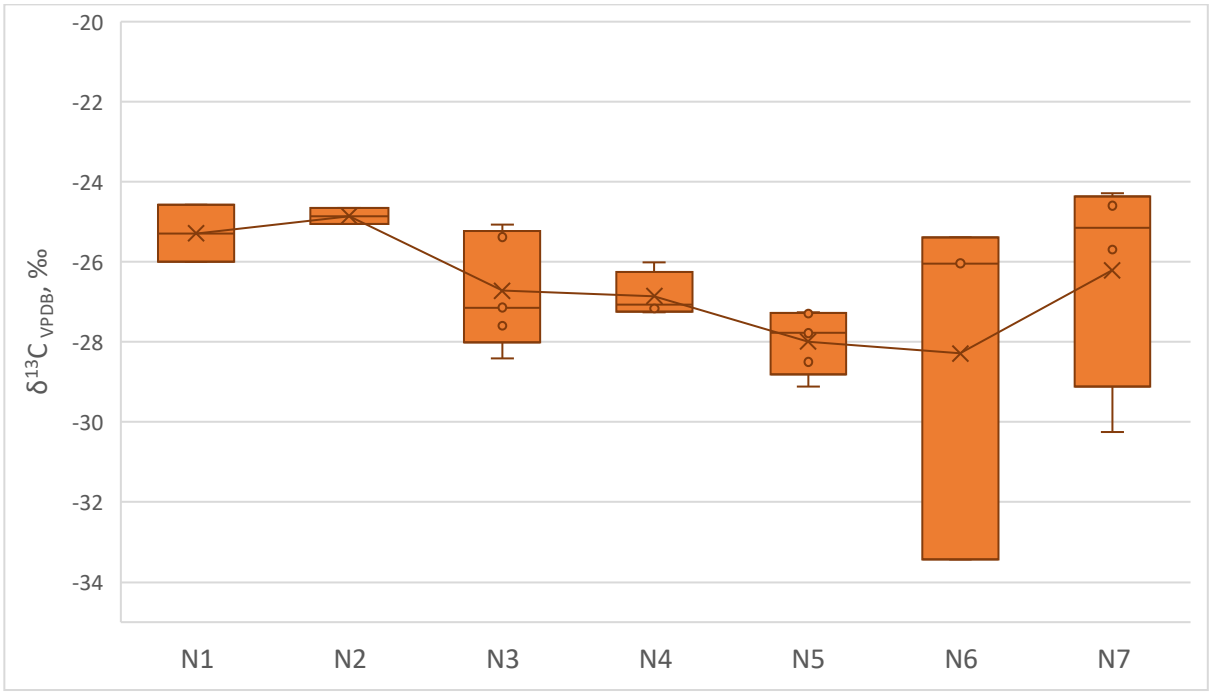

Figure 18: *Example of high natural abundance $\delta^{13}C_{VPDB}$ inter-nematode variability in an unlabelled casing sample.* The nematodes for the sample were extracted at day 21. N stands for nematode, demarking the numerical order of the nematode with all its belonging measurements.

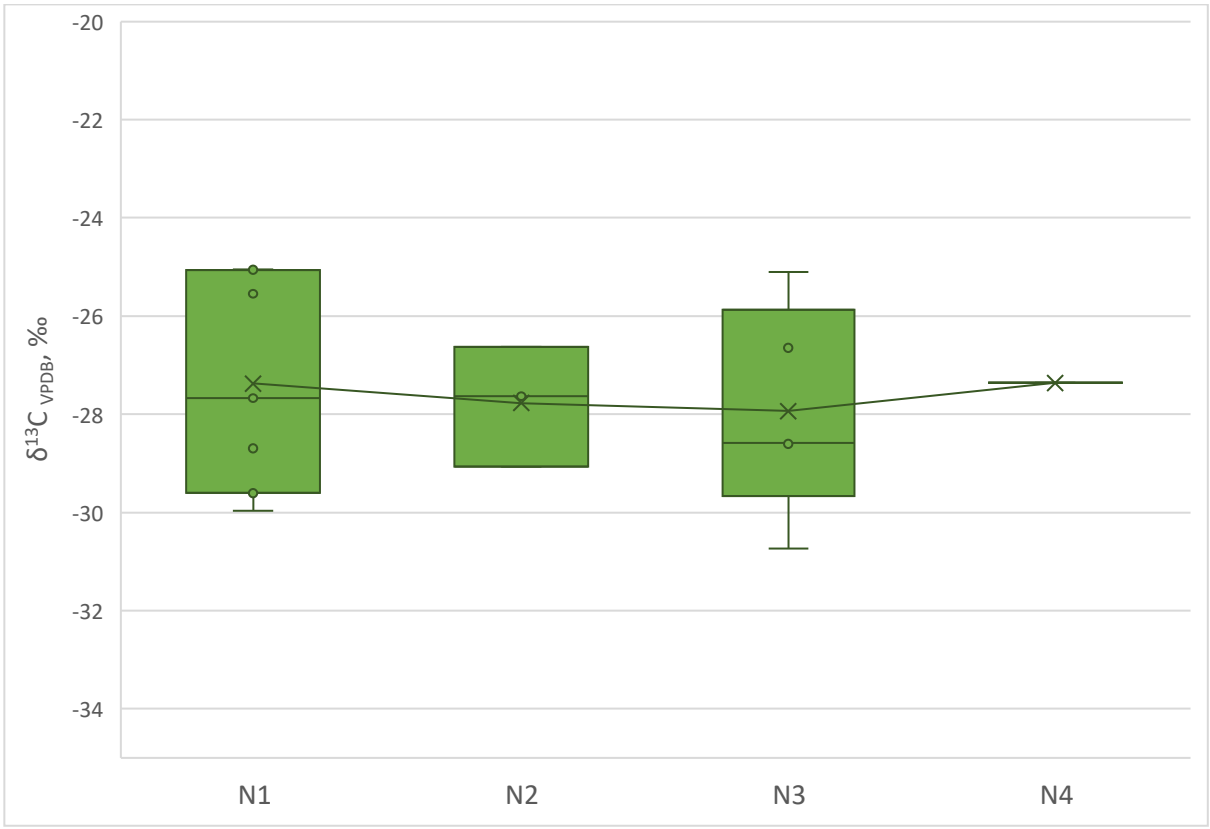

Figure 19: *Example of low natural abundance $\delta^{13}C_{VPDB}$ inter-nematode variability in an unlabelled casing sample.* The nematodes for the sample were extracted at day 14. N stands for nematode, demarking the numerical order of the nematode with all its belonging measurements.

Inter-nematode variability was tested for statistical significance between corresponding L+ and L- treatments. Significant differences were found for inter-nematode variability between L+ and L- casing, replicate A [$H(1) = 13.2408$, $p = 0.00027$] and compost, replicate A [$H(1) = 30.9819$, $p < 0.00001$] samples sampled at day 14. Significant differences were also found between L+ and L- casing, replicate A [$H(1) = 5.1634$, $p = 0.02307$] and compost, replicate A [$H(1) = 31.9269$, $p < 0.00001$] samples sampled at day 21, as well as compost, replicate B [$H(1) = 35.3741$, $p < 0.00001$]. Finally, significant differences were also found for inter-nematode variability between L+ and L- casing [$H(1) = 11.211$, $p = 0.00081$] and compost [$H(1) = 7.0108$, $p = 0.0081$] samples acquired at day 30.

The results and subsequent statistical analysis showed significant differences in inter-nematode variability of both tracer and natural abundance $\delta^{13}C_{VPDB}$ values between corresponding L+ and L- nematode samples in most cases where such direct comparison was viable.

Excess labelling in nematodes from L+ treatments

Distributions of excess in nematodes from compost and casing samples sourced from L+ experiments across all replicates, averaged per time and soil type, can be seen in **Figure 20**.

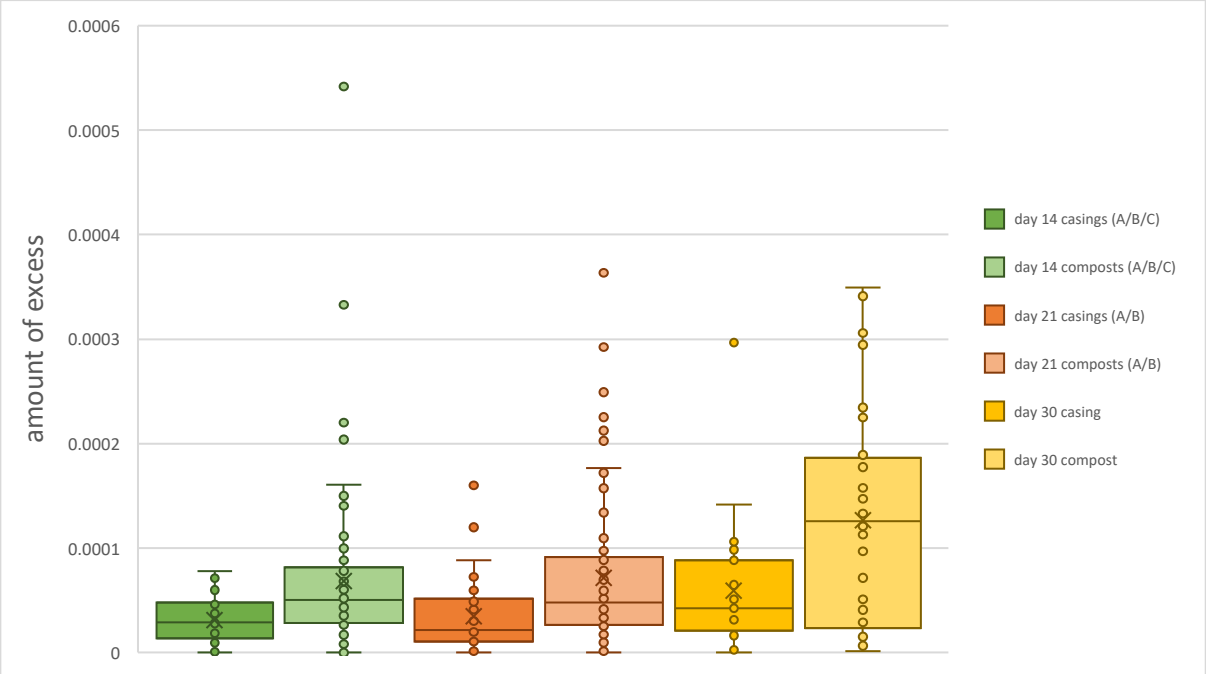

Figure 20: *Excess distribution in labelled samples, averaged per substrate type and per sampling time.* Distribution of excess in nematodes from labelled casing (dark green, dark orange and dark yellow) and compost (light green, light orange and light yellow) samples, with replicate values averaged per substrate and sampling time.

Table 10: Overview of excess values calculated from labelled nematode samples, with calculated minimums, maximums, medians and means for two types of substrate (casing and compost), divided by sampling times.

	Day 14		Day 21		Day 30	
Substrate	Casing	Compost	Casing	Compost	Casing	Compost
Min. excess	5×10^{-7}	7.95×10^{-7}	2.12×10^{-7}	5.78×10^{-7}	1.45×10^{-8}	1.56×10^{-6}
Max. excess	7.79×10^{-5}	5.41×10^{-4}	1.6×10^{-4}	3.63×10^{-4}	2.97×10^{-4}	3.49×10^{-4}
Median excess	2.91×10^{-5}	5.09×10^{-5}	2.18×10^{-5}	4.8×10^{-5}	4.24×10^{-5}	1.26×10^{-4}
Mean excess	3.1×10^{-5}	6.99×10^{-5}	3.48×10^{-5}	7.15×10^{-5}	5.96×10^{-5}	1.27×10^{-4}

For all sampling timepoints and soil types, minimum possible value was zero, in which case a certain hit for a certain sample showed no excess. General trends noted was the small abundance of excess, and the propensity for increase in excess abundance with consequent sampling time points. This result was evident in casing substrate, but featured more prominently in the compost substrate. In both substrates, a difference of 2 to 4 orders of magnitude between minimum and maximum recorded excess values was noted, with a higher spread of values noted in compost. A full overview of descriptive values can be found in **Table 10**.

Kruskal-Wallis non-parametric testing revealed significant differences in label excess among different soil types: between nematodes from day 14 casing and compost samples [$H(1) = 17.8008$, $p = 0.00002$], between nematodes from day 21 casing and compost samples [$H(1) = 12.5968$, $p = 0.00039$] and between nematodes from day 30 casing and compost samples [$H(1) = 6.2831$, $p = 0.01219$]. Statistical testing likewise revealed significant differences in label excess among different sampling timepoints: between nematodes from day 14, day 21 and day 30 casing samples [$H(2) = 6.505$, $p = 0.03868$] and between nematodes from day 14, day 21 and day 30 compost samples [$H(2) = 8.6879$, $p = 0.01299$].

LA-IRMS straw testing and subsequent nematode identification

LA-IRMS analysis was also performed on two separate samples of thick straws (sourced from a day 14 compost sample and a day 30 compost sample), one sample of thick debris (sourced from a day 21 compost sample), one sample of thin debris (sourced from a day 21 compost sample) and one nematode (sourced from a day 21 compost sample), where all tested components were commonly found in all original extracted nematode samples. All samples used were from L+ experiments (**Figure 21**).

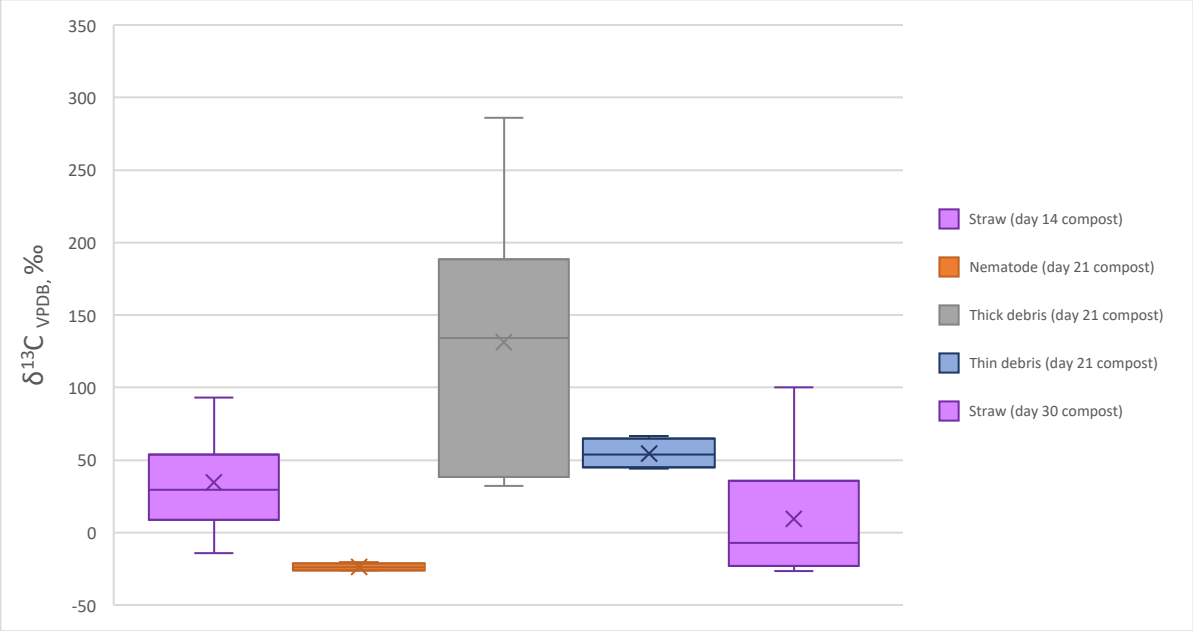

Figure 21: *Results of the straw, nematode and debris testing on the LA-IRMS.* $\delta^{13}C_{VPDB}$ values as a result from LA-IRMS testing on straw (purple), thick debris (grey), thin debris (blue) and nematodes (orange).

Straw sourced from both day 14 compost and day 30 compost showed large intra-sample variation in $\delta^{13}C_{VPDB}$ values within the straw, unseen in any of the measured nematode samples. The same result was noted for thicker and thinner debris sourced from day 21 compost. However, statistical testing showed that the measured nematode did not differ significantly from previously measured unlabelled compost nematodes. A full overview of values can be found in **Table 11**.

Kruskal-Wallis non-parametric statistical testing showed significant differences between $\delta^{13}C_{VPDB}$ values of all components [$H(4) = 41.2746$, $p < 0.00001$]. The testing further showed significant differences between $\delta^{13}C_{VPDB}$ values of both straw samples and nematodes previously sourced from day 21 compost for the purpose of analysis [$H(2) = 63.002$, $p < 0.00001$]. Similarly, testing showed significant differences between $\delta^{13}C_{VPDB}$ values of the day 21 compost nematodes used for analysis and thick debris [$H(1) = 31.5$, $p < 0.00001$], as well as for the thin debris [$H(1) = 14.0722$, $p = 0.00018$]. However, testing did not show significant differences between $\delta^{13}C_{VPDB}$ values of the day 21 compost nematodes used for analysis, and the nematode sampled from day 21 compost for the purposes of this test [$H(1) = 0.1242$, $p = 0.72448$]. Therefore, the results displayed statistically significant distinctiveness between thick debris, nematode-like straws and nematodes.

Table 11: Overview of $\delta^{13}C_{VPDB}$ values calculated from the straw testing run, with calculated minimums, maximums, medians and means for two types of substrate (casing and compost), divided by sampling times.

	Day 14	Day 21			Day 30
Substrate and type	Compost straw	Compost nematode	Compost thick debris	Compost thin debris	Compost straw
Min. $\delta^{13}C$	+93.27‰	-20.22‰	+286.045‰	+66.79‰	+100.09‰
Max. $\delta^{13}C$	-14‰	-26‰	+32.115‰	+44.23‰	-26.57‰
Median $\delta^{13}C$	+29.6‰	-23.7‰	+134.16‰	+53.91‰	7.145‰
Mean $\delta^{13}C$	+34.5‰	-23.58‰	+131.33‰	+54.71‰	+9.49‰

Biomarker studies on bacteria and fungi

Total PLFA concentrations for bacteria and fungi

In measured compost samples, both total bacterial PLFA concentrations and total fungal PLFA concentrations displayed a decrease over the first 14 days of the experiment, following a similar trend (**Figure 22**). In compost, both bacteria (3954.2 ± 320.8 nmol C g^{-1}) and fungi (381.5 ± 54.0 nmol C g^{-1}) had high biomass at the start of the experiment. Within the initial 7 days of the experiment, the total biomass of bacteria (4255.7 ± 397.1 nmol C g^{-1}) and fungi (474.3 ± 26.6 nmol C g^{-1}) in compost increased. However, by day 14 of the experiment, both bacteria and fungi saw a severe decrease in biomass. Bacterial biomass fell to 1035.3 ± 44.6 nmol C g^{-1}, a 75.7% decrease from day 7. Fungal biomass fell to 37.2 ± 9.0 nmol C g^{-1}, a 92.2% decrease from day 7. However, the rest of the experiment was marked with different trends in the measured biota. Bacterial biomass experienced a slight decrease from day 21 until the end of the experiment. Conversely, fungal biomass displayed a gradual linear increase during day 21 (88.7 ± 34.1 nmol C g^{-1}) and day 30 (170.4 ± 4.9 nmol C g^{-1}). Overall, in compost, bacteria showed higher concentrations than the fungi at all times of the experiment.

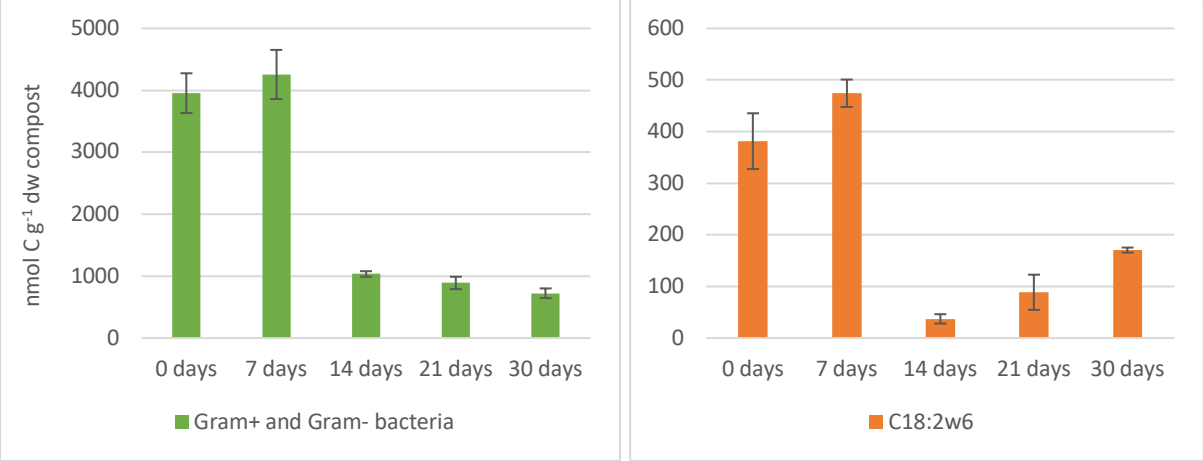

Figure 22: *Total bacterial biomass in compost (left) and total fungal biomass in compost (right).* Total PLFA concentration after 0, 7, 14, 21 and 30 days for industry standard spawn density experiments. Error bars represent standard deviation, n = 2.

In casing samples, total bacterial and fungal PLFA concentrations showed similar trends for the entire duration of the experiment, presenting with a linear increase (**Figure 23**). In bacteria, concentrations were lowest at day 14 (97.1 ± 0.1 nmol C g^{-1}), linearly increasing by day 21 (158.5 ± 14.7 nmol C g^{-1}) and day 30 (213.6 ± 91.8 nmol C g^{-1}). In fungi, concentrations were likewise lowest at day 14, showing no PLFA fungal biomarkers, but linearly increasing by day 21 (183.5 ± 73.2 nmol C g^{-1}) and day 30 (452.2 ± 291.8 nmol C g^{-1}). Overall, in casing, fungi showed higher concentrations than the bacteria at all times of the experiment, except at day 14.

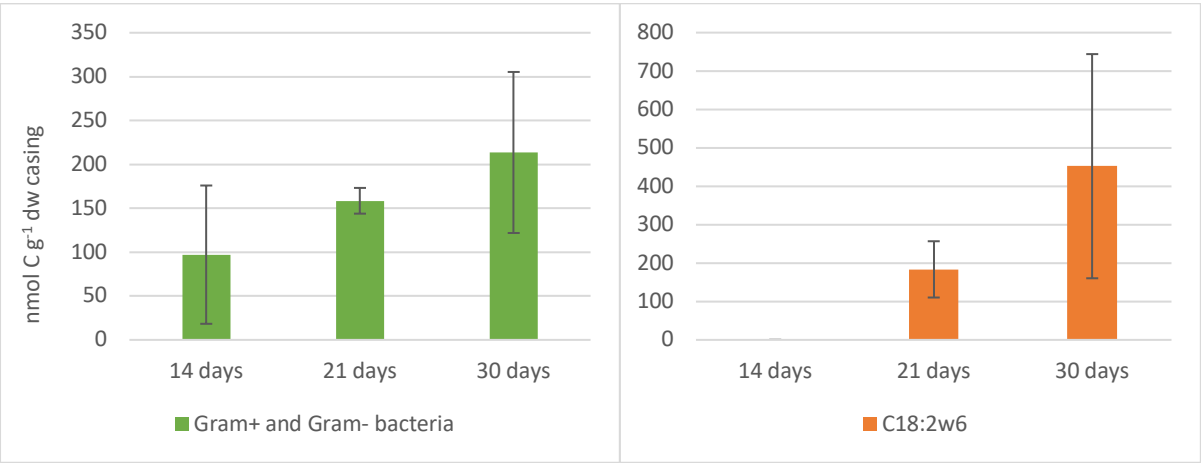

Figure 23: *Total bacterial biomass in casing (left) and total fungal biomass in casing (right).* Total PLFA concentration after 14, 21 and 30 days for industry standard spawn density experiments. Error bars represent standard deviation, n = 2.

Incorporation of label into bacterial and fungal PLFAs

Similarly to trends noticed with PLFA concentrations, labelled biomass of bacteria and fungi demonstrated similar trends during the first 14 days of the experiment in compost. Bacteria initially started off with a very low amount of labelled biomass at day 0 (0.15 ± 0.04 nmol C g^{-1}). The labelled biomass of bacteria rapidly increased during the next 7 days (43.52 ± 5.57 nmol C g^{-1}), only to fall by day 14 of the experiment (6.83 ± 0.68 nmol C g^{-1}), displaying an 84.3% decrease (**Figure 24**). Similar observations were made for fungi, with a very low amount of labelled biomass at day 0 (0.01 ± 0.0001 nmol C g^{-1}), a rapid increase in the next 7 days (0.64 ± 0.08 nmol C g^{-1}), and a rapid, 86% labelled biomass decrease by day 14 of the experiment (0.09 ± 0.05 nmol C g^{-1}). Trends again diverged at day 21, where labelled bacterial biomass showed a 50% decrease (3.61 ± 0.8 nmol C g^{-1}), with a further slight decrease continuing until day 30 (3.63 ± 0.37 nmol C g^{-1}). Conversely, fungal labelled biomass showed a drastic linear increase of 267% on day 21 (0.33 ± 0.19 nmol C g^{-1}), continuing to day 30 when the labelled biomass was 121% higher than on day 21 (0.73 ± 0.21 nmol C g^{-1}) and the overall highest in the experiment. Despite these increases, overall labelled biomass of fungi was lower than that of labelled biomass of bacteria in the compost, during the entire experiment.

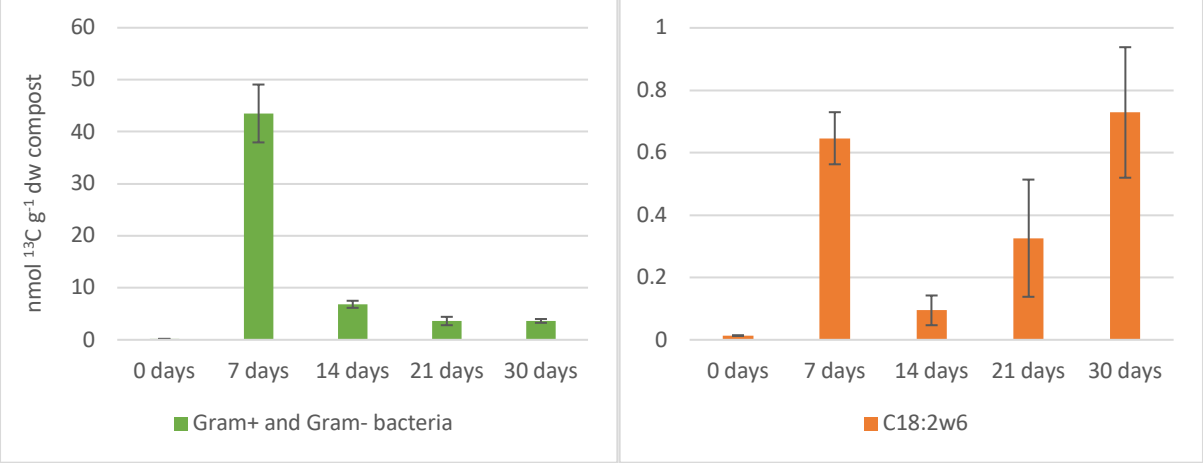

Figure 24: *Labelled bacterial biomass in compost (left) and labelled fungal biomass in compost (right).* ^{13}C absolute uptake as reflected in bacterial and fungal PLFAs. Error bars represent standard deviation, n = 2.

In casing, labelled biomass of both bacteria and fungi showed trends of linear growth (**Figure 25**). Bacteria exhibited very low amounts of labelled biomass on day 14 (0.0004 ± 0.00001 nmol C g^{-1}), with a marked increase at day 21 (0.16 ± 0.02 nmol C g^{-1}) and a 150% increase at day 30 (0.4 ± 0.13 nmol C g^{-1}). Fungi exhibited similar behaviour, with no fungal biomarkers found at day 14, but a marked increase at day 21 (0.96 ± 0.26 nmol C g^{-1}) and a 106% increase at day 30 (1.98 ± 0.47 nmol C g^{-1}). Overall, fungi had a higher amount of labelled biomass than bacteria in casing for the duration of

the experiment.

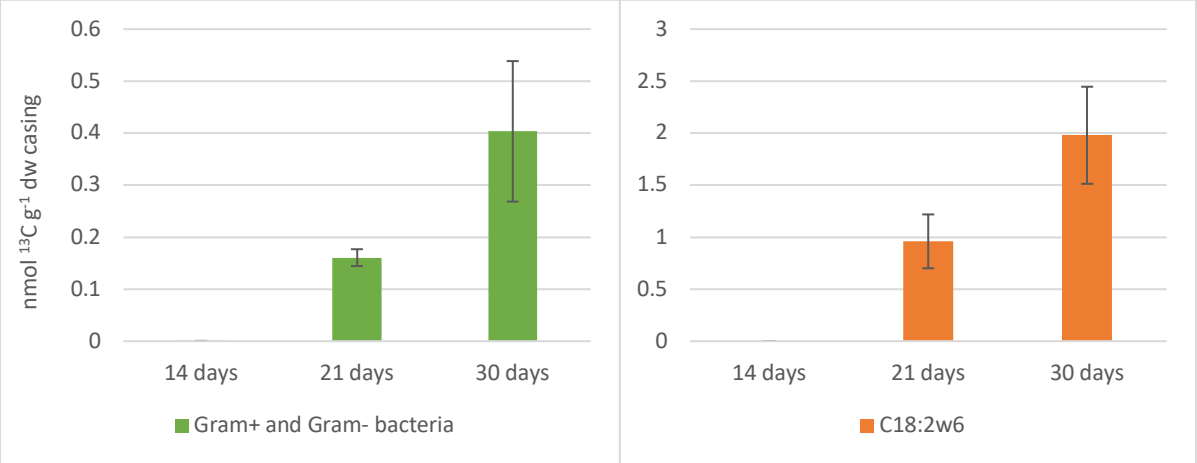

Figure 25: *Labelled bacterial biomass in casing (left) and labelled fungal biomass in casing (right).* ^{13}C absolute uptake as reflected in bacterial and fungal PLFAs. Error bars represent standard deviation, n = 2.

Modelling the food web environment in R

The total carbon food-web model

A scenario of a normal mushroom compost environment without any additional resource injections was considered for model calibration. Several possible scenarios were considered for the model, for which the intensity of degradation rates, uptake rates, predation rates, mortality rates, Monod rates, efficiency rates and state variables were modified. The optimal model was reached through trial-and-error calibration of known values and empirical knowledge on biomass fluctuations across a span of time from real-life experiments. The result was an interactive model which was able to answer post-hoc questions of a changing environment with the real-time change in modelled variables (**Figure 26**).

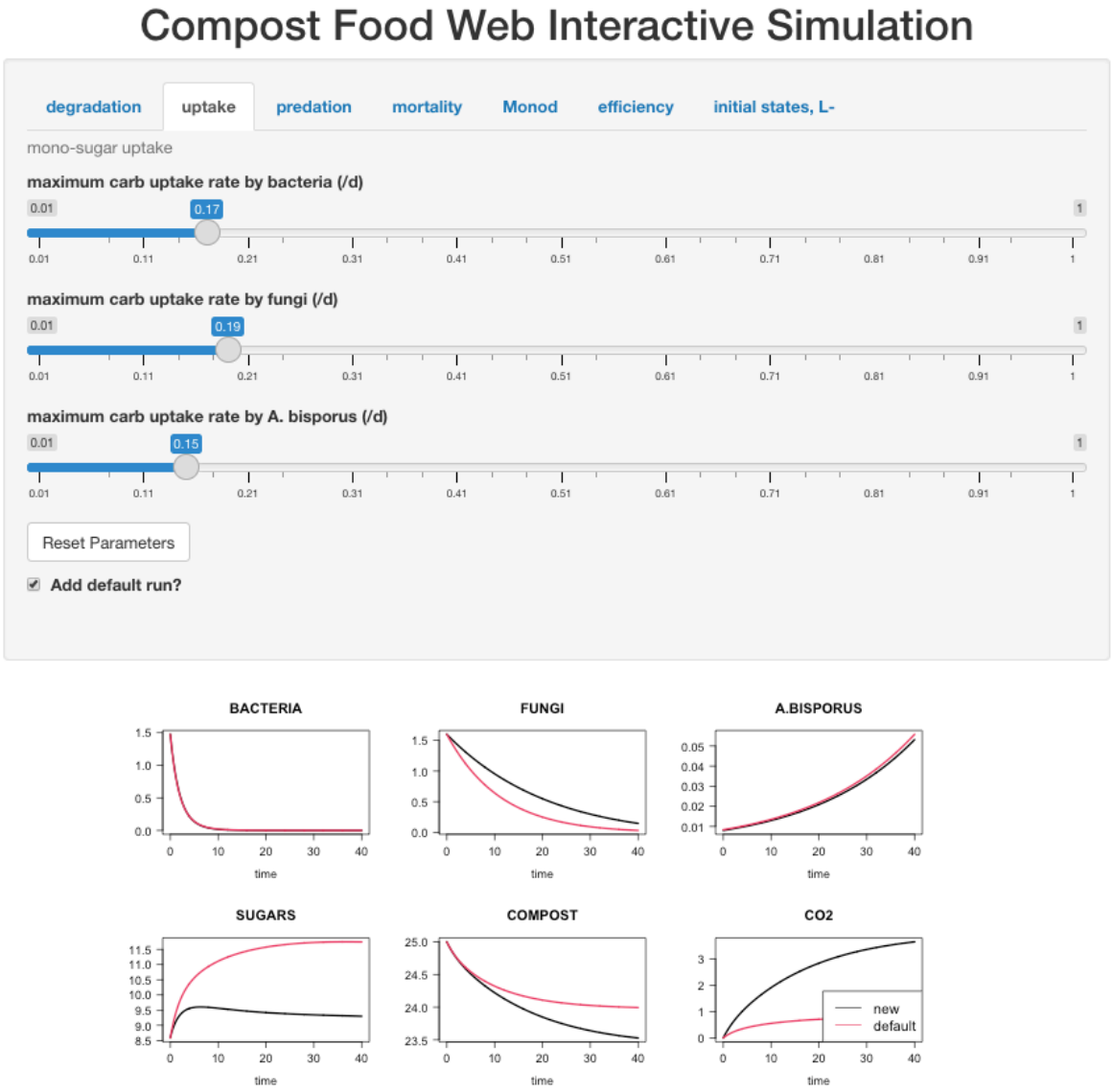

Figure 26: User interface of the model, coded in R (version 4.1.2) and based on the package shiny, seen open in a RStudio window on the MacOS environment. **Top to bottom:** interactive tabs which allowed changing of related parameters, explanation of parameters contained in the tab, interactive sliders which allowed real-time adjustments to select variables, which were applied to the output and visible immediately, "Reset Parameters" button which returned the sliders and the output to original state, as mandated by the code, "Add default run?" checkbox which allowed direct comparison between a new run (any run that occurred due to a change in any offered variable) and a default run (the run which immediately preceded the run commenced by a new change in variables), graphical output which allowed tracking change of biomass through a certain time.

Calibrated model showed a graphical output which tracked a rapid fall in biomass of bacteria to nearly zero in compost over the span of 40 days, where already by day 20 of the experiment, most of bacterial biomass would be rapidly depleted, with no later changes (**Figure 27**). Fungi, likewise, demonstrated a fall in amounts of biomass present, however, with a much more gradual slope. The fall progressed gently over the span of 40 days, and fungal biomass was fully depleted only towards the end of the experiment. Conversely, *A. bisporus* started off with nearly no detectable biomass (due

to its incorporation into compost in the form of a rye grain, from which the mycelium formed gradually, over time). However, the biomass of the white button mushroom increased by 100% by day 20 of inoculation, and by another 100% about 8-10 days later. 40 days into the experiment, *A. bisporus* had the highest biomass. The total amount of sugars increased during the experiment, with the increase being the highest from day 0 to day 10, by 33%. From day 10 to day 30, the amount of sugar in compost increased slowly, by 8% in total over the course of 20 days, levelling off afterwards. The total amount of recalcitrant polysaccharides in compost decreased gradually, by about -10% over the course of 40 days of the experiment. The emission of CO_2 from compost due to metabolic activity (i.e. respiration) exponentially increased, with the highest amount of CO_2 produced in the first 5 days of the experiment. The production and emission of CO_2 decreased considerably after day 15. In the last 35 days of the experiment, the emission of CO_2 was equal to the emission during the first 5 days.

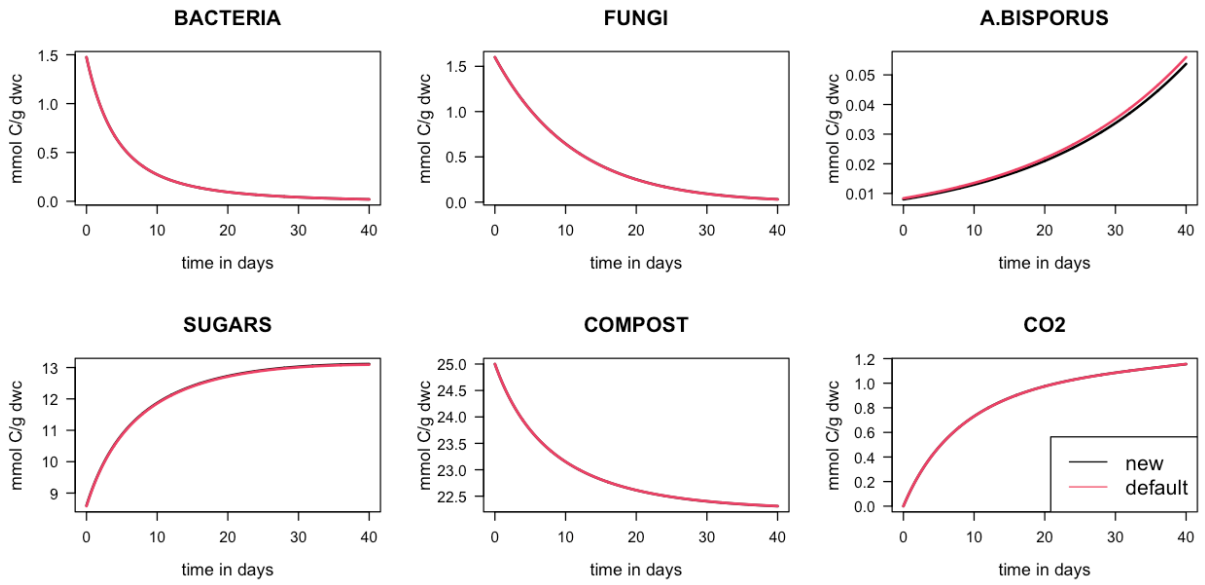

Figure 27: Graphical output of the model for the scenario of a regular mushroom compost food web, without any nutrient additions, tracing the total carbon flow through various biomass compartments of the food web participants (bacteria, fungi, A. bisporus, sugars in the form of monosaccharides, sugars in the form of polysaccharides, and CO_2 emitted from the compost). Y-axis of all graphs represents the amount of biomass in mmol C per gram dry weight compost, and the X-axis of all graphs represents the duration of the experiment in days.

Tracing the label uptake through a calibrated food web model

Addition of ^{13}C-glucose to the compost setting allowed for tracing of ^{13}C-label uptake through incorporation of label into the biomass of white button mushroom food web participants (**Figure 28**). Graphical output showed that bacteria gradually took up the injected label over the course of the first 5 days of the experiment, until full depletion of the label. Fungal population displayed similar trends, gradually taking up labelled glucose from the first day of the experiment, afterwards taking it up almost

exponentially with a peak around day 10. Fungal consumption of labelled glucose levelled off around day 15, and then consistently decreased over the course of the next 30 days, until the end of the experiment. *A. bisporus* initially showed a very slow uptake of the label in the first 10 to 15 days of the experiment, after which uptake increased exponentially, not demonstrating deceleration until the end of the experiment. The label in monosaccharide sugars compartment grew exponentially initially, quadrupling in the first 10 days of the experiment. In the subsequent 30 days of the experiment, label in monosaccharide sugars compartment increased by 25% of the increase that occurred during the first 10 days. No results were modelled for the compost, as the label did not in any way interact with the recalcitrant polysaccharides compartment in the model setup, since the ^{13}C-glucose was a direct injection into the compartment of simple, monosaccharide sugars. In the case of exuded CO_2, the highest degree of emissions from compost due to respiration occurred within the first 10 days of the experiment, with the day 10 amount demonstrating a 100% increase in emissions compared to day 0. During the consecutive 30 days of the experiment up until its termination, equal amount of CO_2 was emitted from the compost as during the first 10 days.

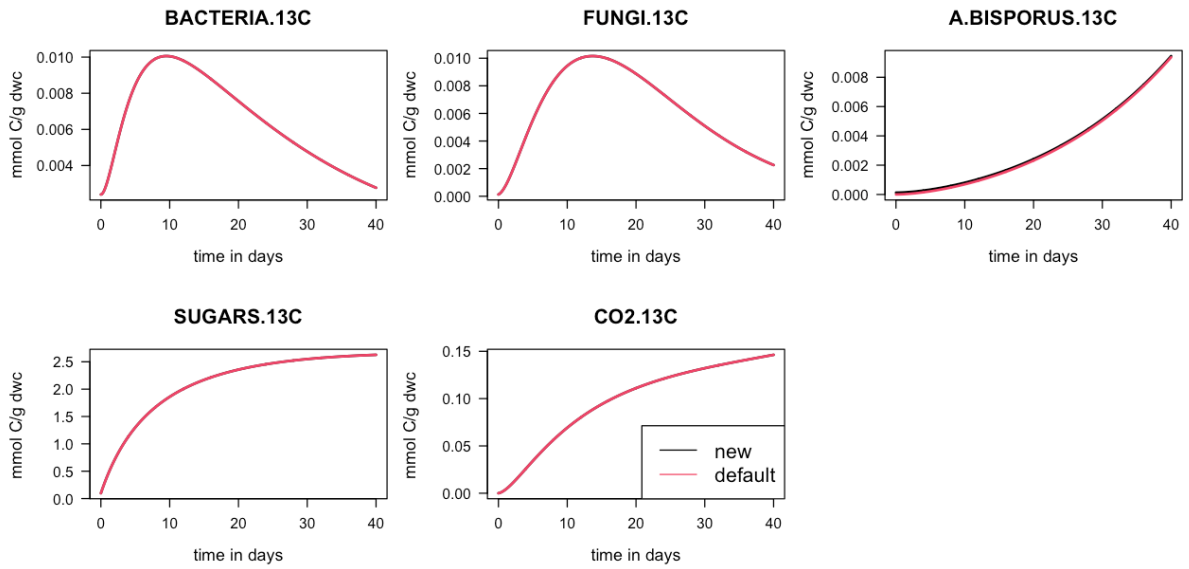

Figure 28: Graphical output of the model for the scenario of a mushroom compost food web, where a one-time injection of ^{13}C-labelled glucose has been dispersed through the compost. In this scenario, the carbon flow of the injected label, rather than total carbon, is traced through biomass compartments of the food web participants (labelling in bacteria, labelling in fungi, labelling in A. bisporus, labelling in monosaccharide sugars, and labelling emitted from the compost in the form of exuded CO_2). Y-axis of all graphs represents the amount of biomass in mmol C per gram compost, and the X-axis of all graphs represents the duration of the experiment in days.

Discussion

Nematodes are present in various niches of decomposition ecosystems, including in commercial *A. bisporus* mushroom beds, and they populate this environment together with various bacterial and fungal taxa, as well as the white button mushroom itself. Microbiota directly participates in cycling of nutrients and elements in the niche they populate, contributing through direct competition between taxa (predation, inhibition or suppression of competitors), as well as through biological behaviours (feeding on present sugars, breaking down complex carbohydrates for easier uptake, increasing population numbers through reproduction, respiration, cellular death) to name a few. While bacterial and fungal populations of compost ecosystems have been well-described by existing literature, as well as the mechanisms of their biological behaviours and competition, the literature on both feeding preferences and behaviour of nematodes in artificial compost networks is scant. Additionally, it is unclear how the behaviours of compost biota and their interaction with one another in the compost environment amalgamate, and in turn, explain changes in population numbers and resources in the compost. Stable isotope analysis performed on nematodes which have consumed isotopically labelled resources such as glucose can help elucidate their role in the *A. bisporus* compost food web in relation to other participants. PLFA biomarker analysis can facilitate recognition of biomass amounts of specific biological participants in the compost and aid their differentiation. Combining the two approaches allows for the creation of an interactive model which can present real-time consequences and further understanding of compost biota behaviours in the compost environment, as well as further understanding of changes in population densities and ecological parameters of the niche.

Nematode counts and their impact on the food web of the compost

Nematodes were extracted from labelled and unlabelled microcosm samples, and nematode populations were counted, after which the effect of treatments (presence of label, substrate type and sampling time) on the numbers of nematodes present was assessed. Through absolute and normalised population counts, a significant nematode count decrease was identified in all substrate types with progressive sampling times, as well as a strong trend towards lower overall nematode counts in labelled over unlabelled samples. Percent decreases in population densities between 12% and 87% with progressive sampling time were found in all replicates. Furthermore, compost to casing population density ratios displayed higher nematode counts in compost samples compared to casing samples, at the same sampling timepoint within the same replicates, possibly due to nematodes initially originating from compost. However, tests performed prior to choosing a method of nematode extraction showed that no nematodes were extracted at any sampling timepoint from either Phase II or Phase III compost, while nematodes were extracted from casing alone, and from casing combined with Phase III compost, possibly indicating that nematodes originate from casing, and

proliferate at the interface with compost during the later stages of incubation. Furthermore, when nematode numbers are normalised by volume, instead of by weight, the calculation gives indication towards the likelihood that, on average, nematodes are possibly higher in numbers in casing than in compost counterparts. This might be due to compacting of casing over time that creates an unliveable environment for nematodes, or possibly due to the need of juveniles for compost for development. In addition, results showed that in both compost and casing, the number of nematodes present is generally lower in samples where *A. bisporus* wasn't present, and is generally higher where *A. bisporus* was present, regardless of whether label was added. A possible explanation could be that with the lack of presence of the white button mushroom, the nematodes in compost lose access to a significant resource, which could particularly impact the fungivorous nematodes present, causing them to die off, and leaving a smaller overall number of nematodes in both substrates.

While microscopic in size, high abundance of nematodes displaying certain feeding habits in certain habitats can prove extremely destructive. In the artificial *A. bisporus* compost ecosystem, nematodes have been observed to infest mushroom beds and cause mycelial sparsity, changing the white spawn run primordia to brown. Resulting diseased substrate would emit a foul smell and cause decreasing total mushroom yield, if not outright total crop failure (Thind et al., 2004). Previous studies agree that the most important predictors for ways in which nematodes affect mycelial growth are nematode species present in the system/substrate, their feeding habits, and their densities (Kumar et al., 2007). Depending on preferential nutrient consumption, populations of nematodes in soil are known to be bacterivores, fungivores, predators, herbivores, saprovores, or omnivores (Freckman, 1982; Wasilewska, 1998; Yeates et al., 1993). The possible roles which nematodes play in compost environments all tie into their feeding preferences as a second-level consumer. In particular, bacterivore and fungivore nematodes do not feed directly on soil organic matter, but rather on first-level consumers (Beare et al., 1992). In *A. bisporus* mushroom bed environments, mycophagous and saprophagous nematodes are both the most common, and the most destructive. While mycophagous nematodes have been shown to have greater destructive potential, with only 3 nematodes per 100 grams compost enough to precipitate destruction of the entire mycelium within 70 days (Singh et al., 2011), saprophagous nematodes present less of a threat, with 300 - 500 nematodes per gram casing substrate necessary for an infestation which can damage the *A. bisporus* mycelium (Ansari et al., 2020). On top of that, fast multiplication is a trait common to most nematode species, with a fertility optimum matching *A. bisporus* cropping period compost temperatures (14 - 18°C), spawn run period temperatures of an actively growing mycelium (22 - 28°C) being unsuitable for reproduction, and most species regardless of feeding habits dying off in environmental temperatures higher than 30°C (Grewal, 1991). However, the occurrence of mycophagous nematodes in mushroom culture is rare under modern mushroom farming techniques (Rinker, 2017). As such, mycophagous nematodes are unlikely to be present, as they would be highly destructive even at the low population densities found in the microcosms of this study. Conversely,

saprophagous nematodes are generally more common, and can form resistant stages which enable their survival during pasteurisation temperatures (Leblanc et al., 2014), with declining nematode densities generally observed in cultures containing saprophytic over mycorrhizal fungi (Ruess & Dighton, 1996). While most studies see mycophagous nematodes as dangerous to the white button mushroom mycelium, there is disagreement on saprophagous nematodes, with some studies viewing them as destructive (Keshari & Kranti, 2020) and other as beneficial or neutral participants in small densities (Hesling, 1966; Moreton et al., 1956). Survival of saprophagous nematodes in very small numbers is indicative of high presence of suitable bacteria on which they can feed and multiply, if compost has been well prepared and pasteurised (Keshari & Kranti, 2020). Nematodes in compost being predominantly bacterivores also aligns with previous research (Briar et al., 2007; Bulluck III et al., 2002; Forge et al., 2005; Hu & Qi, 2010). However, fungivory is also possible, especially in manure-treated soil (Forge et al., 2005; Griffiths, 1994; Villenave et al., 2003).

In this study, nematode population densities were observed to decrease over time, but more intensely so in compost than in casing. A study by Grewal and Richardson (Grewal & Richardson, 1991) observed that, in instances when nematodes originate from compost, their population levels drop sharply over time, simultaneously increasing in the casing substrate. In all cases of nematodes originating from casing instead of migrating to casing from compost, nematode multiplication was characteristically intensive, resulting in high end-numbers and mushroom beds affected both in total crop yield and outward appearance. The findings of this study are in line with those of Grewal and Richardson, who found that initial lower numbers of nematodes in casing yield no significant effects during spawn run and reported that nematode population densities necessary in casing for an explosion in later population densities and subsequent nematode-caused mycelium inhibition were equal or larger than 267 nematodes/gram of casing substrate. The findings are further supported by studies finding infestation numbers to be as small as 100 and as large as 5000 nematodes/gram casing substrate, both extremes being much higher than densities present in this study (Ingratta & Olthof, 1979; Khanna & Sharma, 1988). The highest outlier nematode density found both in casing and compost of this study was measured to be 15 nematodes/gram substrate, with a general range of 1 to 6 nematodes/gram casing substrate and 1 to 9 nematodes/gram compost substrate, depending on the sampling time and replicate.

The proposed hypothesis is that nematodes in *A. bisporus* mushroom beds could be predominantly bacterivores or minor fungivores and possibly saprovores in feeding habits, placing them on the second trophic level in the compost food web, ultimately originating from the compost substrate. A hypothesis that nematodes migrate to casing from compost substrate is further supported by the fact that casing is rarely sterilised, has lower mycelial density and an abundant and naturally-occurring bacterial biota, with higher overall moisture levels compared to compost (Eger, 1972; Hayes et al., 1969). As the nematode population densities displayed a decrease over time, as opposed

to an increase, ultimately the nematodes present in mushroom beds did not lead to any visible sign of disease in primordia. While the scope of the experiment does factor in for the cropping period, sampling times for nematodes fall under the spawn run period, with the last sampling time point just after pinning. This further explains the drop in nematode populations, as they would be unable to withstand high compost temperatures brought on by mycelial growth, because nematodes cannot reproduce at temperatures higher than 22 - 28°C. The hypothesis is additionally supported by the calculated compost to casing population density ratio, which decreased over time in all instances, possibly suggesting an initial intensification in population growth in compost, followed by a shift of population levels via migration, decreasing the nematode population levels in compost with regards to casing.

Furthermore, growth of *A. bisporus* mycelium creates a nematostatic environment by producing volatile antibiotic substances (Grewal & Richardson, 1991; Keshari & Kranti, 2020). The decrease in nematode densities might also be pointing towards a general decrease in the preferred food source in compost, where a general decline of biomass of bacteria during the progression of the experiment would directly influence a strong decline in bacterivore nematodes (Ruess & Dighton, 1996). *A. bisporus* likewise creates a bacteriostatic environment, which reduces the availability of bacteria as a food resource (Barron, 1988; Grewal & Richardson, 1991; Tschierpe & Sinden, 1965). As the microcosms of this study had healthy and strong mycelium leading to vital and edible pins, it is likely that *A. bisporus* mycelia indirectly acted as the strongest competitor to any extant nematodes by creating toxic antibiotic enzymes and consuming and destroying nematode food supplies, exterminating the nematodes that otherwise remained after farming prevention procedures, hygienic measures and unsuitable environmental temperature conditions. When displaying healthy growth, *A. bisporus* mycelium's high use of all available compost moisture disables nematodes from moving (Flegg et al., 1985). Nematode have been found unable to compete with a healthy mycelium even in high numbers (Grewal & Richardson, 1991; Hesling, 1966; Tomalak & Lipa, 1991). Ross and Burden (Ross & Burden, 1981) have further found that presence of nematodes produces an effect where usually, either the mycelium or the nematode population is nearly fully suppressed, usually by direct competition for nutrients with the mushroom mycelium, where nematodes require bacteria as food and *A. bisporus* requires them as sporophore inductors, coupled with a simultaneous inability of the nematodes to structurally damage *A. bisporus*. Coupled with the preferential artificial propagation of conditions meant to be optimal for development of *A. bisporus*, nematodes found in this study likely didn't enjoy favourable conditions to multiply in. Alternatively, a possibility exists that nematode densities and present species are consistent with mycelial decline, but the length of the experiment is too short for it to present itself, with one study indicating no mycelial decline observed before day 57 after inoculation (Hesling, 1966). Mycelial disease could possibly manifest itself in less pronounced flushes over time, instead of total yield, which could be ultimately unaffected (Hesling, 1966).

Effect of ^{13}C-labelled glucose addition on nematodes

While statistical analysis showed no significant differences between ^{12}C and ^{13}C-glucose being utilised as a carbon source in the ecosystem, there was a strong trend pointing towards lower nematode populations in inoculums where ^{13}C-glucose was added (**Figure 6 and 7**). While the reason for this outcome is possibly random feeding of nematodes in compost on tracer and naturally abundant carbon, it is theoretically possible that the effect is due to isotopic fractionation, where primary consumers grazing on the glucose substrate preferentially choose simple sugars which are naturally abundant over those that have been isotopically enriched. The discrimination against ^{13}C is common and well-described in biological pathways (Volk et al., 2018), as living organisms tend to preferentially take up lighter isotopes (^{12}C rather than ^{13}C) due to a lower activation energy barrier associated with the lighter isotope, allowing for preferential formation into products. As nematodes are secondary consumers, any label consumed by primary consumers will take time before being incorporated into nematode tissue and organs, even after consumption of labelled organisms has already occurred (Middelburg et al., 2000; Moens et al., 2002; Van Oevelen et al., 2006).

Stable isotope analysis and δ^{13}C nematode signatures as trophic designators

Isotopic measurements were performed to acquire natural abundance δ^{13}C signatures of bulk nematodes. Furthermore, natural abundance δ^{13}C signatures were acquired from individual nematodes which fed on regular (unlabelled) glucose, as well as tracer δ^{13}C signatures from nematodes which fed on ^{13}C-labelled glucose. Extensive literature review has shown that LA-IRMS stable isotope measurements of δ^{13}C signatures in *A. bisporus* commercial beds presented here are the first of their kind. Therefore, measurements introduced are experimental in their nature and difficult to put into previous contexts. Furthermore, this study presents with the first known usage of LA-IRMS methods for stable isotope studies on nematodes, straying from its usual use-case in dinoflagellate and palynomorph measurements.

Extant literature on this topic generally concerns a broader variety of soil nematodes, with a focus on different feeding groups, with tracer δ^{13}C signatures usually obtained by the means of EA-IRMS. One of the first trophic studies of this type was performed by Neilson and Brown (Neilson & Brown, 1999). Stable isotope analysis on plant-parasitic nematodes in compost showed tracer δ^{13}C signature values of -28‰, -27.5‰, -26.4‰, -24.6‰, and -28.1‰, respectively, for five different species of nematodes observed, with a marked -1.6‰ to -3.3‰ depletion in δ^{13}C respective to the plant material they were fed on, the values of which are in line with the results of this study (Neilson & Brown, 1999). Sampedro and Dominguez reported tracer δ^{13}C values of -26‰ for nematodes extracted from pig slurry vermicomposting bins, the values of which align with the results of this study for labelled nematodes (Sampedro & Domínguez, 2008). Findings by Estifanos et al. indicated that bacterivores presented with tracer δ^{13}C = -23.33‰ to -21.19‰, meaning that a 1‰ enrichment could align

known bacterivores with the tracer $\delta^{13}C$ signature range presented in labelled compost nematodes of this study (Estifanos et al., 2013). In labelled experiments, stronger labelling evident in compost over casing would support this hypothesis, given that in the experimental approach of this study, label was added only in the compost substrate, allowing widespread availability of labelled simple sugars in compost, but not in the casing. Likewise, nematode life stages might affect the isotopic composition derived experimentally, with younger stages possibly feeding on different substrates to adult specimens (Yeates, 1987). For nematodes that are isotopically enriched, bacterivory offers a possible explanation as it could reflect direct nematode consumption on bacteria which are likewise directly feeding on labelled resources (Middelburg et al., 2000; Moens et al., 2002; Schmidt et al., 2004). As nematodes display isotopic labelling even in casing, it gives additional credence to the previously presented theory that nematodes will travel from compost to casing at some point during the experiment. However, lower relative tracer $\delta^{13}C$ can also be explained by biochemical differences over feeding habits, especially in the measurements derived from LA-IRMS, as the spot-focused measuring style of the instrument might preferentially hit a lipid reserve over proteins or carbohydrates, which tend to be higher in $\delta^{13}C$ (Schmidt et al., 2004). Natural abundance studies such as that of Crotty et al. reported $\delta^{13}C$ values of -26.75‰ for grassland ecosystem nematode fauna and -27.65‰ for woodland ecosystem nematode fauna, with no discernment among feeding types or species, likewise in line with unlabelled nematodes of this study (Crotty et al., 2013). Kudrin et al. further found that soil nematodes sourced from a boreal forest floor had distinct isotopic values at natural abundance level, representing trophic differences between microbial and predatory feeders, with natural abundance $\delta^{13}C$ ranging from -24.6‰ to -23.8‰ (Kudrin et al., 2015). Their measurements included those of the fungal mycelium as well, with a natural abundance $\delta^{13}C$ value range of roughly -28.8‰ to -26.5‰. As trophic fractionation is estimated to cause an approximate $\delta^{13}C$ increase of 0.5‰ - 1‰ (Post, 2002), certain nematode taxa of this study would fall within the range necessary to identify them as fungal feeders, supporting the findings made so far. Bacterivores tend to be on average 1‰ higher in natural abundance $\delta^{13}C$ than fungal feeders, which tend to be more depleted (Kudrin et al., 2015), which could indicate a likelihood that, on average, casing nematodes are preferentially bacterial and fungal feeders, while compost nematodes might prefer detrital resources instead, such as plant material or simple sugars.

In general, the distance between trophic levels in soils is known to be less intelligible than in other systems, due to soil food webs having more trophic levels than other food webs, omnivory of food web participants, and the levels being directly influenced by the dominant energy pathways within compost (Digel et al., 2014; Illig et al., 2005). Even though stable isotope values found in detrital consumers depend on the consumer's metabolism and type of diet (McCutchan Jr et al., 2003), individuals of different species fed the same diet may differ significantly in both their natural abundance and tracer $\delta^{13}C$ signatures, possibly due to differences in trophic fractionation due to varied ability to assimilate nutrients in the food, with a further

unclear relationship between ingested and assimilated food (Estifanos et al., 2013; Levey & Rio, 2001; Melody et al., 2016). This is apparent in the experimental measurements performed in this study with the LA-IRMS, which indicate high probability of not all present nematodes consuming the label, and in those that do, not all nematodes fully incorporating it into their tissues and organs by day 30 of the experiment. Likewise, nematodes have been found in labelled samples which measured values identical to those of unlabelled nematodes. Additionally, some labelled nematodes had a combination of highly labelled measurements and unlabelled measurements within a single run. This might hypothetically be due to feeding rates and physiology (Zanden & Rasmussen, 2001) or metabolization of carbon (Macko et al., 1987), meaning that nematodes which practice bacterivory or fungivory could ultimately present with slightly different $\delta^{13}C$ signatures within a trophic group despite consuming the same sources of food at the same location, presenting possible challenges to accurate determination of trophic levels.
The results of this study are in line with known literature values for soil nematodes, with the marked difference of labelled nematodes where some measurements of labelled nematodes display enrichment, while other measurements display a lack of enrichment, regularly within the same measured nematode. It is likely to conclude that intense labelling present is a result of direct feeding on bacteria and/or fungi which have consumed large amounts of the labelled glucose substrate, with a high probability of incomplete digestion of label in nematode tissues and organs. Labelling is likelier to be a product of dietary affinity rather than spatial distribution, as labelled glucose was well-mixed into the compost.

Comparison of EA-IRMS and LA-IRMS methods for nematode stable isotope analysis

Comparison between values acquired with the EA-IRMS and the LA-IRMS and the general higher relative depletion shown in results acquired through LA-IRMS may stem from the fact that EA-IRMS samples featured smaller and larger debris pieces stuck to nematode individuals transferred into tin cups for analysis, which were not possible to be fully removed or washed out from the nematodes prior to measurements. Upon incineration in the EA-IRMS, the isotopic signatures of the organic debris mix with those of the nematodes, inevitably reporting an overall higher isotopic signature. Conversely, on the LA-IRMS, while the nematode samples remained tainted with debris clinging to their surface, the precision of the laser allows for spot-targeting and the ability to fully target and incinerate only nematodes in desired quantities. Furthermore, as EA-IRMS incinerated ethanol-preserved samples, resulting $\delta^{13}C$ values may be biased, however, excess values calculated from LA-IRMS can provide an unbiased $\delta^{13}C$ value of measured nematodes, considering the calculation of excess values was based on tracer $\delta^{13}C$ signature measurements of the labelled nematode samples subtracted by the natural abundance $\delta^{13}C$ signature measurements of unlabelled nematode samples used as control.

Measurements were also performed on the LA-IRMS which purposefully targeted debris of the kinds which could be found adhering to the nematode surface in order to elucidate their isotopic signatures. Debris and straw present in original nematode samples were found to be significantly isotopically higher than nematodes. It is therefore possible that even very minor additions of debris to the tin cups skewed the natural abundance $\delta^{13}C$ signature results and calculated them to be more enriched than they truly were. Contaminating carbon effects of the EA-IRMS due to carrier material use are well-described in existing literature (van Roij et al., 2017).

Failure of visual observations of nematode mouthparts and subsequent use of LA-IRMS for nematode identification

Due to the lack of success with the visual observations of nematode mouthparts and their feeding preferences, LA-IRMS was used as a testing instrument for various types of components found in extracted nematodes samples. Among these were samples of thick straw, thick debris, thin debris and a suspected nematode individual. Visually, nematodes may appear similar to straw and debris under a compound microscope. However, completed LA-IRMS measurements showed nearly no overlap in natural abundance $\delta^{13}C$ signatures of straw and debris sourced from nematode samples. All samples tested showed considerably higher values, with natural abundance $\delta^{13}C$ ranging from -10‰ to +100‰ for straw, +30‰ to +270‰ for thick debris and +40‰ to +60‰ for thin debris. The results presented may partly be due to the matrix-dependent nature of the LA-IRMS, producing a biased matrix effect where the laser is possibly better at incinerating one type of substrate rather than another, resulting in quantifications of non-target analytes which can be unreliable (Zhang et al., 2020). For most accurate results, material tested on the LA-IRMS should have similar chemical make-up, and thickness as well as quantity of the tested material could prove problematic. However, resulting isotopic signatures measured for suspected nematodes align well with those of literature values.

$\delta^{13}C$ signature variability within and between nematodes

In both unlabelled and labelled nematodes, variability of natural abundance and tracer $\delta^{13}C$ signatures was analysed. Results indicated that isotopic signatures acquired via LA-IRMS vary, both within a single nematode (intra-nematode variability) and between nematodes of the same sample (inter-nematode variability).

The inter-variability was shown to be low in unlabelled nematodes, and high in labelled nematodes. One hypothesis is that inter-variability in unlabelled nematodes was low because feeding on natural abundance substrates would display more uniform $\delta^{13}C$ signatures. Contrastingly, high inter-variability in labelled nematodes was likely because not all nematodes in labelled samples fed on the same substrates, with same feeding rates and habits, and with the same rates of digestion, metabolization and

assimilation (Macko et al., 1987; Zanden & Rasmussen, 2001). The hypothesis is further supplemented by intra-nematode variability data. While in unlabelled nematodes, natural abundance $\delta^{13}C$ can vary 1‰ - 4‰ depending on the laser hit, in labelled nematodes tracer $\delta^{13}C$ signature range can be as high as 10‰ - 15‰ within a single nematode. These findings lend additional credence to previously presented hypothesis that positional incineration by the means of a precise laser could preferentially burn lipids, which tend to be isotopically more negative, proteins or carbohydrates which tend to be isotopically higher, and even possibly incinerate positions in nematode digestion systems which contain labelled food undigested at the time of preservation and extraction, leading to very enriched values compared to the mean isotopic signature of a particular nematode (Schmidt et al., 2004). Likewise, nematodes which have efficiently incorporated the label into their tissues and organs would present with less varied, more uniform, but overall higher isotopic values than unlabelled nematode counterparts.

Isotopic excess of ^{13}C-tracer in labelled nematodes as trophic indicator

In labelled nematodes, excess of the ^{13}C isotopic tracer versus the natural abundance was calculated based on measured isotopic signatures and calculated fractions and ratios of each LA-IRMS laser hit. The calculated excess proves translocation of the label into nematodes, with primary consumers as proxies to the labelled substrate. One hypothesis is that as secondary consumers, nematodes need more time for label to be consumed, processed and assimilated by primary consumers, after which primary consumers are consumed and assimilated by nematodes that feed on them, depositing label into their own tissues through metabolization. This is further corroborated by the fact that the amounts of excess present are small, in the 10^{-4} to 10^{-8} orders of magnitude, pointing towards nematodes acting as top controls of the food chain in *A. bisporus* ecosystem. Comparison between different substrates showed that, for a certain sampling time points, compost substrate nematodes have a higher amount of excess label than casing substrates. The increase of excess label in casing substrates is likewise, slower than observed in compost counterparts over the same time period, presenting an additional argument towards the theory of nematode migration from compost to casing, with the added possibility of nematodes which grow in casing beginning to feed on labelled substrate later on in the experiment (Christensen et al., 2007; Gibbs et al., 2005; Kenney et al., 2006; Scheepmaker et al., 1997). As label is uniformly distributed in the compost, nematodes consuming primary consumers which in turn, consumed labelled substrate, are both more abundant in compost and more intensely labelled. Through the act of upward migration, labelled nematodes habituate casing once it's applied atop compost, increasingly migrating over time. Once these nematodes inhabit compost, it is possible they feed increasingly on primary consumers which consume naturally abundant substrate present in casing. This behaviour could cause a far less rapid increase in excess over time. An increase already present could be owed to increased migration of nematodes from compost to casing as the time of the experiment progresses, as well as the possibility that their feeding rates are slow enough for the

excess to still be present in tissues at a significant level, despite switching the dietary source from labelled substrate found in compost to naturally abundant substrate found in casing.

Total concentrations and label incorporation in bacterial and fungal PLFA biomarkers in compost and casing

In compost, bacterial and fungal PLFA biomarker concentrations displayed a similar trend, with concentrations sharply rising through the first 7 days and sharply falling during the second week of the experiment. Much like with total PLFA concentrations, bacterial and fungal active biomass label incorporation observed similar trends, with active biomass nearly non-existent on the first day of the experiment, henceforth sharply rising through the first 7 days and sharply falling during the second week of the experiment. The results observed are consistent with previously performed PLFA analysis on smaller-scale mesocosms within this project. High amounts of PLFA concentrations already apparent on the first day of the experiment are consistent with previous findings that bacteria and fungi are present in the soil during the first days of the experiment. Active biomass of bacteria and fungi in compost at the first day of the experiment is near zero, indicating that while bacteria and fungi are present in the compost before the start of the experiment, most contribute in the form of deceased biomass, brought on from previous stages of preparation, niche formation and composting. One possible explanation for the sharp drop in both total and active biomass at day 14 lies in rapid consumption, suppression or outcompetition of bacteria and fungi by the developing *A. bisporus* mycelium. *A. bisporus* is well-documented for its capability of utilising active and deceased biomass as a resource, showing ability to survive solely off fungal biomass in compost (Fermor & Grant, 1985) as well as utilise bacterial biomass as nutrients (Vos et al., 2017), though it is unknown which resource it prefers.

Bacterial and fungal biomass presents with an apparent propensity for growth until inoculation with *A. bisporus*, at which point the two kingdoms both witness a sharp drop. From the point of 14 days onwards, the trends between different biota diverge, with bacterial concentrations continuing a decline, and fungal concentrations seeing a gradual increase towards the end of the experiment. Similar trends are mirrored in label uptake measurements, where active biomass activity diverged at day 14, with bacterial active biomass declining, and fungal active biomass seeing a sharp increase towards the end of the experiment. After a rapid biomass decline, and after casing is applied, bacterial biomass experiences a decrease in compost but a simultaneous increase in casing, possibly due to bacteria transport by bioturbation to casing once it's applied atop the compost. This theory is further supported by the fact that in casing, concentration trends were similar in both bacteria and fungi, displaying a linear increase until the end of the experiment. Active biomass trends were likewise similar in both bacteria and fungi, displaying a linear increase until the end of the experiment. An increase in fungal biomass is likewise seen in casing, at a more rapid pace and in

double the concentrations of bacteria, but the growth in fungal biomass is likewise mirrored in compost. One possible explanation for this is natural growth of *A. bisporus*, which colonises and penetrates the casing layer rapidly from the moment of inoculation, growing hyphae upwards into the casing and ultimately creating primordia on top. Overall, higher concentrations of fungi than bacteria in casing might likewise indicate a higher ability of fungi to colonise casing, with bacteria possibly utilising fungal hyphae for their own transport, with limited ability to do so on their own (Barto et al., 2012; Cameron et al., 2013; Schmidt et al., 2019). The reasons for increasing active fungal biomass in compost is unknown, however, it is theorised that either a succession of fungal communities occurs during the time of proliferation of *A. bisporus*, with fungal taxa appearing which are better suited for co-existing with *A. bisporus*, or that *A. bisporus* is partially at fault for the observed increase, as it shares the PLFA biomarker with that of the common PLFA biomarker for fungi (C18:2w6), possibly demonstrating a skewed result. However, as test cultivars previously created in which *A. bisporus* was inoculated in autoclaved compost displayed similar propensity for rebounded growth after day 14, *A. bisporus* might not be the reason behind the sudden biomass increase in fungi.

Unification of isotopic and biomarker data with the model

Isotopic data and biomarker data was tied together with a functional model representation of the *A. bisporus* mushroom bed ecosystem. The two-part model focused on modelling total carbon flow and modelling labelled carbon flow in the compost.

Total carbon food-web model scenario

The total carbon food-web model can be interpreted simply as displaying a marked decrease in biomasses of both bacteria and fungi, albeit at different rates, while at the same time displaying marked and consistent proliferation of *A. bisporus* biomass, which is consistent with biological experimental observations of compost beds. A possible reason for this is both a natural succession of organisms in the compost, but more likely, the reason is in *A. bisporus'* direct consumption of both active and deceased bacterial and fungal biomass, as indicated by PLFA biomarker studies. Bacterial biomass features a slightly sharper decline than fungal biomass, while fungal population biomass declines slowly, possibly due to a preference of *A. bisporus* towards disintegrating bacterial biomass, but also likely due to the fact that other fungal specimens contained in the compost likewise feed on bacteria, as well as bacterivorous nematodes, making bacteria a scarcer nutrient resource. Simultaneously to the drop in biomass of bacteria and fungi, *A. bisporus* biomass is shown to increase, initially at a slow rate, but subsequently almost exponentially, with biomass doubling towards the end of the experiment. This outcome matches what is seen in bioecological experiments, considering that day 17 to day 19 of the experiment usually mark the commencement of Phase IV, which is instigated by casing. While *A. bisporus* biomass does steadily

increase during the Phase III from the rye grain inoculate (which is considered in the model to be close to no biomass), true intensification in biomass amount is seen with the mycelial colonisation of the added casing and, consequently, the fruiting phase with formation of primordia on casing surface.

Additionally, to modelling carbon flow through biomass, the model further shows the fates of carbon by modelling flow through simple sugars, complex carbohydrates and emitted carbon dioxide. Simple sugars show an exponential, but overall small increase initially, which begins to level off at day 10 of the experiment, and levels off fully by day 20. These findings are validated by the findings of Jurak et al. well, where simple sugars (expressed in %w/w) were found to be ultimately higher at day 16 of the experiment, compared to the beginning of the experiment, with a similar overall percent increase (28% increase measured by Jurak et al. versus 35% increase seen in the model output) (Jurak et al., 2014). Conversely, complex carbohydrates display a steep decline, which likewise levels off around day 30 of the experiment. This outcome is likewise supported by Jurak et al., where complex carbohydrates are shown to decrease over the progress of the experiment, by a total of 14% by day 16 of the experiment, compared to Phase II (Jurak et al., 2015). The model displays a similar decrease on a smaller scale, for a total of 5% decrease compared to the beginning of the experiment. Carbon dioxide emitted from the compost shows steep growth up until day 10 of the experiment, after which slow levelling-off commences, tapering off around the end of the experiment. The model output matches well with cumulative carbon dioxide emission experimental measurements (van Dam, 2020), displaying fast growth during the first 10 days of the experiment, which is the period of most intense activity within the compost (feeding, breakdown of complex carbohydrates, growth of *A. bisporus* mycelium, etc.).

Labelled carbon flow model scenario

The version of the model tracing labelled carbon flow interprets a gradual initial consumption of ^{13}C-labelled glucose by the bacteria, similar to that of the fungal population. As validated by the PLFA biomarker studies, active bacterial and fungal biomass is shown to be at low levels during the first days of experiment but peaking 10 to 15 days in. Uptake of the label does not closely follow the biomass, which was likewise validated by PLFA biomarker studies, showing that a large portion of biomass in compost is deceased, and brought on from previous composting stages and biological communities. In the first few days of the experiment, little to no uptake of the label is seen in fungal populations. However, about 2-3 days in, fungi begin exponentially and rapidly depleting the labelled glucose. Peak glucose consumption is reached between day 12 and day 16 of the experiment, during a time when bacterial and fungal biomass has already decreased by 65% of the initial values, indicating high assimilation efficiency by living biomass in the compost. A hypothesis for the high ^{13}C label incorporation despite a heavily decreased biomass could lay in a possibility that *A. bisporus*, whose mycelium would be growing steadily for about two weeks by day 12

to day 16 of the experiment, at this point suppresses the pre-existing fungal population and outcompetes them, after which significant die-off of fungal biomass is observed. *A. bisporus* specific ^{13}C-label uptake shows consistency throughout the experiment, matching that of growing biomass. The same trends are seen in ^{13}C-labelled simple sugars and emitted carbon dioxide, with both outputs showing similar trends to natural abundance counterparts, albeit in smaller amounts, consistent with the original input of the glucose tracer.

Nematode feeding preferences in the context of the labelled carbon flow model output

While modelling nematodes as a carbon flow compartment of the compost food web has been omitted due to a lack of literature-based modelling parameters, as well as the lack of PLFA data, it is possible to discuss nematodes in the context of the current model output. Day 14 of the experiment generally showed highest densities of nematodes across all treatments, substrates and replicates. This was followed by day 21 nematode densities, with day 30 densities shown to be the smallest. Placing this knowledge in the context of modelling data, the previously discussed hypothesis of nematodes being predominantly bacterivores or minor fungivores is given additional traction. By day 14 of the experiment, most of the bacteria will have been already consumed. Conversely, by day 14, about 66% of fungal populations (not accounting for *A. bisporus*) will have been consumed. Highest nematode densities sampled at day 14 could be specimens of juvenile or adult bacterivore nematodes in high numbers, having just depleted bacterial sources. Persistence of nematodes in smaller densities past the point of depletion of compost bacteria alludes to nematode which persist being fungivores. However, it is likely that extant fungivore nematodes, in much smaller densities than with larger populations of bacteria, must compete versus rapidly growing *A. bisporus* for the fungal biomass as a source of food. As *A. bisporus* has been previously shown to aggressively attack other fungal populations (Atkey & Wood, 1983; Kertesz & Thai, 2018), it is likely that present densities of fungal nematodes are simply not high enough to proliferate in the power struggle against *A. bisporus*, or that *A. bisporus* is prolific at creating a nematode-hostile environment, or a combination of both of the aforementioned hypotheses. Extant nematodes being fungivores would likewise explain the tendency for large percent decreases in nematode densities between day 21 and day 30 (-28% to -86% decreases for individual replicates), as bacterivore nematodes would die out due to a lack of nutritive sources.

Model validation with biomarker studies and parameter calibration

The built model was validated using directly measured and analysed PLFA concentrations for total biomass and for active biomass. Total biomass was used to validate the total carbon food web model, while active biomass was used to validate the labelled tracer food web model. Both models followed general trends of respective compartments well, with the exception of fungi in both the total carbon and tracer carbon model. Even with careful calibration, the model was unable to replicate the

increase in PLFA biomarker concentrations in fungi after day 21 of the experiment, as visible in both active and total biomass. It is theorised that the model cannot replicate the behaviour of the experimental data due to the uncertainty as to which fungal behaviour causes the biomass increase. As there is uncertainty in the theoretical background, it is likely that the unknown behaviour needs to be separately added into the model and linked with existing compartments, depending on what kind of ecological function the resulting behaviour represents.

Theoretical, literature-sourced parameters agreed well with the model representation, except in the case of bacteria, where the parameters had to be calibrated away from literature values. Mortality of the bacteria was lowered to 0.1 from the minimum 0.24 mmol C/g/day, which was a concession made in lieu of values sourced from aquatic environments, versus the decomposing soil environment. Bacterial assimilation efficiency was raised to 40%, up from 30%, which aligned with original literature stating that general assimilation efficiency of bacteria is higher than that of fungi, sometimes up to 10 times. Bacterial uptake of simple sugars was raised to 0.2, just slightly higher than the literature maximum.

Study limitations, implications and future directions

Identification of feeding guilds via nematode head morphology

The strongest limitation of this study are the unsuccessful visual observations of nematode heads and identification of nematode taxa and feeding guilds via mouthparts. Purported reason for failure likely lies in the length of time during which deceased nematodes were preserved in ethanol, which is a drying agent. Considering that nematodes were preserved only in ethanol for almost a year, mouthparts and tails were likely severely dehydrated and suffered breakage and mechanical damage. Dehydration and mechanical damage likewise probably affected internal structures and organs, most notably stylets found in mouths of some nematode taxa, the intact presence of which is imperative for proper determination of feeding habits. Literature focusing on population analysis and nematode counts and identification generally employed fresh, living and recently extracted nematodes (Kanzaki, 2013; Wyss & Grundler, 1992). If nematodes were killed for the purposes of easier counting, fixation methods were immediately performed in order to preserve structures, necessitating use of preservative and fixative agents such as formaldehyde, methanol, or DESS solution, which should be applied immediately post-mortem (Van Bezooijen, 2006; Yoder et al., 2006). Accurate determination of nematode taxa, even if only at the level of feeding guilds, would serve a dual purpose: as a validation of measured isotopic $\delta^{13}C$ signatures of nematodes, but also deeper elucidation and validation of nematode trophic preferences at various points in time during *A. bisporus* cultivation. Without a sequestration of nematodes into feeding guilds with certainty and an insufficient number of nematodes sampled to perform a PLFA biomarker study, building the model with a nematode compartment for carbon flow would be difficult, if not inaccurate. As the model

requires precise descriptions of behaviours, including feeding, ascertaining either the exact species or direct feeding guilds is likely the only possible way to construct a conceptual model with certainty.

Expanding the *A. bisporus* compost food web with $\delta^{15}N$ signatures

A part of the limitation in elucidation of trophic levels lies in $\delta^{13}C$ signatures. While trophic level can be indicated from $\delta^{13}C$ signatures, which are found to increase by 0.5 - 1‰ with each trophic level due to isotope fractionation, $\delta^{15}N$ ($^{15}N/^{14}N$) has been found to increase by as much as 3 - 5‰ per successive trophic level (DeNiro & Epstein, 1978; Minagawa & Wada, 1984; Wada et al., 1993), allowing for more precise delineation of trophic categories and allowing more detailed reconstructions of dietary habits, as well as eliminating one-dimensional bias which can occur when using only one isotopic pair. Furthermore, incorporation of $\delta^{15}N$ measurements together with $\delta^{13}C$ allows for higher precision in food web mapping and differentiation between main and secondary food sources, especially in complex food webs with many possible primary and secondary dietary sources. Increases of $\delta^{15}N$ relative to diet make $\delta^{15}N$ useful for ranking animals into relative trophic levels, while $\delta^{13}C$ is better suited for direct tracing of energy resources (Neilson & Brown, 1999). However, usage of $\delta^{15}N$ is limited by a great diversity of soil-dwelling organisms and a small body of literature containing necessary information for building of more detailed food webs (Kudrin et al., 2015). In this study, measurements of this kind were likewise limited by equipment (LA-IRMS cannot measure nitrogen isotopic values) and comparatively small sample sizes (robust measurements on the EA-IRMS require more material than extracted from compost microcosms). Likewise, robust food web building necessitates a wide variety of $\delta^{13}C$ and $\delta^{15}N$ isotopic values of all other compost food web participants, which is both beyond the scope of the study, and scarcely covered in existing literature concerning *A. bisporus* mushroom beds and stable isotope studies.

Necessity for further LA-IRMS measurements on organic matter

The LA-IRMS measurements on nematodes presented in this study are the first of their kind, which in turn limits the scope of generalisations which can be made using the data. There is a general need for more LA-IRMS measurements on nematodes from compost and casing substrates in all stages of their life cycles, nematodes preserved in other fixatives, fresh, recently deceased nematodes, as well as nematodes for which feeding guilds or specific taxa have been predefined. There is also a tentative necessity for measurements to be performed on other *A. bisporus* food web participants, including *A. bisporus* itself. The utilisation of LA-IRMS on soft organic matter is a novel topic in biogeochemistry, and more measurements are needed for a robust validation of measurements performed thus far.

PLFA biomarker analysis limitations

PLFA analysis in fungal communities should be done with caution. The limitation lies in PLFA 18:2w6, which is a proxy PLFA found in fungal communities, but also in *A. bisporus*. In some conditions, using this PLFA makes it so that the effects of various autochthonous fungal populations vs the effects of allochthonous *A. bisporus* cannot always be elucidated with certainty. Furthermore, PLFAs are not ideal proxies for biomass, especially in cases of successive generations of fungi occurring in compost. Ways to combat this included creating microcosms which included industry standard fungal densities, but also microcosms which included low fungal densities and those that had no *A. bisporus* inoculum added. PLFAs measured from such microcosms served to mechanically separate the effect displayed by PLFA analysis from niches where both *A. bisporus* and other fungal communities could be found, compared to niches where *A. bisporus* wasn't present. However, this method isn't exact, and relies heavily on experimental data which may be dependent on growth conditions, incubation conditions, environmental controls, and possible microbiota dynamics which shift with changing populations.

Food web model constraints

Model parameters have been validated by using real-world values, usually acquired experimentally or through existing literature on the topic of soil food webs. However, this literature is scarce, and parametrisation sometimes dependent on using values from very different ecological settings to that of the *A. bisporus* compost food web. While it is imperative to define parameters as closely to reality as possible, some of the parameters utilised for calibration are very difficult to directly measure.

Besides the need for accurate, detailed and direct measurements of parameters of real-life behaviours, this model could be additionally improved by statistical analysis. Identifiability analysis could be performed for determination of how well the model parameters were estimated, both by quantity and quality of experimental data. Markov Chain Monte Carlo (MCMC) algorithm could also be utilised to assess the model parameters, construct probability intervals and ensure statistical consistency (Soetaert & Petzoldt, 2010).

Finally, the quality of the model output is highly affected by the model's design. Models are simplified representations of observed and known reality. As such, complex behaviours are often simplified due to a lack of scientific knowledge on the topic or a lack of readily available data. However, simplification is often also done for the sake of easier understanding of the processes, easier relaying to the wider scientific community, and easier implementation, which in turn assures less error, a faster runtime and a more stable base on which to add more complex behaviours in future iterations. As an example, an obvious future direction of the model includes the addition of nematodes as a carbon flux compartment. In doing so, one would have to consider whether to

separate the feeding guilds into separate compartments, as some nematodes could possibly act predatory towards other nematodes in compost, while some might feed on complex carbohydrates. For this, visual observations of mouthparts, PLFA analysis and possibly even DNA analysis would be necessary in order to obtain values for parameters needed for an accurate model. Furthermore, while behaviours describing nematode feeding are complex, and the differential equations, rate laws and mass balances affect different carbon compartments in different ways, as predator-prey relations are ecologically modelled via Lotka-Volterra differential equations, and simple degradation via maximum uptake rate differential equations.

Conclusion

Nematode stable isotope analysis, together with PLFA biomarker analysis, nematode density counts, visual observations of nematode mouthparts and interactive carbon flow modelling in *A. bisporus* compost has been performed. Nematodes have been shown to more densely populate compost substrates than casing substrates, with percent decreases in population densities between 20 to 80% with each consecutive sampling week of the experiment. Sampling time has been proven to affect nematode densities in substrate, while labelling showed elements of a trend with generally lower counts in labelled than unlabelled samples. Decreases of population densities could be due to unsuitable conditions within compost and casing for development of nematodes, possibly further exacerbated by *A. bisporus* creating a hostile environment. Nematode densities were shown to be on average 2 to 5 times higher in compost substrate versus casing substrate. The likely reason nematodes were found in casing is due to nematode transport from compost to casing substrate. EA-IRMS analysis on nematodes indicated, on average, higher natural abundance $\delta^{13}C$ signatures than those acquired via LA-IRMS analysis, by 1.61‰ to 1.93‰. The higher $\delta^{13}C$ signatures were likely measured due to presence of debris which are impossible to fully eliminate from nematode samples for the EA-IRMS measurements but are possible to purposefully not target during LA-IRMS measurements. LA-IRMS measurements on labelled nematodes further indicated higher tracer $\delta^{13}C$ values in compost, than in casing nematodes, ranging from 2.69‰ to 5.19‰ and increasing with each sampling time point, likely due to labelled glucose being spread in compost, but not in casing substrate. In unlabelled nematodes, natural abundance $\delta^{13}C$ signature difference between casing and compost nematodes varied from 0.15 to 1.09‰. Labelled nematodes were found to have higher tracer $\delta^{13}C$ signatures overall compared to unlabelled nematodes sourced from same substrates and at the same sampling times. Labelled nematodes were further found to be very variable in tracer $\delta^{13}C$ signatures both within individual measured nematodes (highest span 31‰) and between nematodes of the same sample (highest span 18.2‰), with a possible explanation of LA-IRMS randomly targeting specific parts of nematode bodies which preferentially contained isotopically lower or higher organic matter. Variability could further possibly point to the fact that not all nematodes incorporate labelled glucose, and those who do, do not fully process it during the experiment. A considerably lesser variability was found in unlabelled nematodes, with a natural abundance $\delta^{13}C$ signature span of 9.1‰ between nematodes and 8‰ within nematodes. Tracer ^{13}C isotopic label excess was found in labelled nematodes, with excess being higher in compost than in casing-sourced nematodes. Excess steadily increased in both casing and compost-sourced nematodes within each subsequent sampling time, indicating that nematode in general need a lot of time to uptake the label from food sources, especially if they are the last trophic step in the food web. Simultaneously, LA-IRMS measurements were used to prove that natural abundance and tracer $\delta^{13}C$ signatures of measured nematodes align with those of literature values. Measurements performed with the same instrument on

thinner and thicker debris, as well as straw which can visually be quite similar to nematode individuals, showed much more positive values, with almost no $\delta^{13}C$ signature overlap with nematode values. PLFA biomarker studies showed that, in the performed experiments, total bacterial and fungal biomass had a trend of rising until day 7, abruptly falling by day 14, and then continuing the decline in bacteria, but displaying a rapid increase in fungi. PLFA active biomass analysis showed similar trends, proving that at day 0 most of the biomass is from previous composting cycles and not active. However, active biomass sees an increase by day 7, decrease by day 14, and a subsequent decrease in bacteria and increase in fungi. This phenomenon is as of yet unexplained, though possibly influenced by the shared fungal biomarker during a period of rapid *A. bisporus* growth, or otherwise, a succession of different species of fungi proliferating in the compost parallel to *A. bisporus'* growth. Finally, a model was built in R in two versions. The total carbon flow version of the model tracked carbon flows between compartments of bacterial biomass, fungal biomass, *A. bisporus* biomass, simple sugars, complex carbohydrates and CO_2. Bacterial biomass was shown to rapidly deplete within the first 10 days of the experiment, while fungal biomass depleted gradually, and fully only around the end of the experiment. Simultaneously, *A. bisporus* biomass grew steadily during the experiment, showing more intensive growth 15 days into the experiment. Simple sugars initially increased, before an equilibrium appeared about 20 days in. Concurrently, amounts of complex carbohydrates showed a slow decline, before equilibrating after about 30 days of the experiment. Emitted CO_2 grew rapidly during the first 20 days, equilibrating afterwards. Isotopic tracer version of the model showed that bacteria swiftly consume the label within the first 10 days, while fungal populations lag in food consumption at first, afterwards showing exponential consumption, topping off around 15 days into the experiment, and slowly levelling-off after the peak. *A. bisporus* consumed label gradually, increasing consumption about 20 days in. Simple sugars, complex carbohydrates and emitted CO_2 displayed similar behaviour as in the total carbon version of the model. Visual observations of nematode mouthparts proved unsuccessful, likely due to the agent used for preservation, failure to use fresh samples or mechanical damage to mouths and tails. Future studies are advised to continue expansion of the model, either by the addition of a nematode compartment to the model, by adding more behaviours, especially those of complex nature, as well as shifting focus to real-life measurements of parameters from biogeochemical behaviours needed for ecological modelling and subsequent statistical validation of derived parameters. Further LA-IRMS measurements on both nematodes and other organic interactors of the *A. bisporus* food web is likewise encouraged, due to a lack of body of literature on this novel scientific method. This study has improved on existing knowledge on nematodes in soil, particularly on population counts, composition, and isotopic signatures of nematodes as dietary indicators in commercial white button mushroom compost and casing, as well as validated experimentally observed and theorised trophic and behavioural interactions of soil food web collaborators.

References

Agnew, J., & Leonard, J. (2003). The physical properties of compost. *Compost Science & Utilization*, *11*(3), 238-264.

Ahlgren, G., Gustafsson, I. B., & Boberg, M. (1992). FATTY ACID CONTENT AND CHEMICAL COMPOSITION OF FRESHWATER MICROALGAE 1. *Journal of phycology*, *28*(1), 37-50.

Anderson, R. V., Gould, W. D., Ingham, R. E., & Coleman, D. C. (1979). A staining method for nematodes: determination of nematode resistant stages and direct counts from soil. *Transactions of the American Microscopical Society*, 213-218.

Ansari, R. A., Rizvi, R., & Mahmood, I. (2020). *Management of phytonematodes: recent advances and future challenges*. Springer.

Atila, F., Owaid, M. N., & Shariati, M. A. (2021). The nutritional and medical benefits of Agaricus bisporus: a review. *Journal of Microbiology, Biotechnology and Food Sciences*, *2021*, 281-286.

Atkey, P., & Wood, D. (1983). An electron microscope study of wheat straw composted as a substrate for the cultivation of the edible mushroom (Agaricus bisporus). *Journal of applied bacteriology*, *55*(2), 293-304.

Attiwill, P. M., & Adams, M. A. (1993). Nutrient cycling in forests. *New phytologist*, *124*(4), 561-582.

Bååth, E., Frostegård, Å., & Fritze, H. (1992). Soil bacterial biomass, activity, phospholipid fatty acid pattern, and pH tolerance in an area polluted with alkaline dust deposition. *Applied and Environmental Microbiology*, *58*(12), 4026-4031.

Barron, G. (1988). Microcolonies of bacteria as a nutrient source for lignicolous and other fungi. *Canadian Journal of Botany*, *66*(12), 2505-2510.

Barto, E. K., Weidenhamer, J. D., Cipollini, D., & Rillig, M. C. (2012). Fungal superhighways: do common mycorrhizal networks enhance below ground communication? *Trends in plant science*, *17*(11), 633-637.

Basting, D., & Marowsky, G. (2005). Excimer laser technology.

Beare, M. H., Parmelee, R. W., Hendrix, P. F., Cheng, W., Coleman, D. C., & Crossley Jr, D. (1992). Microbial and faunal interactions and effects on litter nitrogen and decomposition in agroecosystems. *Ecological Monographs*, *62*(4), 569-591.

Berendsen, R. L., Baars, J. J., Kalkhove, S. I., Lugones, L. G., Wösten, H. A., & Bakker, P. A. (2010). Lecanicillium fungicola: causal agent of dry bubble disease in white-button mushroom. *Molecular plant pathology*, *11*(5), 585-595.

Bhushan, A., & Kulshreshtha, M. (2018). The medicinal mushroom Agaricus bisporus: review of phytopharmacology and potential role in the treatment of various diseases. *Journal of Nature and Science of Medicine*, *1*(1), 4.

Bligh, E. G., & Dyer, W. J. (1959). A rapid method of total lipid extraction and purification. *Canadian journal of biochemistry and physiology*, *37*(8), 911-917.

Bongers, T., & Bongers, M. (1998). Functional diversity of nematodes. *Applied Soil Ecology*, *10*(3), 239-251.

Bongers, T., & Ferris, H. (1999). Nematode community structure as a bioindicator in environmental monitoring. *Trends in Ecology & Evolution*, *14*(6), 224-228.

Boschker, H., & Middelburg, J. (2002). Stable isotopes and biomarkers in microbial ecology. *FEMS Microbiology Ecology*, *40*(2), 85-95.

Bowman, J. P., Sly, L. I., Nichols, P. D., & Hayward, A. (1993). Revised taxonomy of the methanotrophs: description of Methylobacter gen. nov., emendation of Methylococcus, validation of Methylosinus and Methylocystis species, and a proposal that the family Methylococcaceae includes only the group I methanotrophs. *International Journal of Systematic and Evolutionary Microbiology*, *43*(4), 735-753.

Briar, S. S., Jagdale, G. B., Cheng, Z., Hoy, C. W., Miller, S. A., & Grewal, P. S. (2007). Indicative value of soil nematode food web indices and trophic group abundance in differentiating habitats with a gradient of anthropogenic impact. *Environmental Bioindicators*, *2*(3), 146-160.

Broekmans, M., Nijland, T. G., & Jansen, J. B. H. (1994). Are stable isotopic trends in amphibolite to granulite facies transitions metamorphic or diagenetic?-An answer for the Arendal Area (Bamble Sector, southeastern Norway) from Mid-Proterozoic carbon-bearing rocks. *American Journal of Science*, *294*(9), 1135-1165.

Bulluck III, L., Barker, K., & Ristaino, J. (2002). Influences of organic and synthetic soil fertility amendments on nematode trophic groups and community dynamics under tomatoes. *Applied Soil Ecology*, *21*(3), 233-250.

Bybd Jr, D., Kirkpatrick, T., & Barker, K. (1983). An improved technique for clearing and staining plant tissues for detection of nematodes. *Journal of nematology*, *15*(1), 142.

Cameron, D. D., Neal, A. L., van Wees, S. C., & Ton, J. (2013). Mycorrhiza-induced resistance: more than the sum of its parts? *Trends in plant science*, *18*(10), 539-545.

Castilho, R. C., de Moraes, G. J., Silva, E. S., Freire, R. A., & Da Eira, F. C. (2009). The predatory mite Stratiolaelaps scimitus as a control agent of the fungus gnat Bradysia matogrossensis in commercial production of the mushroom Agaricus bisporus. *International Journal of Pest Management*, *55*(3), 181-185.

Chang, S. T., & Wasser, S. P. (2017). The cultivation and environmental impact of mushrooms. In *Oxford Research Encyclopedia of Environmental Science*.

Chang, W., Cheng, J., Allaire, J., Xie, Y., & McPherson, J. (2015). Package 'shiny'. *See http://citeseerx. ist. psu. edu/viewdoc/download*.

Chmura, G., & Aharon, P. (1995). Stable carbon isotope signatures of sedimentary carbon in coastal wetlands as indicators of salinity regime. *Journal of Coastal Research*, 124-135.

Christensen, S., Alphei, J., Vestergård, M., & Vestergaard, P. (2007). Nematode migration and nutrient diffusion between vetch and barley material in soil. *Soil Biology and Biochemistry*, *39*(7), 1410-1417.

Coplen, T. B., Brand, W. A., Gehre, M., Gröning, M., Meijer, H. A., Toman, B., & Verkouteren, R. M. (2006). New guidelines for δ 13C measurements. *Analytical chemistry*, *78*(7), 2439-2441.

Crotty, F. V., Adl, S. M., Blackshaw, R. P., & Murray, P. J. (2013). Measuring soil protist respiration and ingestion rates using stable isotopes. *Soil Biology and Biochemistry*, *57*, 919-921.

De Kluijver, A., Bart, M. C., Van Oevelen, D., De Goeij, J. M., Leys, S. P., Maier, S. R., Maldonado, M., Soetaert, K., Verbiest, S., & Middelburg, J. J. (2021). An integrative model of carbon and nitrogen metabolism in a common deep-sea sponge (Geodia barretti). *Frontiers in Marine Science*, *7*, 596251.

de Vries, F. T., & Caruso, T. (2016). Eating from the same plate? Revisiting the role of labile carbon inputs in the soil food web. *Soil Biology and Biochemistry*, *102*, 4-9.

DeNiro, M. J., & Epstein, S. (1978). Influence of diet on the distribution of carbon isotopes in animals. *Geochimica et cosmochimica acta*, *42*(5), 495-506.

Derikx, P., De Jong, G., Op den Camp, H., Van der Drift, C., Van Griensven, L., & Vogels, G. (1989). Isolation and characterization of thermophilic methanogenic bacteria from mushroom compost. *FEMS Microbiology Ecology*, *5*(4), 251-257.

Dias, E. S., Zied, D. C., & Rinker, D. L. (2013). Physiologic response of Agaricus subrufescens using different casing materials and practices applied in the cultivation of Agaricus bisporus. *Fungal biology*, *117*(7-8), 569-575.

Digel, C., Curtsdotter, A., Riede, J., Klarner, B., & Brose, U. (2014). Unravelling the complex structure of forest soil food webs: higher omnivory and more trophic levels. *Oikos*, *123*(10), 1157-1172.

Dijkman, N. A., Boschker, H. T., Stal, L. J., & Kromkamp, J. C. (2010). Composition and heterogeneity of the microbial community in a coastal microbial mat as revealed by the analysis of pigments and phospholipid-derived fatty acids. *Journal of Sea Research*, *63*(1), 62-70.

Dungait, J., Kemmitt, S., Michallon, L., Guo, S., Wen, Q., Brookes, P., & Evershed, R. (2011). Variable responses of the soil microbial biomass to trace concentrations of 13C-labelled glucose, using 13C-PLFA analysis. *European Journal of Soil Science*, *62*(1), 117-126.

Dunn-Coleman, N. S., & Michaels, T. J. (1989). Composting process for the production of mushroom cultivation substrates. In: Google Patents.

Eger, G. (1972). Experiments and comments on the action of bacteria on sporophore initiation in Agaricus bisporus. *Mushroom Sci*, *8*, 719-725.

Estifanos, T. K., Traunspurger, W., & Peters, L. (2013). Selective feeding in nematodes: a stable isotope analysis of bacteria and algae as food sources for free-living nematodes. *Nematology*, *15*(1), 1-13.

Federle, T. W., Dobbins, D. C., Thornton-Manning, J. R., & Jones, D. D. (1986). Microbial biomass, activity, and community structure in subsurface soils. *Groundwater*, *24*(3), 365-374.

Fermor, T., & Grant, W. (1985). Degradation of fungal and actinomycete mycelia by Agaricus bisporus. *Microbiology*, *131*(7), 1729-1734.

Fermor, T., Randle, P., & Smith, J. (1985). Compost as a substrate and its preparation. *Biology and technology of the cultivated mushroom/edited by PB Flegg, DM Spencer, and DA Wood*.

Flegg, P. B., Spencer, D. M., & Wood, D. A. (1985). *Biology and technology of the cultivated mushroom*. Wiley.

Flint, M. L., & Dreistadt, S. H. (1998). *Natural enemies handbook: the illustrated guide to biological pest control* (Vol. 3386). Univ of California Press.

Forge, T., Bittman, S., & Kowalenko, C. (2005). Responses of grassland soil nematodes and protozoa to multi-year and single-year applications of dairy manure slurry and fertilizer. *Soil Biology and Biochemistry*, *37*(10), 1751-1762.

Foucreau, N., Puijalon, S., Hervant, F., & Piscart, C. (2013). Effect of leaf litter characteristics on leaf conditioning and on consumption by G ammarus pulex. *Freshwater Biology*, *58*(8), 1672-1681.

Francisco, R., Stone, D., Creamer, R. E., Sousa, J. P., & Morais, P. V. (2016). European scale analysis of phospholipid fatty acid composition of soils to establish operating ranges. *Applied Soil Ecology*, *97*, 49-60.

Freckman, D. (1982). Parameters of the nematode contribution to ecosystems [Soil fauna].

Frostegård, A., & Bååth, E. (1996). The use of phospholipid fatty acid analysis to estimate bacterial and fungal biomass in soil. *Biology and fertility of soils*, *22*(1), 59-65.

Frostegård, Å., Tunlid, A., & Bååth, E. (1993). Phospholipid fatty acid composition, biomass, and activity of microbial communities from two soil types experimentally exposed to different heavy metals. *Applied and Environmental Microbiology*, *59*(11), 3605-3617.

Frostegård, Å., Tunlid, A., & Bååth, E. (2011). Use and misuse of PLFA measurements in soils. *Soil Biology and Biochemistry*, *43*(8), 1621-1625.

Gibbs, D. S., Anderson, G. L., Beuchat, L. R., Carta, L. K., & Williams, P. L. (2005). Potential role of Diploscapter sp. strain LKC25, a bacterivorous nematode from soil, as a vector of food-borne pathogenic bacteria to preharvest fruits and vegetables. *Applied and Environmental Microbiology*, *71*(5), 2433-2437.

Gillan, F. T., Stoilov, I. L., Thompson, J. E., Hogg, R. W., Wilkinson, C. R., & Djerassi, C. (1988). Fatty acids as biological markers for bacterial symbionts in sponges. *Lipids*, *23*(12), 1139-1145.

Grassineau, N. V. (2006). High-precision EA-IRMS analysis of S and C isotopes in geological materials. *Applied Geochemistry*, *21*(5), 756-765.

Grewal, P. (1991). Relative contribution of nematodes (Caenorhabditis elegans) and bacteria towards the disruption of flushing patterns and losses in yield and quality of mushrooms (Agaricus bisporus). *Annals of applied biology*, *119*(3), 483-499.

Grewal, P., & Richardson, P. (1991). Effects of Caenorhabditis elegans (Nematoda: Rhabditidae) on yield and quality of the cultivated mushroom Agaricus bisporus. *Annals of applied biology*, *118*(2), 381-394.

Grewal, P., Richardson, P., Collins, G., & Edmondson, R. (1992). Comparative effects of Steinernema feltiae (Nematoda: Steinernematidae) and insecticides on yield and cropping of the mushroom Agaricus bisporus. *Annals of applied biology*, *121*(3), 511-520.

Grewal, P. S. (1989). Nematicidal effects of some plant-extracts to Aphelenchoides composticola (Nematoda) infesting mushroom, Agaricus bisporus. *Revue de nématologie*, *12*(3), 317-322.

Griffiths, B. (1994). Microbial-feeding nematodes and protozoa in soil: Their effectson microbial activity and nitrogen mineralization in decomposition hotspots and the rhizosphere. *Plant and soil*, *164*(1), 25-33.

Gujarathi, G., & Pejaver, M. K. (2011). Study of Diversity of compost fauna from different Biocompost samples.

Hallmann, J., & Subbotin, S. A. (2018). Methods for extraction, processing and detection of plant and soil nematodes. *Plant Parasitic Nematodes in Subtropical and Tropical Agriculture, 3rd ed.; Sikora, RA, Coyne, D., Hallmann, J., Timper, P., Eds*, 87-119.

Hassan, M. (2013). MORPHOLOGICAL STRUCTURES AND CHARACTERS OF PLANT PARASITIC NEMATODE UNDER SCANNING ELECRON MICROSCOPY (SEM). *Malaysian Journal of Microscopy*, *9*(1).

Hayes, J. M. (2004). An introduction to isotopic calculations. *Woods Hole Oceanographic Institution, Woods Hole, MA*, *2543*.

Hayes, W., Randle, P. E., & Last, F. (1969). The nature of the microbial stimulus affecting sporophore formation in Agaricus bisporus (Lange) Sing. *Annals of applied biology*, *64*(1), 177-187.

Hesling, J. (1966). The effect of some microphagous saprobic nematodes on mushroom culture. *Annals of applied biology*, *58*(3), 477-486.

Hu, C., & Qi, Y. (2010). Effect of compost and chemical fertilizer on soil nematode community in a Chinese maize field. *European Journal of Soil Biology*, *46*(3-4), 230-236.

Iiyama, K., Stone, B. A., & Macauley, B. J. (1994). Compositional changes in compost during composting and growth of Agaricus bisporus. *Applied and Environmental Microbiology*, *60*(5), 1538-1546.

Illig, J., Langel, R., Norton, R. A., Scheu, S., & Maraun, M. (2005). Where are the decomposers? Uncovering the soil food web of a tropical montane rain forest in southern Ecuador using stable isotopes (15N). *Journal of Tropical Ecology*, *21*(5), 589-593.

Ingham, R. E. (1994). Nematodes. *Methods of Soil Analysis: Part 2 Microbiological and Biochemical Properties*, *5*, 459-490.

Ingratta, F., & Olthof, T. H. (1979). influence of saprophagous nematodes on the production of Agaricus brunnescens (Bisporus). *Mushroom science*.

Jagadish, L. K., Krishnan, V. V., Shenbhagaraman, R., & Kaviyarasan, V. (2009). Comparitive study on the antioxidant, anticancer and antimicrobial property of Agaricus bisporus (JE Lange) Imbach before and after boiling. *African Journal of Biotechnology*, *8*(4).

Jurak, E., Kabel, M. A., & Gruppen, H. (2014). Carbohydrate composition of compost during composting and mycelium growth of Agaricus bisporus. *Carbohydrate polymers*, *101*, 281-288.

Jurak, E., Punt, A. M., Arts, W., Kabel, M. A., & Gruppen, H. (2015). Fate of carbohydrates and lignin during composting and mycelium growth of Agaricus bisporus on wheat straw based compost. *PloS one*, *10*(10), e0138909.

Kabel, M. A., Jurak, E., Mäkelä, M. R., & De Vries, R. P. (2017). Occurrence and function of enzymes for lignocellulose degradation in commercial Agaricus bisporus cultivation. *Applied microbiology and biotechnology*, *101*(11), 4363-4369.

Kanzaki, N. (2013). Simple methods for morphological observation of nematodes. *Nematological Research (Japanese Journal of Nematology)*, *43*(1), 15-17.

Kenney, S. J., Anderson, G. L., Williams, P. L., Millner, P. D., & Beuchat, L. R. (2006). Migration of Caenorhabditis elegans to manure and manure compost and potential for transport of Salmonella newport to fruits and vegetables. *International journal of food microbiology*, *106*(1), 61-68.

Kertesz, M. A., & Thai, M. (2018). Compost bacteria and fungi that influence growth and development of Agaricus bisporus and other commercial mushrooms. *Applied microbiology and biotechnology*, *102*(4), 1639-1650.

Keshari, N., & Kranti, K. (2020). Integrated management of phytopathogenic nematodes infesting mushroom. In *Management of Phytonematodes: Recent Advances and Future Challenges* (pp. 141-170). Springer.

Khanna, A. S., & Sharma, N. K. (1988). Effect of population levels and time of infestation of Aphelenchoides agarici on the mycelial growth of Agaricus bisporus. *Nematologia Mediterranea*.

Kohlmeier, S., Smits, T. H., Ford, R. M., Keel, C., Harms, H., & Wick, L. Y. (2005). Taking the fungal highway: mobilization of pollutant-degrading bacteria by fungi. *Environmental science & technology*, *39*(12), 4640-4646.

Kozarski, M., Klaus, A., Niksic, M., Jakovljevic, D., Helsper, J. P., & Van Griensven, L. J. (2011). Antioxidative and immunomodulating activities of polysaccharide extracts of the medicinal mushrooms Agaricus bisporus, Agaricus brasiliensis, Ganoderma lucidum and Phellinus linteus. *Food chemistry*, *129*(4), 1667-1675.

Kroppenstedt, R. (1985). Fatty acid and menaquinone analysis of actinomycetes and related organisms. *Chemical methods in bacterial systematics*, 173-199.

Kudrin, A. A., Tsurikov, S. M., & Tiunov, A. V. (2015). Trophic position of microbivorous and predatory soil nematodes in a boreal forest as indicated by stable isotope analysis. *Soil Biology and Biochemistry*, *86*, 193-200.

Kumar, S., Khanna, A., & Chandel, Y. (2007). Effect of population levels of Aphelenchoides swarupi and Aphelenchus avenae inoculated at spawning on mycelial growth of mushrooms and nematode multiplication. *Nematologia Mediterranea*.

Leblanc, M., Berry, K., Graciano, S., Becker, B., & Reuter, J. D. (2014). False-positive results after environmental pinworm PCR testing due to rhabditid

nematodes in corncob bedding. *Journal of the American Association for Laboratory Animal Science*, *53*(6), 717-724.

Levey, D. J., & Rio, C. M. d. (2001). It takes guts (and more) to eat fruit: lessons from avian nutritional ecology. *The Auk*, *118*(4), 819-831.

Logatcheva, K., Smit, P., & van der Meulen, H. (2014). Market intelligence champignons: productie en handel van Nederlandse champignons in context.

Macko, S. A., Fogel, M. L., Hare, P. E., & Hoering, T. (1987). Isotopic fractionation of nitrogen and carbon in the synthesis of amino acids by microorganisms. *Chemical Geology: Isotope Geoscience section*, *65*(1), 79-92.

McCutchan Jr, J. H., Lewis Jr, W. M., Kendall, C., & McGrath, C. C. (2003). Variation in trophic shift for stable isotope ratios of carbon, nitrogen, and sulfur. *Oikos*, *102*(2), 378-390.

McGee, C. F. (2018). Microbial ecology of the Agaricus bisporus mushroom cropping process. *Applied microbiology and biotechnology*, *102*(3), 1075-1083.

Meire, L., Soetaert, K., & Meysman, F. (2013). Impact of global change on coastal oxygen dynamics and risk of hypoxia. *Biogeosciences*, *10*(4), 2633-2653.

Melody, C., Griffiths, B., Dyckmans, J., & Schmidt, O. (2016). Stable isotope analysis (δ13C and δ15N) of soil nematodes from four feeding groups. *PeerJ*, *4*, e2372.

Mercer, D. K., Iqbal, M., Miller, P., & McCarthy, A. (1996). Screening actinomycetes for extracellular peroxidase activity. *Applied and Environmental Microbiology*, *62*(6), 2186-2190.

Middelburg, J. (2014). Stable isotopes dissect aquatic food webs from the top to the bottom. *Biogeosciences*, *11*(8), 2357-2371.

Middelburg, J. J., Barranguet, C., Boschker, H. T., Herman, P. M., Moens, T., & Heip, C. H. (2000). The fate of intertidal microphytobenthos carbon: An in situ 13C-labeling study. *Limnology and oceanography*, *45*(6), 1224-1234.

Minagawa, M., & Wada, E. (1984). Stepwise enrichment of 15N along food chains: further evidence and the relation between δ15N and animal age. *Geochimica et cosmochimica acta*, *48*(5), 1135-1140.

Moens, T., Luyten, C., Middelburg, J. J., Herman, P. M., & Vincx, M. (2002). Tracing organic matter sources of estuarine tidal flat nematodes with stable carbon isotopes. *Marine Ecology Progress Series*, *234*, 127-137.

Moran, J. J., Newburn, M. K., Alexander, M. L., Sams, R. L., Kelly, J. F., & Kreuzer, H. W. (2011). Laser ablation isotope ratio mass spectrometry for enhanced sensitivity and spatial resolution in stable isotope analysis. *Rapid Communications in Mass Spectrometry*, *25*(9), 1282-1290.

Moreton, B., John, M., & Goodey, J. (1956). Aphelenchoides sp. destroying mushroom mycelium. *Nature*, *177*(4513), 795-795.

Mouthier, T. M., Kilic, B., Vervoort, P., Gruppen, H., & Kabel, M. A. (2017). Potential of a gypsum-free composting process of wheat straw for mushroom production. *PloS one*, *12*(10), e0185901.

Muszynska, B., Kala, K., Rojowski, J., Grzywacz, A., & Opoka, W. (2017). Composition and biological properties of Agaricus bisporus fruiting bodies-a review. *Polish journal of food and nutrition sciences*, *67*(3).

Naem, S., Pagan, C., & Nadler, S. A. (2010). Structural restoration of nematodes and acanthocephalans fixed in high percentage alcohol using DESS solution and rehydration. *Journal of Parasitology*, *96*(4), 809-811.

Nardi, J. B. (2009). Life in the Soil. In *Life in the Soil*. University of Chicago Press.

Neilson, R., & Brown, D. J. (1999). Feeding on Different Host Plants Alters the Natural Abundances of δ ^{13}C and δ ^{15}N in Longidoridae (Nemata). *Journal of nematology*, *31*(1), 20.

Nichols, P. D., Glen A, S., Antworth, C. P., Hanson, R. S., & White, D. C. (1985). Phospholipid and lipopolysaccharide normal and hydroxy fatty acids as potential signatures for methane-oxidizing bacteria. *FEMS Microbiology Ecology*, *1*(6), 327-335.

Noble, R., Dobrovin-Pennington, A., Evered, C., & Mead, A. (1999). Properties of peat-based casing soils and their influence on the water relations and growth of the mushroom (Agaricus bisporus). *Plant and soil*, *207*(1), 1-13.

O'Leary, W., Wilkinson, S., & Ratledge, C. (1988). Microbial lipids. *Ratledge C., Wilkinson SG, editors*, *1*.

Perrier, V., Meyer, F., & Granjon, D. (2019). shinyWidgets: Custom inputs widgets for Shiny. *R package version*.

Pimm, S. L., Lawton, J. H., & Cohen, J. E. (1991). Food web patterns and their consequences. *Nature*, *350*(6320), 669-674.

Polis, G. A., & Strong, D. R. (1996). Food web complexity and community dynamics. *The American Naturalist*, *147*(5), 813-846.

Post, D. M. (2002). Using stable isotopes to estimate trophic position: models, methods, and assumptions. *Ecology*, *83*(3), 703-718.

Rajavat, A. S., Mageshwaran, V., Bharadwaj, A., Tripathi, S., & Pandiyan, K. (2022). Spent mushroom waste: An emerging bio-fertilizer for improving soil health and plant productivity. In *New and Future Developments in Microbial Biotechnology and Bioengineering* (pp. 345-354). Elsevier.

Rashid, M. I., Mujawar, L. H., Shahzad, T., Almeelbi, T., Ismail, I. M., & Oves, M. (2016). Bacteria and fungi can contribute to nutrients bioavailability and aggregate formation in degraded soils. *Microbiological research*, *183*, 26-41.

Reyes, J. E., Venturini, M. E., Oria, R., & Blanco, D. (2004). Prevalence of Ewingella americana in retail fresh cultivated mushrooms (Agaricus bisporus, Lentinula edodes and Pleurotus ostreatus) in Zaragoza (Spain). *FEMS Microbiology Ecology*, *47*(3), 291-296.

Richter, A., Kern, T., Wolf, S., Struck, U., & Ruess, L. (2019). Trophic and non-trophic interactions in binary links affect carbon flow in the soil micro-food web. *Soil Biology and Biochemistry*, *135*, 239-247.

Rinker, D. L. (2017). Insect, mite, and nematode pests of commercial mushroom production. *Edible and medicinal mushrooms: technology and applications*, 221-237.

Ross, R., & Burden, J. (1981). unusual problem--saprophagous nematodes. *Mushroom journal*.

Royse, D. J., Sanchez, J. E., Beelman, R. B., & Davidson, J. (2008). Re-supplementing and re-casing mushroom (Agaricus bisporus) compost for a second crop. *World Journal of Microbiology and Biotechnology*, *24*(3), 319-325.

Ruess, L., & Chamberlain, P. M. (2010). The fat that matters: soil food web analysis using fatty acids and their carbon stable isotope signature. *Soil Biology and Biochemistry*, *42*(11), 1898-1910.

Ruess, L., & Dighton, J. (1996). Cultural studies on soil nematodes and their fungal hosts. *Nematologica*, *42*(3), 330-346.

Ruess, L., Schütz, K., Haubert, D., Häggblom, M. M., Kandeler, E., & Scheu, S. (2005). Application of lipid analysis to understand trophic interactions in soil. *Ecology*, *86*(8), 2075-2082.

Sampedro, L., & Domínguez, J. (2008). Stable isotope natural abundances (δ13C and δ15N) of the earthworm Eisenia fetida and other soil fauna living in two different vermicomposting environments. *Applied Soil Ecology*, *38*(2), 91-99.

Sánchez, C. (2009). Lignocellulosic residues: biodegradation and bioconversion by fungi. *Biotechnology advances*, *27*(2), 185-194.

Savoie, J.-M., & Mata, G. (2016). Growing Agaricus bisporus as a contribution to sustainable agricultural development. In *Mushroom Biotechnology* (pp. 69-91). Elsevier.

Scheepmaker, J., Geels, F., Smits, P., & Van Griensven, L. (1997). Location of immature stages of the mushroom insect pest Megaselia halterata in mushroom-growing medium. *Entomologia experimentalis et applicata*, *83*(3), 323-327.

Schmidt, O., Curry, J. P., Dyckmans, J., Rota, E., & Scrimgeour, C. M. (2004). Dual stable isotope analysis (δ13C and δ15N) of soil invertebrates and their food sources. *Pedobiologia*, *48*(2), 171-180.

Schmidt, R., Ulanova, D., Wick, L. Y., Bode, H. B., & Garbeva, P. (2019). Microbe-driven chemical ecology: past, present and future. *The ISME journal*, *13*(11), 2656-2663.

Seinhorst, J. W. (1950). *De betekenis van de toestand van de grond voor het optreden van aantasting door het stengelaaltje (Ditylenchus dipsaci (Kühn) Filipjev)* Veenman].

Semerok, A., Chaléard, C., Detalle, V., Lacour, J.-L., Mauchien, P., Meynadier, P., Nouvellon, C., Sallé, B., Palianov, P., & Perdrix, M. (1999). Experimental investigations of laser ablation efficiency of pure metals with femto, pico and nanosecond pulses. *Applied Surface Science*, *138*, 311-314.

Sharma, A., Khanna, A. S., Raina, R., Kapoor, R., & Thakur, K. S. (2019). Faunistic survey of insect-pests associated with Agaricus bisporus. *International Journal of Economic Plants*, *6*(3), 122-125.

Simon, A., Bindschedler, S., Job, D., Wick, L. Y., Filippidou, S., Kooli, W. M., Verrecchia, E. P., & Junier, P. (2015). Exploiting the fungal highway:

development of a novel tool for the in situ isolation of bacteria migrating along fungal mycelium. *FEMS Microbiology Ecology*, *91*(11), fiv116.

Singh, M., Vijay, B., Kamal, S., & Wakchaure, G. (2011). Mushrooms: cultivation, marketing and consumption. *Mushrooms: cultivation, marketing and consumption.*

Soetaert, K., & Herman, P. M. (2008). Practical Guide to Ecological Modelling: Using R as a Simulation Platform. In: Springer.

Soetaert, K., & Petzoldt, T. (2010). Inverse modelling, sensitivity and Monte Carlo analysis in R using package FME. *Journal of statistical software*, *33*, 1-28.

Soetaert, K., Petzoldt, T., & Setzer, R. W. (2010). Solving differential equations in R: package deSolve. *Journal of statistical software*, *33*, 1-25.

Soetaert, K., Provoost, P., & van Rijswijk, P. (2015). Rlims: utilities for processing laboratory analyses from NIOO-CEME. *v1.03*(NIOZ Yerseke).

Stahl, P. D., & Klug, M. J. (1996). Characterization and differentiation of filamentous fungi based on fatty acid composition. *Applied and Environmental Microbiology*, *62*(11), 4136-4146.

Steel, H., & Bert, W. (2012). Biodiversity of compost mesofauna and its potential as an indicator of the composting process status. *Dynamic Soil Dynamic Plant*, *5*(spec. iss. 2), 45-50.

Steel, H., de la Peña, E., Fonderie, P., Willekens, K., Borgonie, G., & Bert, W. (2010). Nematode succession during composting and the potential of the nematode community as an indicator of compost maturity. *Pedobiologia*, *53*(3), 181-190.

Straatsma, G., Gerrits, J. P., Thissen, J. T., Amsing, J. G., Loeffen, H., & Van Griensven, L. J. (2000). Adjustment of the composting process for mushroom cultivation based on initial substrate composition. *Bioresource technology*, *72*(1), 67-74.

Straatsma, G., Samson, R. A., Olijnsma, T. W., Op Den Camp, H. J., Gerrits, J. P., & Van Griensven, L. J. (1994). Ecology of thermophilic fungi in mushroom compost, with emphasis on Scytalidium thermophilum and growth stimulation of Agaricus bisporus mycelium. *Applied and Environmental Microbiology*, *60*(2), 454-458.

Team, R. C. (2013). R: A language and environment for statistical computing.

Thind, T. S., N., G. H., & D., P. S. (2004). *Annual review of plant pathology, volume 2, 2003*. Scientific Publishers (India) on behalf of Indian Society of Mycology and Plant Pathology.

Tomalak, M., & Lipa, J. (1991). Factors affecting entomophilic activity of Neoaplectana feltiae in mushroom compost. *Entomologia experimentalis et applicata*, *59*(2), 105-110.

Treonis, A. M., Ostle, N. J., Stott, A. W., Primrose, R., Grayston, S. J., & Ineson, P. (2004). Identification of groups of metabolically-active rhizosphere microorganisms by stable isotope probing of PLFAs. *Soil Biology and Biochemistry*, *36*(3), 533-537.

Tschierpe, H., & Sinden, J. (1965). Über leicht flüchtige Produkte des aeroben und anaeroben Stoffwechsels des Kulturchampignons, Agaricus campestris var. bisporus (L.) Lge. *Archiv für Mikrobiologie*, *52*(3), 231-241.

Urey, H. C. (1948). Oxygen isotopes in nature and in the laboratory. *Science*, *108*(2810), 489-496.

Van Bezooijen, J. (2006). *Methods and techniques for nematology*. Wageningen University Wageningen.

van Dam, F. (2020). *Carbon flow in Agaricus bisporus' compost: a stable isotope biomarker study* [Master's thesis, Utrecht University]. Utrecht. https://studenttheses.uu.nl/bitstream/handle/20.500.12932/40746/Masterthesis_FvD.pdf?sequence=1&isAllowed=y

Van Oevelen, D., Soetaert, K., Middelburg, J. J., Herman, P. M., Moodley, L., Hamels, I., Moens, T., & Heip, C. H. (2006). Carbon flows through a benthic food web: Integrating biomass, isotope and tracer data. *Journal of Marine Research*, *64*(3), 453-482.

van Roij, L., Sluijs, A., Laks, J. J., & Reichart, G. J. (2017). Stable carbon isotope analyses of nanogram quantities of particulate organic carbon (pollen) with laser ablation nano combustion gas chromatography/isotope ratio mass spectrometry. *Rapid Communications in Mass Spectrometry*, *31*(1), 47-58.

Vestal, J. R., & White, D. C. (1989). Lipid analysis in microbial ecology. *Bioscience*, *39*(8), 535-541.

Villenave, C., Bongers, T., Ekschmitt, K., Fernandes, P., & Oliver, R. (2003). Changes in nematode communities after manuring in millet fields in Senegal. *Nematology*, *5*(3), 351-358.

Volk, M., Bassin, S., Lehmann, M. F., Johnson, M. G., & Andersen, C. P. (2018). 13C isotopic signature and C concentration of soil density fractions illustrate reduced C allocation to subalpine grassland soil under high atmospheric N deposition. *Soil Biology and Biochemistry*, *125*, 178-184.

Vos, A. M., Heijboer, A., Boschker, H. T., Bonnet, B., Lugones, L. G., & Wösten, H. A. (2017). Microbial biomass in compost during colonization of Agaricus bisporus. *AMB Express*, *7*(1), 1-7.

Wada, E., Kabaya, Y., & Kurihara, Y. (1993). Stable isotopic structure of aquatic ecosystems. *Journal of Biosciences*, *18*(4), 483-499.

Warmink, J., Nazir, R., Corten, B., & Van Elsas, J. (2011). Hitchhikers on the fungal highway: the helper effect for bacterial migration via fungal hyphae. *Soil Biology and Biochemistry*, *43*(4), 760-765.

Wasilewska, L. (1998). Changes in the proportions of groups of bacterivorous soil nematodes with different life strategies in relation to environmental conditions. *Applied Soil Ecology*, *9*(1-3), 215-220.

Watzinger, A. (2015). Microbial phospholipid biomarkers and stable isotope methods help reveal soil functions. *Soil Biology and Biochemistry*, *86*, 98-107.

Willers, C., Jansen van Rensburg, P., & Claassens, S. (2015). Phospholipid fatty acid profiling of microbial communities–a review of interpretations and recent applications. *Journal of applied microbiology*, *119*(5), 1207-1218.

Willis, K. (2018). State of the World's Fungi. *Report. Royal Botanic Gardens, Kew: London, 92p.*

Wilschut, R. A., Geisen, S., Martens, H., Kostenko, O., de Hollander, M., Ten Hooven, F. C., Weser, C., Snoek, L. B., Bloem, J., & Caković, D. (2019). Latitudinal variation in soil nematode communities under climate warming-related range-expanding and native plants. *Global change biology*, *25*(8), 2714-2726.

Wood, D., & Leatham, G. (1983). Lignocellulose degradation during the life cycle of Agaricus bisporus. *FEMS microbiology letters*, *20*(3), 421-424.

Wyss, U., & Grundler, F. (1992). Feeding behavior of sedentary plant parasitic nematodes. *Netherlands Journal of Plant Pathology*, *98*(2), 165-173.

Yeates, G. (1987). Nematode feeding and activity: the importance of development stages. *Biology and fertility of soils*, *3*(1), 143-146.

Yeates, G. W., Bongers, T., De Goede, R. G., Freckman, D. W., & Georgieva, S. (1993). Feeding habits in soil nematode families and genera—an outline for soil ecologists. *Journal of nematology*, *25*(3), 315.

Yoder, M., De Ley, I. T., King, I. W., Mundo-Ocampo, M., Mann, J., Blaxter, M., Poiras, L., & De Ley, P. (2006). DESS: a versatile solution for preserving morphology and extractable DNA of nematodes. *Nematology*, *8*(3), 367-376.

Zanden, M. J. V., & Rasmussen, J. B. (2001). Variation in δ15N and δ13C trophic fractionation: implications for aquatic food web studies. *Limnology and oceanography*, *46*(8), 2061-2066.

Zelles, L. (1997). Phospholipid fatty acid profiles in selected members of soil microbial communities. *Chemosphere*, *35*(1-2), 275-294.

Zelles, L. (1999). Fatty acid patterns of phospholipids and lipopolysaccharides in the characterisation of microbial communities in soil: a review. *Biology and fertility of soils*, *29*(2), 111-129.

Zhang, H., Lai, W., Xu, L., Jia-Ni, W., Qiu-Yue, S., & Zhang, X. (2020). In Situ Carbon Stable isotope Analysis of Organic Carbon by Laser Ablation-Isotope Ratio Mass Spectrometry. *Chinese Journal of Analytical Chemistry*, *48*(6), 774-779.

Zhang, X., Zhong, Y., Yang, S., Zhang, W., Xu, M., Ma, A., Zhuang, G., Chen, G., & Liu, W. (2014). Diversity and dynamics of the microbial community on decomposing wheat straw during mushroom compost production. *Bioresource technology*, *170*, 183-195.

Appendices

Appendix A: Visualisation of the process of nematode counting

Figure 29: Two vials, with the larger vial representing a product of nematode extraction, and the smaller vial representing a product of counting. Top row represents a typical compost sample, while the lower row represents a typical casing sample. Nematode counting included separating nematodes from the extraction sample and cleaning them, after which they were placed in ethanol in the smaller vial. In the right column, both larger vials were shaken before the image was taken, showing the amount of material in suspension which was intertwined with present nematodes, and the comparable cleanliness of the smaller sample with counted nematodes. The smaller vial was used as a working sample, from which nematodes were extracted further for isotopic analyses.

Appendix B: Illustrated modified Bligh and Dyer method

First step of the modified Bligh and Dyer method

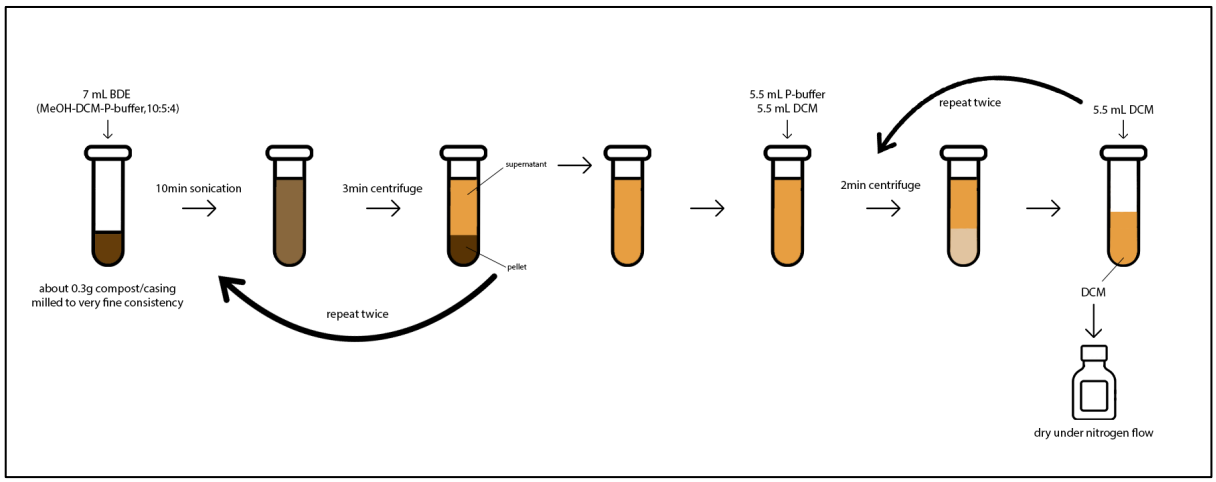

Figure 30: Illustration of the first step of modified Bligh-Dyer method.

Second step of the modified Bligh and Dyer method

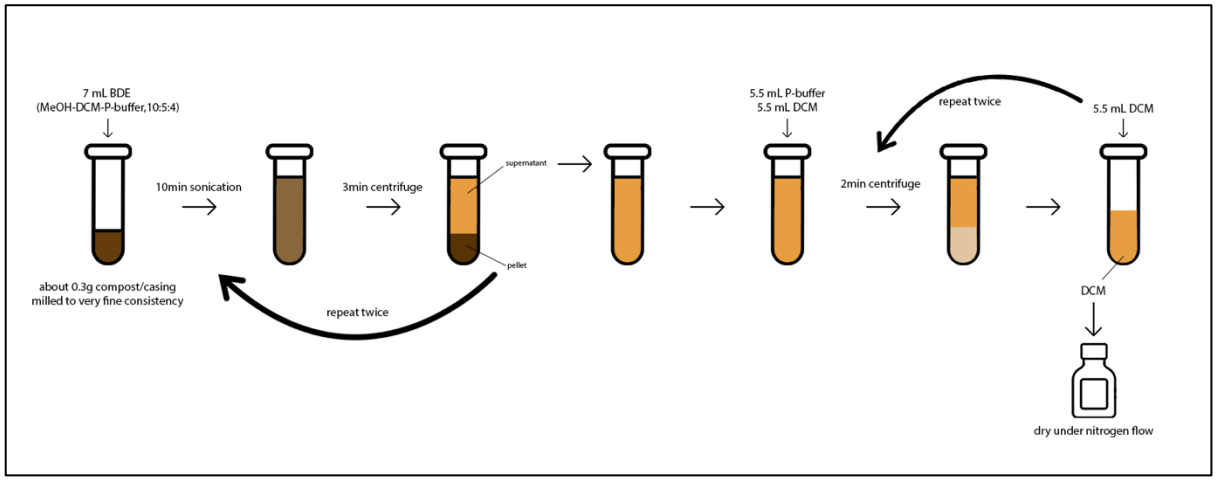

Figure 31: Illustration of the second step of modified Bligh-Dyer method.

Third step of the modified Bligh and Dyer method

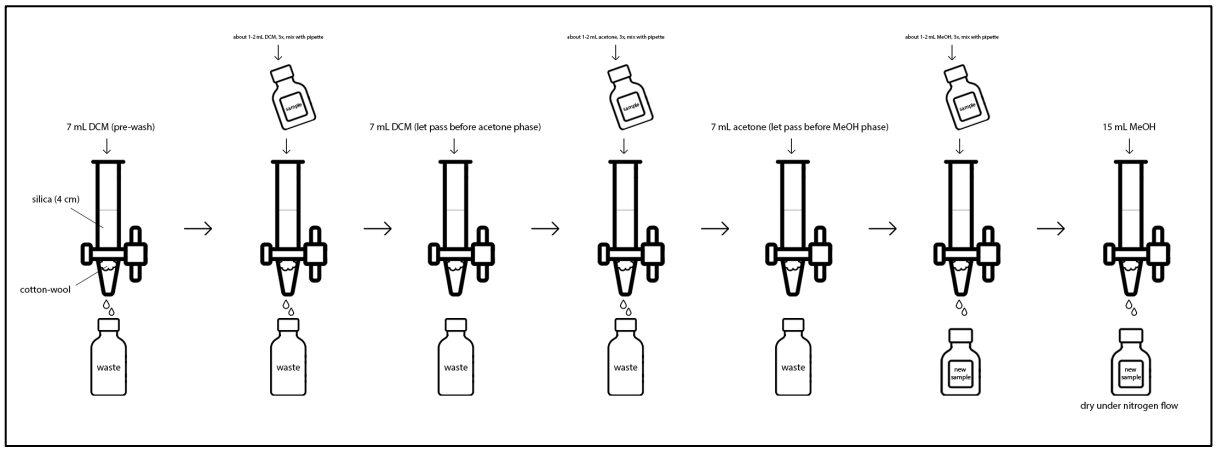

Figure 32: Illustration of the final step of modified Bligh-Dyer method.

Appendix C: Complete food web model code, as written in R

Full version of the code can be found on the github repository: https://github.com/liusaydh/compost-food-web/blob/main/food-web-code-May22.Rmd

Appendix D: Parameters used in the total carbon food-web model with literature sources

Total carbon food-web parameters can be found on the github repository: https://github.com/liusaydh/compost-food-web#-natural-abundance-parameters-and-state-variables-

Appendix E: Parameters used in the ^{13}C-tracer model with literature sources

^{13}C-tracer model parameters can be found on the github repository: https://github.com/liusaydh/compost-food-web#-13c-model-addition-parameters-and-state-variables-

Appendix F: Tables containing absolute and normalised nematode counts

Table 12: Absolute nematode counts between treatments L- A+, L+ A+ and L+ A-. Each treatment was conducted on two distinctive soil types (compost and casing) per replicates (A, B, C...). Results were divided per sampling timepoint (sampled at day 0, day 14, day 21, or day 30 of the experiment).

treatment	L- A+						L+ A+						L+ A-			
substrate	compost				casing		compost			casing			compost		casing	
replicate	A	B	D	F	A	B	A	B	C	A	B	C	A	B	A	B
Day 0	-	-	-	-	275	-	-	-	-	-	-	-	-	-	-	-
Day 14	440	178	-	-	89	64	98	181	163	65	93	51	89	82	13	36
Day 21	248	35	255	305	27	22	87	199	31	14	34	11	42	26	192	21
Day 30	31	22	-	-	46	29	23	27	23	8	8	30	-	-	-	-

Table 13: Nematode counts normalised per weight of substrate, for L- A+, L+ A+ and L+ A- treatments. Values are in units of nematodes per 10 grams compost. Unavailable values (N/A, where indicated) occurred due to missing values for the weight of the sample of casing or compost, disabling the conversion from absolute to normalised counts.

treatment	L- A+						L+ A+						L+ A-			
substrate	compost				casing		compost			casing			compost		casing	
replicate	A	B	D	F	A	B	A	B	C	A	B	C	A	B	A	B
Day 0	-	-	-	-	N/A	-	-	-	-	-	-	-	-	-	-	-
Day 14	145.5	61.3	-	-	40.5	33.1	27.6	54.3	53.2	33.9	48.4	24.5	32.7	26.6	5.6	15.2
Day 21	94.1	13	60.2	70.5	17.9	13.6	24.2	59.2	9.5	9	29.1	8.6	12.7	8.2	140.3	18.8
Day 30	12.4	6.2	-	-	36.1	N/A	7.3	8.1	6.8	5.6	7.5	30.1	-	-	-	-

Appendix G: Complete set of images taken during visual observations of nematode mouthparts

Images taken of samples before rehydration

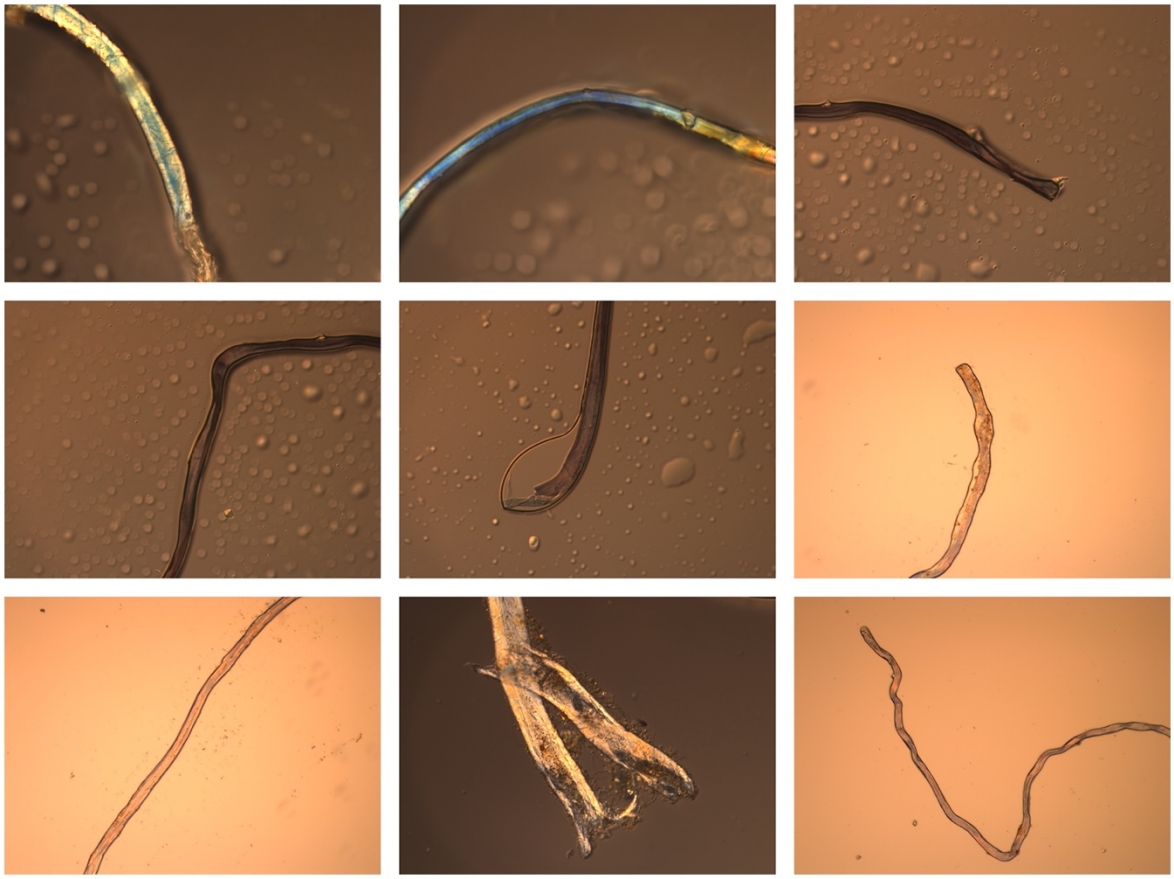

Figure 33: An assortment of images made of nematodes taken from casing after 14 days at various magnifications, of extremities, as well as full body lengths.

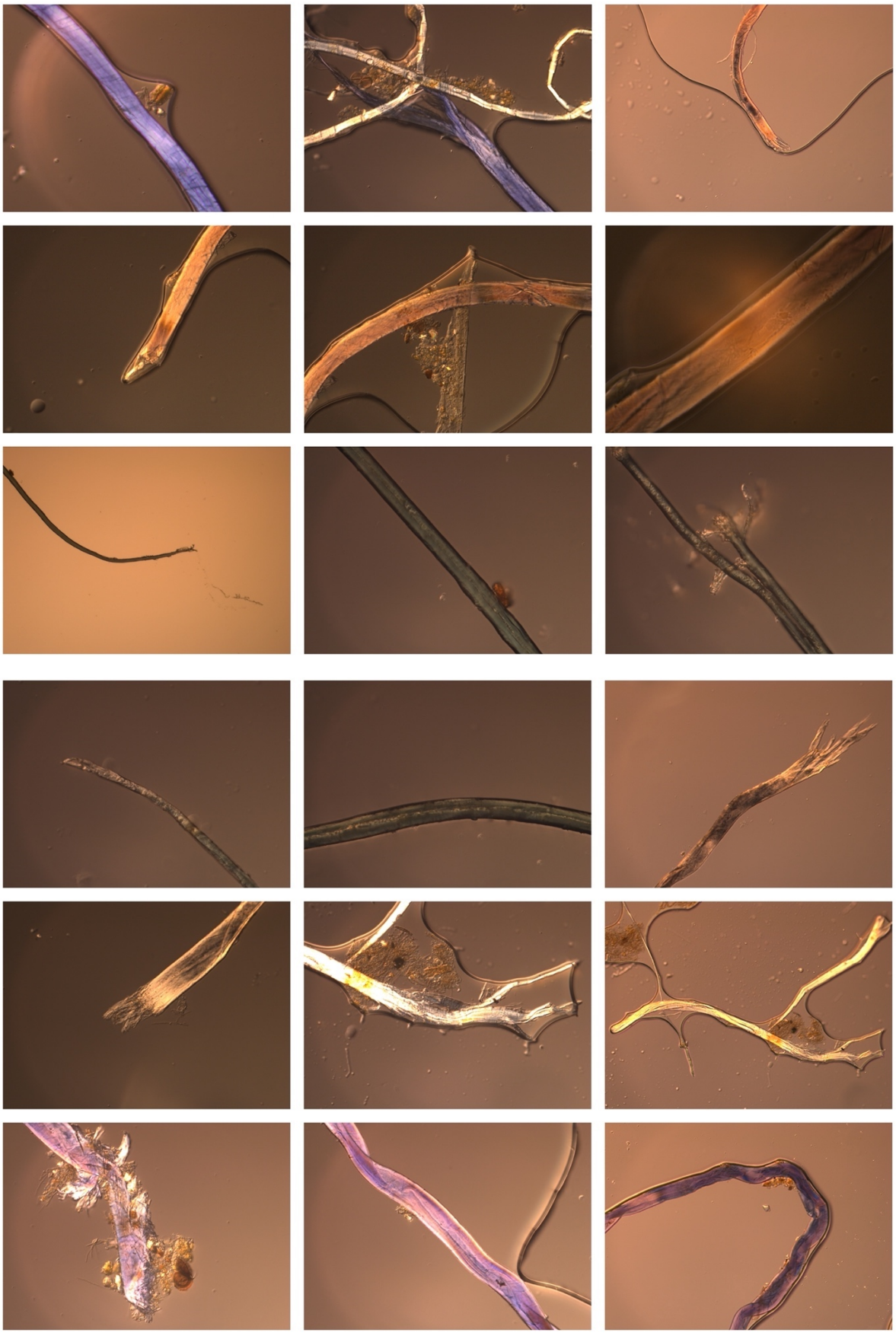

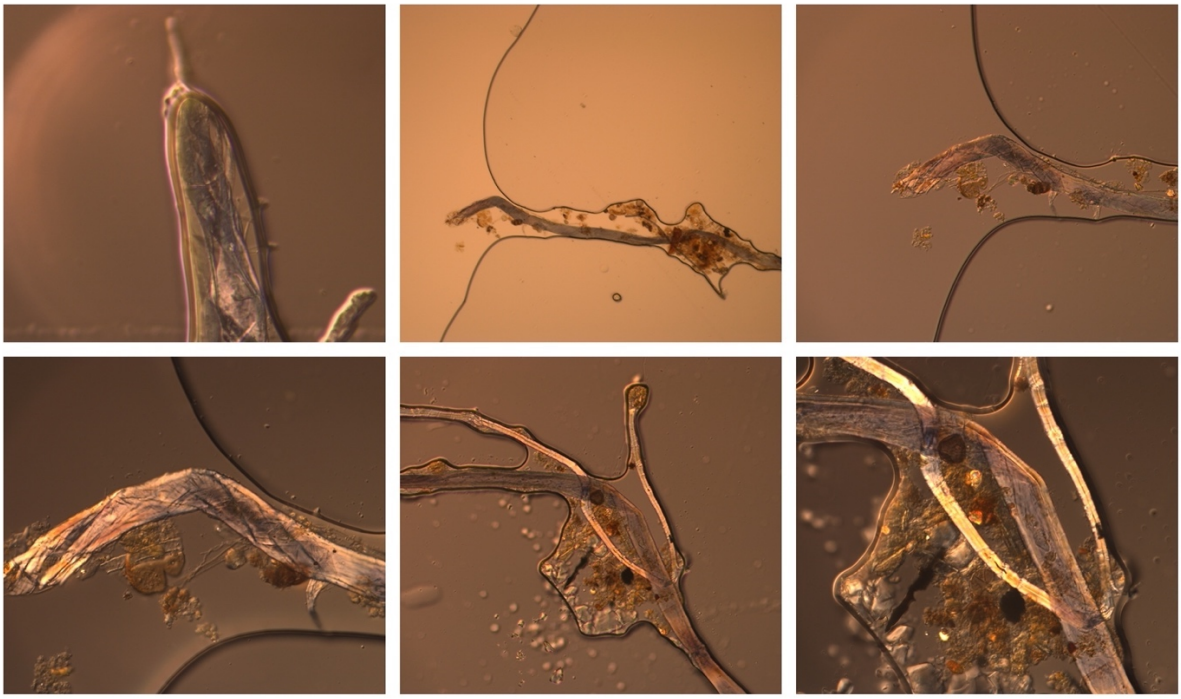

Figure 34: An assortment of images made of nematodes taken from compost after 14 days at various magnifications, of extremities, as well as full body lengths.

Images taken of samples after 24 hours rehydration

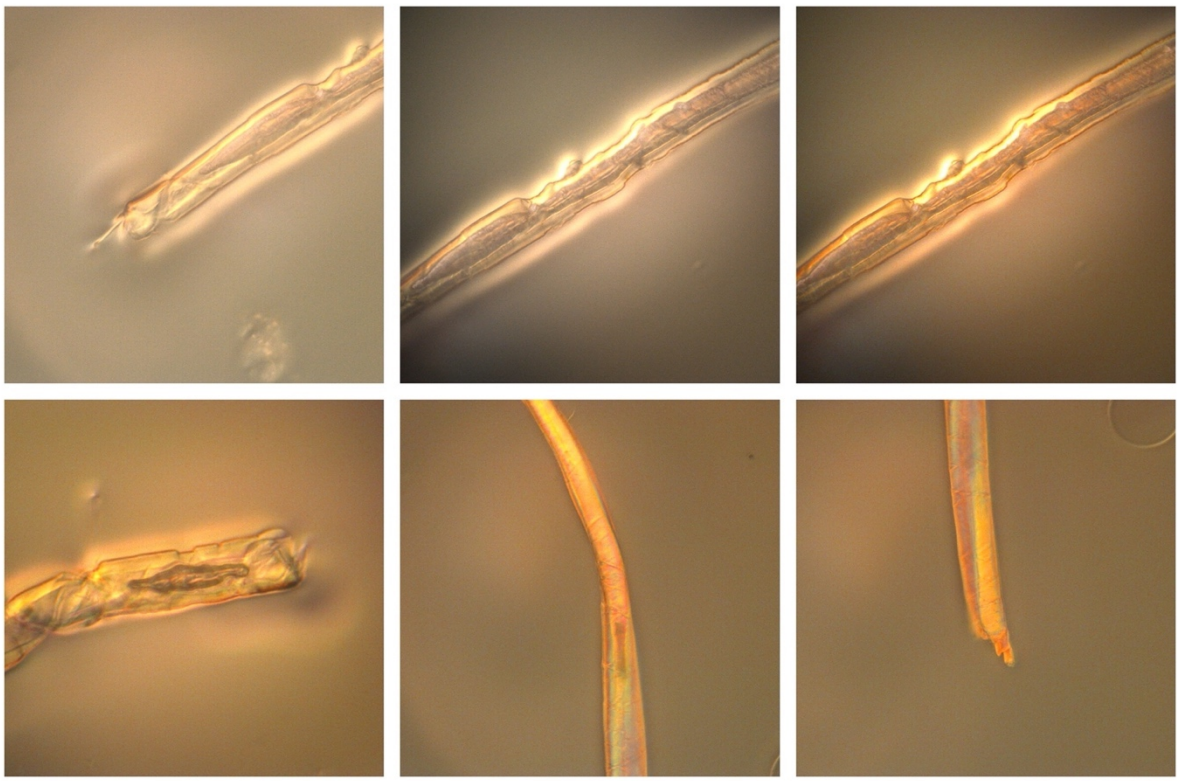

Figure 35: An assortment of images made of nematodes taken from casing after 14 days at various magnifications, of extremities, as well as full body lengths, after 24 hours rehydration method was performed on the sample.

Images taken of samples after 65 hours rehydration

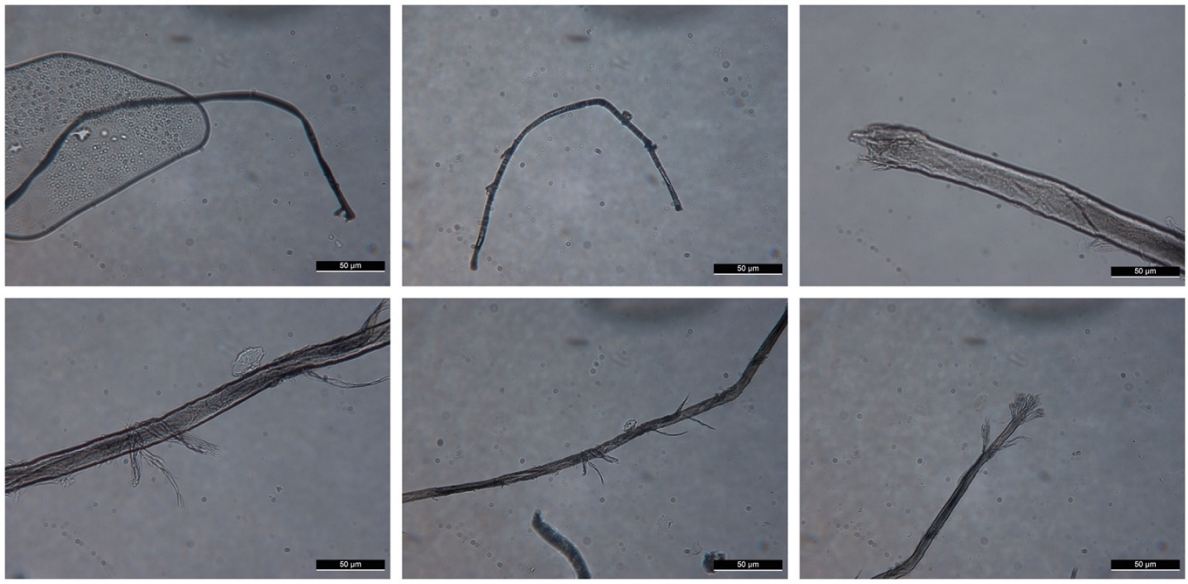

Figure 36: An assortment of images made of nematodes taken from casing after 14 days at various magnifications, of extremities, as well as full body lengths, after 65 hours rehydration method was performed on the sample.

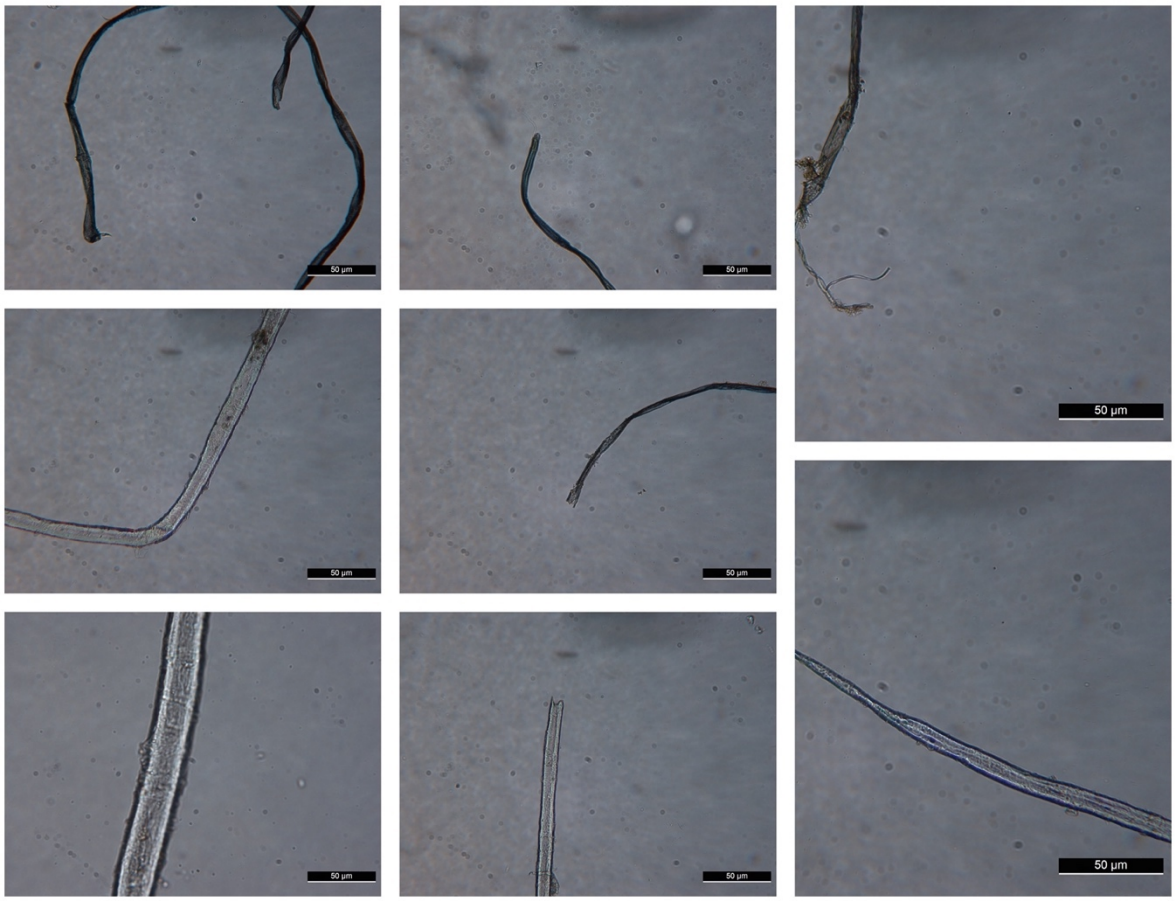

Figure 37: An assortment of images made of nematodes taken from compost after 14 days at various magnifications, of extremities, as well as full body lengths, after 65 hours rehydration method was performed on the sample.

Acknowledgements

The biggest thank you to my second mentor, Madalina, who was with me every step of the way during the creation of this thesis, privately and professionally, and from whom I had the pleasure of learning from for an entire year. I truly believe you made me a better researcher, and I certainly enjoyed our many lunches and coffees together. Further thanks are in order towards my first mentor, Jack, both for the invaluable advice, as well as encouraging me to write about a topic I really found interesting for my guided research. Many thanks to everyone who was a part of my daily life at GEOLab+, especially Desmond – for all the little daily questions and Chris – for patiently fixing the LA-IRMS more times than I can remember. For all the invaluable help with the model and all the wonderful advice on the written code, a huge thanks to Lubos. Further thanks to everyone who was a fun chat and an interesting part of everydayness in the labs and around, including Salima, Bayan, Tilly, Helen, Koen, Klaas, Antoinette, Natasja, Thom, Mariska, Giovanni and Bernadette. Thanks to all my friends, those from UU and those from before, for listening to concerns both private and professional, and making me feel appreciated even when they were at times overwhelming. An eternal thank you to my best friend Ivan, for gently pushing me when I thought I couldn't go further, for taking care of me for days on end during 10-hour workdays and for binging Star Trek when I felt down, even though he absolutely knows every episode. Finally, thanks are in order to my family – my mum and dad, my sister, my uncle and my grandma, who were all always just a phone call away when things got hard and always made me less alone, and without whom I would most certainly not be what I am today. This accomplishment is as mine as it is all of yours, and I am grateful for that.